NOELY SYLVANIE FOUEDJIO SONFACK

MODELING MISCIBLE $CO_2/N_2$ INJECTION FOR ENHANCED OIL RECOVERY:AIN DAR AREA

MASTER THESIS

2025

**NEAR EAST UNIVERSITY**

**INSTITUTE OF GRADUATE STUDIES**

**DEPARTMENT OF PETROLEUM AND NATURAL GAS ENGINEERING**

# MODELING MISCIBLE $CO_2/N_2$ INJECTION FOR ENHANCED OIL RECOVERY: AIN DAR AREA

**M.Sc. THESIS**

**Noely Sylvanie FOUEDJIO SONFACK**

**Nicosia**

**April, 2025**

**NEAR EAST UNIVERSITY**
**INSTITUTE OF GRADUATE STUDIES**
**DEPARTMENT OF PETROLEUM AND NATURAL GAS ENGINEERING**

# MODELING MISCIBLE $CO_2/N_2$ INJECTION FOR ENHANCED OIL RECOVERY: AIN DAR AREA

**M.Sc. THESIS**

**Noely Sylvanie FOUEDJIO SONFACK**

**Supervisor**
**Prof. Dr. Cavit ATALAR**

**Nicosia**
**April, 2025**

## Approval

We certify that we have read the thesis submitted by Noely Sylvanie FOUEDJIO SONFACK titled "**Modeling miscible $CO_2/N_2$ injection for enhanced oil recovery: Ain dar area** " and that in our combined opinion it is fully adequate, in scope and in quality, as a thesis for the degree of Master of Applied Sciences.

| Examining Committee | Name-Surname | Signature |
|---|---|---|
| Head of the Committee: | Prof.Dr Hüseyin Çamur | ..... |
| Committee Member: | Asst. Prof. Dr. Gamze Ipek | ..... |
| Supervisor: | Prof. Dr. Cavit ATALAR | ..... |

Approved by the Head of the Department

10/04/2025

.....

Prof. Dr Cavit ATALAR

Head of the Department

Approved by the Institute of Graduate Studies

10/04/2025

Prof. Dr. Kemal Hüsnü Can Başer

Head of the Institute of Graduate Studies

## Declaration of Ethical Principles

I hereby declare that all information, documents, analysis and results in this thesis have been collected and presented according to the academic rules and ethical guidelines of Institute of Graduate Studies, Near East University. I also declare that as required by these rules and conduct, I have fully cited and referenced information and data that are not original to this study.

**Noely Sylvanie FOUEDJIO SONFACK**

10/04/2025

## Acknowledgments

First of all, I would like to acknowledge the efforts of my supervisor, Professor Cavit Atalar, for his immense and unwavering support and guidance. I would also like to thank Prof. Dr. Salih Saner, Asst. Prof. Dr. Gamze Ipek, Msc. Palang Moronke Guful, Prof. Dr. Hüseyin Çamur and Dr. Yashar Osgouei for their knowledge and advice. I am overwhelmed in all humility to acknowledge my deep gratitude to Msc. Palang Moronke Guful who has played a crucial role in helping me put these ideas far above the level of simplicity and into something concrete, her simulation suggestions and encouragement have helped me throughout the manufacturing process. I am so grateful to her for the time spent proofreading and correcting my mistakes and for all her advice and follow-ups.

I would like to take this opportunity to thank and recognize the efforts made by my family Kitio Laure, Jean Dubois, Jenny, Stessy ,Florent Fouedjio, Rosine Ngoufack, Ludovic Kana, Louise Tsamo and all my uncles for helping me become what I am today. In addition, I would like to acknowledge the efforts of my friends, I am immensely grateful to Jordan, Irlice, Musa and Ousmane for their uplifting inspiration, valuable and conscientious advice, aspirational motivation, encouragement, invaluable constructive criticism and friendly advice.

Finally, I express my warmth and gratitude for acknowledging and offering my deepest sense of respect to my big sister Chrystie and my fiancé Jores. No one has been more important to me in this quest than they have been in always supporting me morally, giving me encouragement, enthusiasm, invaluable help, endless motivation, advice and the fact is that without their efforts I would not be accomplishing this study. Some of my friends and colleagues whose names have not been mentioned here, I also want to acknowledge their efforts, some have given me valuable and helpful tips that have propelled me to a huge academic success, thank you all.

**Noely Sylvanie FOUEDJIO SONFACK**

## Abstract

### Modeling Miscible $CO_2/N_2$ Injection for Enhanced Oil Recovery: Ain Dar Area

**FOUEDJIO SONFACK, Noely Sylvanie**
**M.Sc, Department of Petroleum and Natural Gas Engineering**
**April 2025, 99 pages**

This study focuses on the injection of miscible carbon dioxide ($CO_2$) as a means to improve oil recovery performance. By analyzing various EOR methodologies, notably miscible flooding with $CO_2$, which enhances oil dissolution and reduces viscosity, the research aims to assess the impact of nitrogen ($N_2$) on recovery efficiency. Our study was conducted in the Ain Dar region of Saudi Arabia, utilizing a computer simulator CMG to model the dynamics of oil recovery and evaluate the effectiveness of pure $CO_2$ flooding compared to mixtures of $CO_2$ and $N_2$.

The simulation results reveal significant findings regarding oil recovery factors, displacement efficiencies, and cumulative oil production. The natural depletion resulted in a recovery factor of 27.3%, pure $CO_2$ flooding achieved a remarkable recovery efficiency of 73.8%, while various $CO_2$ and $N_2$ mixtures yielded recoveries ranging from 60% to 69%. Notably, pure $CO_2$ flooding also demonstrated a lower minimum miscibility pressure compared to mixtures of $CO_2$ with $N_2$, contributing to a peak cumulative output of 38 million barrels. These findings underscore the potential of injecting pure $CO_2$ to optimize oil recovery strategies, while also addressing concerns related to carbon emissions and operational costs.

**Key Words**: enhanced oil recovery, miscible $CO_2$ flooding, minimum miscibility pressure, $CO_2$ sequestration.

# Özet


**Ghawar Petrol Sahasında Gelişmiş Petrol Geri Kazanımı için Karışabilir $CO_2/N_2$ Enjeksiyonunun Modellenmesi: Ain Dar Bölgesi**

**FOUEDJIO SONFACK, Noely Sylvanie**
**Yüksek Lisans, Petrol ve Doğal Gaz Mühendisliği Bölümü**
**Nisan 2025, 99 sayfa**

Bu çalışma, petrol geri kazanım performansını iyileştirmenin bir yolu olarak karışabilir karbondioksit ($CO_2$) enjeksiyonuna odaklanmaktadır. Araştırma, çeşitli EOR metodolojilerini, özellikle de yağ çözünmesini artıran ve viskoziteyi azaltan $CO_2$ ile karışabilir taşmayı analiz ederek, nitrojenin ($N_2$) geri kazanım verimliliği üzerindeki etkisini değerlendirmeyi amaçlamaktadır. Çalışmamız, Suudi Arabistan'ın Ain Dar bölgesinde, petrol geri kazanımının dinamiklerini modellemek ve $CO_2$ ve $N_2$ karışımlarına kıyasla saf $CO_2$ taşkınının etkinliğini değerlendirmek için bir bilgisayar simülatörü CMG kullanılarak gerçekleştirildi.

Simülasyon sonuçları, petrol geri kazanım faktörleri, yer değiştirme verimlilikleri ve kümülatif yağ üretimi ile ilgili önemli bulgular ortaya koymaktadır. Doğal tükenme %27,3'lük bir geri kazanım faktörü ile sonuçlandı, saf $CO_2$ taşkın, %73,8'lik kayda değer bir geri kazanım verimliliği sağlarken, çeşitli $CO_2$ ve $N_2$ karışımları %60 ila %69 arasında değişen geri kazanımlar sağladı. Özellikle, saf $CO_2$ taşkını, $CO_2$ ile $N_2$ karışımlarına kıyasla daha düşük bir minimum karışabilirlik basıncı gösterdi ve bu da 38 milyon varillik bir pik kümülatif çıktıya katkıda bulundu. Bu bulgular, karbon emisyonları ve operasyonel maliyetlerle ilgili endişeleri ele alırken, petrol geri kazanım stratejilerini optimize etmek için saf $CO_2$ enjekte etme potansiyelinin altını çiziyor.



**Anahtar kelimeler**: gelişmiş yağ geri kazanımı, karışabilir $CO_2$ taşma, minimum karışabilirlik basıncı, $CO_2$ sekestrasyonu.

## Table of Contents

CHAPTER III



CHAPTER IV



CHAPTER V



CHAPTER VI

## List of Tables

## List of Figures

## List of Abbreviations

| | |
|---|---|
| **ASP:** | Alkaline/Surfactant/Polymer |
| **BHP:** | Bottom-Hole Pressure |
| **CCS:** | Carbon Capture Sequestration |
| **$CO_2$:** | Carbon-Dioxide |
| **CMG:** | Computer Modeling Group |
| **EOR:** | Enhanced Oil Recovery |
| **EOS:** | Equation Of State |
| **FVF:** | Formation Volume Factor |
| **GOR:** | Gas Oil Ratio |
| **GEM:** | Group Environmental Model |
| **HG:** | Hydrocarbon Gases |
| **IFT:** | Interfacial Tension |
| **IEA:** | International Energy Agency |
| **LPG:** | Liquefied Petroleum Gas |
| **MMP:** | Minimum Miscibility Pressure |
| **MCM:** | Multi-Contact Miscibility |
| **$N_2$:** | Nitrogen |
| **OOIP:** | Oil Originally in Place |
| **OWC:** | Oil-Water Contact |
| **PR:** | Peng-Robinson |
| **PV:** | Pore Volume |

**PSI:** Pounds per Square Inch

**PVT:** Pressure Volume Temperature

**RF:** Recovery Factor

**ROV:** Relative Oil Volume

**SRK:** Soave-Redlich-Kwong

**VLE:** Vapor-Liquid Equilibrium

**WOC:** Water-Oil Contact

# CHAPTER I
# Introduction

This chapter will provide a foundational background on enhanced oil recovery, with a specific focus on modeling miscible $CO_2$ enhanced flooding to improve oil recovery. The discussion will include relevant connections between theories related to the research objectives.

## Study Background

Over the past 150 years, oil has become the world's primary energy source. Production of this commodity has been rapidly increasing, reaching over 30 billion barrels annually at the beginning of the 21st century. Oil now plays a significant role in global politics and the economy. Although more sustainable energy sources are being developed, hydrocarbons remain irreplaceable for the time being. This reality leads to two main outcomes: either new oilfield discoveries are made, or existing ones are utilized more efficiently. To extract more oil from reservoirs that cannot be tapped using primary and secondary recovery methods, the oil industry employs a set of sophisticated techniques known as Enhanced Oil Recovery (EOR) (Mokheimer et al., 2019). EOR is essential for maximizing the yield from older, depleted oil fields. According to Wang et al. (2017), oil companies can extend the productive life of their oil fields by using EOR methods. These methods significantly increase the total recoverable oil from existing wells. This approach is crucial for meeting global energy demands and optimizing the use of our current resources, ultimately enhancing the oil production process in the long run.

Enhanced Oil Recovery (EOR) aims to optimize the extraction of remaining oil from reservoirs. This process involves creating and testing novel agents, such as water, chemicals, gas, and various liquids with different viscosities, which have shown promise in facilitating smoother oil flow during field applications. EOR consists of three main phases: primary, secondary, and tertiary. During the primary extraction phase, mechanical pumps or the reservoir's natural pressure are used to extract oil. However, this stage typically recovers only a small fraction of the oil available in the reservoir (Malozyomov et al., 2023). According to Alagolorni et al. (2015), secondary recovery techniques can enhance extraction by maintaining reservoir pressure and

dispersing oil through the injection of water or gas. Heavy oil poses a particular challenge due to its high viscosity, making both primary and secondary methods less effective. There are various methods for extracting oil from reservoirs, depending on the energy sources used. The two primary approaches for EOR projects on a commercial scale are thermal and non-thermal techniques. Thermal processes include in-situ combustion, electrical heating, and hot water or steam injection. Conversely, non-thermal processes encompass techniques such as gas and chemical injection. EOR methods, like gas injection, modify the characteristics of the oil, increase its mobility, and make it easier to extract, ultimately leading to greater recovery rates. The primary benefit of EOR is the increased production of oil, which can yield up to 30% more, especially in mature oil fields where reservoir pressure has significantly declined (Al-Wahaibi et al., 2017). Additionally, EOR can contribute to reducing carbon emissions through carbon sequestration efforts. To recover heavy oil from aging reservoirs, petroleum engineers often employ gas injection based EOR techniques. This approach helps maintain pressure, reduce the viscosity of reservoir fluids, effectively displace these fluids, and induce the oil swelling effect. The expansion of reservoir oil occurs when an injected solvent dissolves into the reservoir fluid, making gas injection a long-established EOR process in the petroleum industry (Willhite, 1998).

Anthropogenic activities have led to an increase in the concentration of carbon dioxide and other greenhouse gases in the atmosphere since the industrial revolution began. The primary cause of this increase is the combustion of fossil fuels for energy production (Filonchyk et al., 2024). Carbon dioxide ($CO_2$) sequestration is crucial for reducing greenhouse gases, as $CO_2$ accounts for approximately 64% of the overall impact on the greenhouse effect when compared to other greenhouse gases. To mitigate global warming, it is essential to decrease carbon dioxide emissions. One effective strategy for reducing atmospheric $CO_2$ is the use of carbon dioxide for enhanced oil recovery (EOR) through reservoir injection. The International Energy Agency (IEA) estimates that there are between 300 billion to 600 billion barrels of oil resources globally that are suitable for the implementation of $CO_2$ enhanced oil recovery technology (Hall et al., 1983). This represents about 14% to 28% of the world's total recoverable oil resources. Successful examples of carbon dioxide injection for enhanced oil recovery can be found in countries such as China, Russia, the United States, and Canada (Zhao et al., 2021).

One of the most promising techniques among chemical injection in commercial applications is the use of carbon dioxide ($CO_2$) for enhanced oil recovery (EOR). $CO_2$ is preferred over hydrocarbon gases (HC) in gas flooding procedures due to its lower cost, higher displacement efficiency, and potential environmental benefits through its disposal in petroleum reservoirs. $CO_2$ flooding involves injecting carbon dioxide into an oil reservoir to increase its volume and decrease its viscosity, making it easier to extract the oil (Massarweh & Abushaikha, 2022). This method leads to improved oil mobility and higher recovery rates. However, there are challenges associated with $CO_2$ injection, particularly in heavy oil reservoirs. Common issues include poor sweep efficiency and early $CO_2$ breakthrough, which can limit the effectiveness of the process. Oil can be displaced by $CO_2$ through two methods: miscible which is a tertiary recovery and immiscible displacement which is considered as secondary recovery. Miscible processes generally result in higher oil recovery rates compared to immiscible processes. This is because miscible displacement effectively reduces the interfacial tension between the injected fluid and the oil, allowing for more efficient displacement and extraction. Additionally, miscible processes delay gas breakthroughs, which enables the injected gas to remain in contact with the oil for a longer time, ultimately enhancing recovery. In contrast, immiscible processes can impede oil extraction by increasing the oil's viscosity and leaving capillary forces that hold oil within the reservoir. Thus, miscible techniques improve oil recovery by overcoming these challenges.

**Problem Statement**

The primary and traditional secondary recovery methods, such as waterflooding, applied to the Arab-D reservoir have resulted in low recovery rates and left a significant amount of oil in place. This situation necessitates the exploration of enhanced oil recovery (EOR) techniques. Miscible injection is a promising EOR method that can significantly increase the recovery factor while also reducing carbon emissions through carbon sequestration. In our study, we will investigate and model the injection process of this method. However, the efficiency of miscible injection faces several challenges, including the effects of the fluid's properties and composition, particularly due to the presence of contaminants such as nitrogen ($N_2$).

**Aim of the Study**

This thesis aims to enhance oil recovery in the carbonate reservoir known as the Ghawar oil field by studying the miscibility of $CO_2$ with oil and evaluating the effectiveness of various $CO_2$ injection strategies. To achieve this, we utilized CMG GEM to quantitatively assess the viability of Arab-D oil reservoirs for miscible $CO_2$ flooding. The insights gained from this study enhance our understanding of the phase behavior factors involved in soluble displacement processes, including the prerequisites for a multi-contact miscibility (MCM). It will be demonstrated that the minimum miscibility pressure (MMP) is influenced by the composition of the injected fluid, which in turn affects oil recovery. Techniques for calculating this pressure level using CMG Winprop and empirical relationships are employed. Finally, the results of multiple injection scenarios using carbon dioxide and nitrogen are discussed.

**Research Questions**

How can injection strategies be optimized to enhance oil recovery?

What effects does nitrogen ($N_2$) have on oil recovery in the Arab-D reservoir?

What key factors influence the effectiveness of miscible $CO_2$ injection?

What are the environmental impacts of large-scale $CO_2$ injection, and how can they be mitigated?

**Objectives of the Study**

By using simulation studies, the investigation's main objective is to enhance knowledge and design of gas injection with an emphasis on $CO_2/N_2$ miscibility. In light of this, the following are the study's goals:

Performing the miscible $CO_2/N_2$ injection in the Ghawar oil field using CMG GEM modeling.

To determine the MMP during the performance of miscible $CO_2/N_2$ injection using different empirical correlations.

To analyze the effect of impurities such as $N_2$ on injection strategies for maximizing oil recovery.

To assess the potential environmental risks and benefits of $CO_2/N_2$ injection.

**Significance of the Study**

To maximize oil recovery from the Arab-D reservoir, it is essential to implement a miscible approach, as both primary and secondary recovery methods have yielded limited results, leaving a considerable amount of oil still in place. This research aims to address the challenges encountered during miscible $CO_2/N_2$ flooding, particularly focusing on the effects of $CO_2$ purity on oil recovery. High purity $CO_2$ enhances the displacement of oil due to its increased mobility. Conversely, the presence of nitrogen in the system tends to impair oil mobility, displacement efficiency, and overall recovery, limiting the effectiveness of carbon dioxide in the reservoir. However, it is important to note that both carbon dioxide and nitrogen are cost-effective options, which can help lower operational costs, reduce the impact of global warming, and decrease the emission of greenhouse gases into the atmosphere.

**Scope**

The focus of this research is on tertiary enhanced oil recovery, with a particular emphasis on miscible $CO_2$ flooding in carbonate reservoirs. The study utilizes CMG as a tool, specifically the CMG GEM simulator, to explore various aspects of this technique. One key area of investigation is the impact of combining $CO_2$ and $N_2$ on recovery rates, reservoir compliance, and efficiency of oil sweeps. Additionally, the research delves into how the mixture of $CO_2$ and $N_2$ interacts with oil, taking into consideration factors such as miscibility, fluid displacement, extraction efficiency, and the effects induced by nitrogen presence, including changes in oil viscosity and the lowest levels of miscibility achievable. The objective is to refine the miscible $CO_2$ flooding method to enhance oil recovery processes while prioritizing environmental sustainability. This involves identifying critical parameters and optimal reservoir conditions to maximize sweep efficiency in oil production.

**Limitations**

Due to the absence of field data and a properly functioning research laboratory during this study, the investigation relies primarily on a comprehensive review of relevant literature to obtain accurate and valuable information. While the CMG simulator effectively models enhanced oil recovery techniques, the results obtained from laboratory experiments such as slim tube tests along with logistical challenges, economic feasibility, and regulatory issues encountered while scaling the approach for field application may not always align with real-world scenarios. This discrepancy can

lead to variations between anticipated and actual performance. Additionally, external factors like market conditions, technological advancements, and shifts in regulatory frameworks may influence the effectiveness and practical implementation of the $CO_2$ flooding technique, although these aspects may not be directly addressed in this study.

**Structure of the Thesis**

The thesis is organized into six chapters, each focusing on a specific objective outlined in this study. The first chapter presents the research background, introducing key concepts related to enhanced oil recovery, specifically discussing miscible $CO_2$ enhanced flooding. Additionally, it outlines the research problem and the objectives aimed at addressing this issue. The chapter also highlights the study's aim, significance, the overall structure of the thesis, and delineates its scope and limitations.

In the second chapter, a comprehensive literature review is conducted. It begins by establishing a theoretical framework, discussing enhanced oil recovery and reservoir simulation with a focus on the CMG GEM model. This section aims to provide foundational research relevant to the project. Furthermore, it includes details regarding the study area's location and geological context.

The third chapter outlines the methodology employed in this research, detailing the steps taken to investigate miscibility and to maximize oil recovery. This includes the methods for data collection, the refined relationships developed for assessing the minimum miscibility pressure (MMP) of $CO_2$ and $N_2$, the techniques used for data analysis, and the various injection scenarios designed to achieve the research objectives using the CMG GEM simulation tool.

In the fourth chapter, I present significant findings and analyses related to oil recovery across different scenarios. The primary focus of this chapter is to assess the effects of injecting pure $CO_2$ versus $N_2$ on recovery rates, displacement efficiency, cumulative oil production, and other relevant factors.

Chapter five discusses the results regarding the performance of $CO_2$ injection in the presence of nitrogen, along with an examination of the associated environmental impacts.

In conclusion, the thesis captures the study's findings and provides a summary of the research. It also interprets the results in the context of existing literature and highlights the implications of the findings. Importantly, the conclusion offers recommendations for future research avenues.

# CHAPTER II

## Literature Review

### Enhanced Oil Recovery Overview

Oil recovery refers to the extraction of crude oil from subsurface reservoirs. Traditionally, as depicted in figure 1, the stages of oil recovery are categorized into three main phases: primary, secondary, and tertiary recovery.

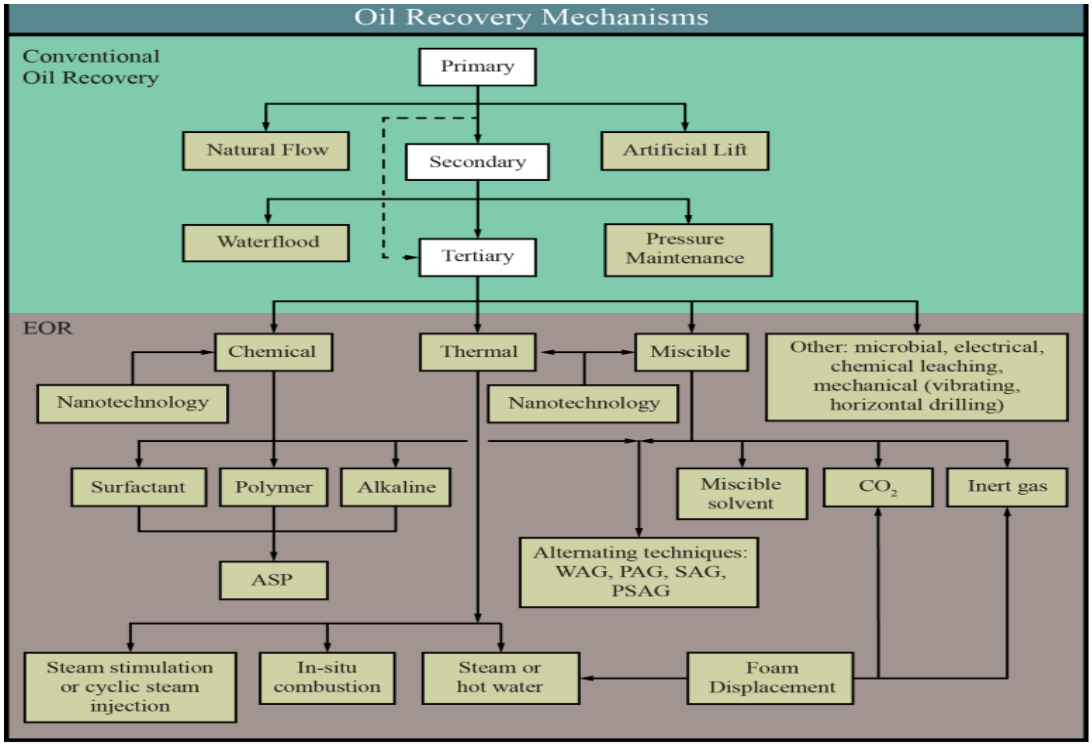


Figure 2.1. Diagram illustrating the steps of extraction of oil and the various strategies utilized in enhanced oil recovery ( Energy, 2019).

**Primary Recovery:** The initial oil production phase relies on the natural energy available within a reservoir to transport oil to the extraction wells. This can involve various natural energy mechanisms such as solution gas drive, gas-cap drive, natural water drive, fluid and rock expansion, and gravity drainage. It is important to note that the classification system does not address the methods used to lift the oil to the surface once it has entered the wellbore.

**Secondary Recovery:** The second phase of oil recovery typically begins when initial production declines. Common methods of conventional secondary recovery include waterflooding, gas injection, and pressure stabilization. This stage, known as secondary recovery, involves enhancing natural energy by injecting gas or water to facilitate the movement of oil towards the production wells. In this process, gas can be introduced into a gas cap to stabilize pressure and expand the gas cap, or it may be injected into an oil-column well for an immiscible process, based on factors like volumetric sweep efficiency and relative permeability. The immiscible gas injection process involves the introduction of gases, such as nitrogen or carbon dioxide, into an oil reservoir at pressures that are below the minimum miscibility pressure (MMP). In this scenario, the gas does not fully blend with the oil, remaining in a separate phase. This method serves multiple purposes: it helps to uphold reservoir pressure, pushes oil toward extraction wells, and induces a slight swelling of the oil, increasing its volume and facilitating easier recovery. While the gas doesn't completely mix with the oil, it can still help vaporize some of the lighter hydrocarbon components, contributing to additional oil recovery. Overall, this technique is both cost-effective and enhances oil recovery, particularly when achieving miscibility is not an option.

**Tertiairy Recovery (EOR):** As secondary recovery methods begin to show diminishing returns, tertiary recovery techniques utilize thermal energy, chemical agents, and/or miscible gases to extract additional oil. In some instances, these tertiary processes may serve as a secondary operation. The decision to implement such methods can depend on various factors, including the specific characteristics of the tertiary process, the availability of injections, and economic considerations. For example, it may be more advantageous to bypass the secondary recovery phase if waterflooding could ultimately compromise the effectiveness of subsequent tertiary recovery efforts. These considerations have led to the increased usage of the term "Enhanced Oil Recovery" (EOR) in the field of petroleum engineering, while "tertiary recovery" has become less commonly used. EOR represents a more holistic strategy for managing oil reservoirs, focusing on maximizing oil extraction from existing deposits (Wang et al., 2017).

## EOR Classification

Tertiary recovery methods aim to extract the oil that remains in the reservoir after the completion of secondary recovery techniques. Essentially, these procedures focus on addressing the residual oil saturation that persists following secondary recovery efforts. Enhanced Oil Recovery (EOR) encompasses four primary techniques: thermal methods, miscible processes, chemical treatments, and additional approaches such as microbial EOR.

**Thermal EOR**: Thermal-enhanced oil recovery methods are employed to elevate the temperature of oil, thereby reducing its viscosity through the introduction of heat into the reservoir. These techniques are primarily applicable to heavy, viscous crude oils. The most commonly utilized thermal recovery methods include in-situ combustion and steam injection. Among steam injection techniques, steam flooding, steam-assisted gravity drainage (SAGD), and cyclic steam stimulation (often referred to as huff and puff) stand out as popular approaches.

When steam flooding occurs, the fluids are pushed toward production wells that are positioned strategically by the injection of steam through specific injection wells. SAGD employs a different strategy, involving the heating of the reservoir through a series of parallel horizontal wells. Conversely, cyclic steam stimulation is a method that focuses on a single well, where steam is injected for a designated duration to enhance oil extraction.

Moreover, in-situ combustion entails injecting air or oxygen into the reservoir, where it combines with oil to produce heat, further reducing its viscosity and facilitating its flow to the production wells. Overall, these thermal techniques harness heat energy to enhance oil mobility, thereby improving recovery rates from challenging reservoirs.

**Chemical EOR:** Introducing specific chemicals into a reservoir to improve oil recovery can alter the properties of the surrounding rock (Malozyomov et al., 2023). The primary aim of chemical flooding, commonly referred to as enhanced oil recovery (EOR), is to boost oil extraction through various methods. These methods include mobility control, which utilizes polymers to reduce the mobility of the injected water,

and the reduction of interfacial tension (IFT) through the application of surfactants and/or alkalis.

In the process of polymer flooding, a water-soluble polymer is introduced to enhance viscosity, thereby facilitating better mobility control during oil displacement. Another technique, known as surfactant flooding, involves injecting surfactants into the reservoir to lower the interfacial tension between oil and water, subsequently enhancing oil recovery. Alkaline flooding also contributes to oil displacement and emulsification by adjusting the reservoir's pH with alkaline substances (Ning et al., 2018). A variation of this method combines the injection of surfactants with alkaline chemicals to optimize the process, while also incorporating polymers for improved mobility control. This combined approach is referred to as an alkaline/surfactant/polymer (ASP) flood.

**Miscible Gas EOR:** Miscible gas processes refer to methods where the miscibility of in-situ oil and the injected fluid is primarily responsible for the oil displacement's effectiveness. Various gases and liquids can serve as effective miscible agents in both first-contact miscibility (FCM) and multiple contact miscibility (MCM) scenarios. Suitable options include low-molecular-weight hydrocarbons, hydrocarbon mixtures such as liquefied petroleum gases (LPGs), carbon dioxide ($CO_2$), nitrogen ($N_2$), and combinations of these substances. Miscible gas injection techniques utilize the distinct properties of gases to facilitate oil movement in order to enhance recovery rates from reservoirs (Wang et al., 2017). A particularly valuable method involves the injection of gases like $CO_2$, which can be effectively employed in both carbonate and sandstone formations containing oil reserves. This technique is anticipated to gain traction for two main reasons: its potential for sequestering a greenhouse gas and its ability to improve oil recovery through miscibility.

**Miscible Gas Process:** The main goal of a soluble process is to ensure that the fluid being injected effectively mixes with the oil at the interface where they meet. Since miscibility prevents direct contact between the oil and the displacing fluid, there are no capillary forces present when no interfaces exist. This procedure primarily involves two types: first contact miscibility (FCM) and multiple-contact miscibility (MCM).

**FCM**: Under specific pressure and temperature conditions in the reservoir, the injected fluid is fully miscible with the reservoir oil in a first-contact miscibility (FCM) process. This method is illustrated in figure 2.

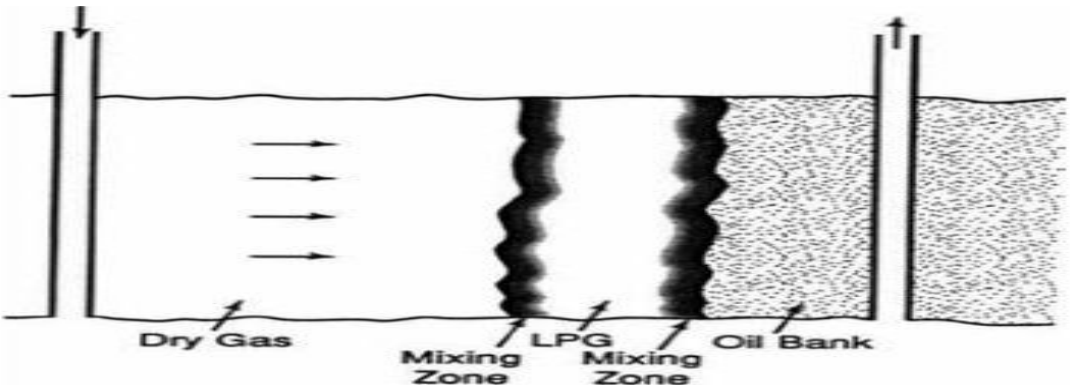


Figure 2.2. FCM process with LPG and dry gas (Willhite, 2018 ).

The FCM process involves the injection of a comparatively small slug of a hydrocarbon fluid, like liquefied petroleum gas (LPG), which serves to push the oil out. Typically, the size of the primary slug ranges from ten to fifteen percent of the pore volume (PV) (Chequer et al., 2019). Subsequently, a larger volume of a more economical gas with a higher methane concentration, commonly referred to as dry gas, is used to displace the liquefied petroleum gas slug. Additionally, water can be used as a secondary displacing solvent in some situations. The key to the effectiveness of this process lies in the miscibility between the oil phase and the primary slug, which facilitates the mobilization of oil droplets and helps to push them ahead of the primary slug, effectively reducing interactions between the two. Additionally, it is advantageous that the secondary displacing fluid (dry gas) and the primary slug are miscible; otherwise, there is a risk that as the process progresses, the main slug can get caught as a residual phase. Clark et al.(1958) outlined the fundamental requirements for both immiscibility and first-contact miscibility in this context.

**MCM:** The multiple-contact-miscible (MCM) process is an alternative approach to the conventional miscible process. With this approach, the fluid that was initially injected is immiscible with the reservoir oil. Instead, the process depends on the mass transfer of various components between the two phases within the reservoir, along with their interactions, to modify the composition of the injected fluid. Under

suitable conditions of pressure, temperature, and composition, this alteration can lead to the development of in situ miscibility between the displacing and displaced fluids. The MCM process can be categorized into two primary types: condensing gas displacements (which involve enriched gas) and vaporizing gas displacements (which use lean gas):

- **Vaporizing-Gas Displacement Process:** The fluid that is typically injected in this process is a lean gas, mainly composed of low-molecular-weight hydrocarbons, particularly methane, although it can include inert gases such as carbon dioxide and nitrogen on occasion. In order to achieve miscibility with the reservoir's existing oil, this procedure involves adjusting the injected gas's composition as it passes through the tank. Essentially, as the gas and oil come into contact, some of the oil's intermediate elements can vaporize into the gas, thereby enhancing the composition of the injected fluid. Under rights conditions, this enhancement can lead to the gas with the modified composition becoming miscible with the oil at specific locations within the reservoir, ultimately resulting in a miscible displacement. However, it is important to note that achieving this miscible condition requires a finite distance, resulting in a transitional zone within the multiple-contact-miscible displacement processes. Laboratory studies indicate that this distance is relatively minimal in reservoir terms (Negahban et al., 1990; Yellig, 1982). Throughout the vaporization process, there may be instances of liquid-phase dropout. The composition of the gas phase can vary between the injection site and the miscible front, as well as behind the front.
- **Condensing Gas Displacement Process:** In this scenario, the fluid being injected is not merely a dry gas; instead, it contains significant quantities of intermediate components, specifically those in the $C_2$ to $C_6$ range. For the process to be effective, these components must condense into the reservoir oil, thus altering its composition. Once this occurs, the injected fluid will mix with the modified oil. A transition zone exists that precedes the miscibility point in this idealized representation of the condensing-type process. This transition is driven by the injected gas moving downstream and continually partially condensing into the oil. The transition zone stabilizes once miscibility is attained. Similar to the behavior observed behind the front in the vaporizing-

gas process, which experiences some liquid condensation, the condensing-gas process shows a minor degree of vaporization occurring in the transition zone downstream of the miscibility point (Zick, 1986).

## Miscible $CO_2$ Flooding

Figure 3 illustrates the process of $CO_2$ miscible displacement, which entails the injection of a significant quantity of $CO_2$ to mobilize and recover the remaining oil from a reservoir. Under optimal conditions, this method can lead to a rapid attainment of miscibility within the reservoir. As this transition occurs, oil experiences swelling, and its viscosity decreases. While enhanced miscibility improves oil displacement and boosts sweep efficiency, the injection of $CO_2$ can also influence interfacial tension by diminishing the capillary forces that trap oil within the pore spaces after water flooding.

In contrast, immiscible $CO_2$ injection occurs when $CO_2$ does not fully mix with the oil, remaining as a distinct phase. This technique operates at pressures below the minimum miscibility pressure (MMP), preventing miscibility from being achieved. Although immiscible $CO_2$ injection lowers interfacial tension, it does not completely eliminate it, which continues to impede oil displacement. Consequently, this approach typically yields lower oil recovery efficiency compared to miscible injection because capillary forces are still at play.

In summary, miscible $CO_2$ injection is more effective for enhancing oil recovery due to complete mixing and the removal of interfacial tension, whereas immiscible $CO_2$ injection functions at reduced pressures and results in partial mixing and lower efficiency. Therefore, the amount of recoverable oil increases since the saturation of oil in a miscible state is less than that of the residual oil that remains (Menouar, 2013).

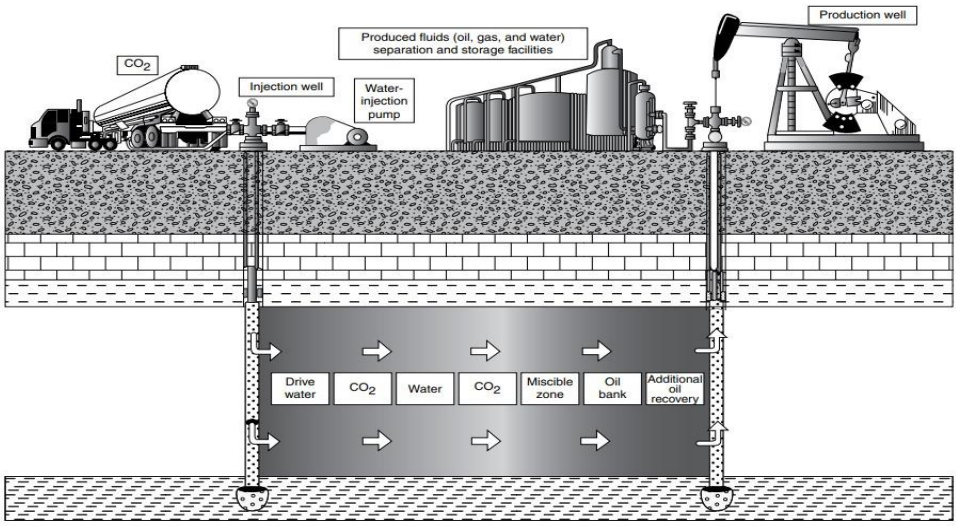


Figure 2.3. $CO_2$ miscible process (US DOE, 2018).

In the context of miscible $CO_2$ injection for enhanced oil recovery, miscibility is achieved once the injection pressure exceeds the MMP (Gao et al., 2013). Several factors that can influence both the MMP and the effectiveness of $CO_2$ injection include reservoir temperature and pressure, the purity of the $CO_2$, the oil composition, fluid properties, and operational conditions, as well as potential $CO_2$ leakage. To enhance oil recovery rates and optimize sweep efficiency, it is crucial for operators to understand the interactions and flow dynamics of these fluids within the reservoir accurately. Key determinants of $CO_2$ miscibility involve parameters such as pressure, residence time, and slug size, as well as the fluid characteristics including surface tension, density, viscosity, and purity (Kurdi et al., 2012; Choubineh et al., 2019; Bhatti et al., 2018). Various approaches, including analytical models and empirical correlations, are applied to estimate the MMP. However, acquiring physical measurements can be resource-intensive and expensive, while mathematical modeling may introduce significant errors in the estimated figures. For this study, the Winprop software is employed, utilizing empirical correlation techniques to evaluate the MMP during the $CO_2$ flooding process.

A simulation model was created by Nasir and Amiruddin (2008) to examine the fluid characteristics' sensitivity to the introduction of miscible $CO_2$. The effects of various fluid characteristics, including viscosity, formation volume factor, and the density of injected gas and oil, were examined for this aim. According to the data, the characteristics of the recovered oil and injected gas determine how well the miscible

$CO_2$ injection goes. Furthermore, the final recovery is far more affected by the formation volume factor than by the oil's density. Miscible $CO_2$ should ideally aid in oil mobility in a number of ways, such as improving microscopic efficiency, decreasing oil density, and lowering interfacial tension (IFT) when in the miscible form.

Al-Abri and Amin (2010) explored how relative permeability relates to interfacial tension and the efficiency of injection displacement in gas condensate reservoirs. To simulate actual reservoir conditions, they conducted experiments using sandstone cores in a high-pressure and high-temperature laboratory environment. The temperature was held at 95°C, and the displacement rate was maintained at 10 cm/h. Their research included displacement experiments at various pressure conditions: immiscible at 1100 and 1200 psi, near-miscible at 3000 psi, and miscible at 4500 and 5900 psi. The core flooding results revealed that pressure was the key factor influencing sweep efficiency. Under near-miscible conditions, only 23% recovery was achieved, whereas miscible flooding resulted in a maximum recovery of 32%, thanks to an improved mobility ratio and delayed gas breakout. The study also highlighted that the characteristics and the phase behavior between $CO_2$ and condensate played a crucial role in stabilizing the displacement front and enhancing recovery due to the interfacial tension effects during miscible displacement. Similarly, Han et al. (2014) investigated $CO_2$ injection under miscible conditions using a 2D vertical sandstone model with unstable gravity drainage. Upon achieving miscibility at 100% oil saturation with $CO_2$ injected from the bottom, they documented an increase in oil production (Bhatti et al., 2019).

In a study conducted by Abbasi et al. (2010), core samples from an Iranian reservoir were subjected to an experimental analysis where they were injected with varying amounts of $CO_2$ and $N_2$ gas. The findings revealed that as the injection pressure approached the conditions for miscibility, there was a noticeable increase in the recovery factor. It was observed that the minimal miscibility pressure (MMP) decreased with an increase in the percentage of $CO_2$, indicating that higher $CO_2$ concentrations facilitate the attainment of miscible conditions (Abbasi et al., 2010).

Additionally, Fath and Pouranfard (2013) explored several scenarios of natural reservoir depletion in one of Iran's oil fields. Utilizing a model consisting of 600 grid

blocks, they simulated the behavior of a slim tube at different pressures to determine the MMP. Their results showed that for $CO_2$ injection, the MMP was approximately 4630 psi (Zene et al., 2019). The simulations indicated that optimal results were 17,000 Mscf/day and 30,000 Mscf/day for the immiscible and miscible injection respectively (Khan et al., 2003). After 20 years of total oil production, the immiscible injection shows a recovery factor of 34.5%, while for miscible injection, it was slightly higher at 36.6%. These results highlighted the greater feasibility of miscible injections, although achieving miscibility in heavy oil reservoirs proved to be challenging at certain points.

A 400 MHz NMR micro-imaging device was used by Yuechao et al. (2011) to investigate the injection of $CO_2$ into a sand pack. They discovered that the differences in viscosity and density between oil and $CO_2$ led to the phenomenon of $CO_2$ fingering during immiscible $CO_2$ displacement. Consequently, 53% of the oil remained in the sand pack. The study indicated that the sweep efficiency for miscible $CO_2$ flooding was significantly better. Notably, the $CO_2$ exhibited low density and viscosity, with a constant flow rate. In contrast to the immiscible injection method, which left 34% of the sand pack containing oil, the findings suggest that miscible injection techniques can significantly enhance oil recovery rates.

## $CO_2$ Enhanced Oil Recovery and Sequestration

As conventional oil reserves become increasingly depleted, the method of carbon dioxide-enhanced oil recovery ($CO_2$-EOR) has gained significant interest. This technique not only aids in extracting additional oil but also plays a vital role in mitigating global greenhouse gas emissions by sequestering $CO_2$ deep within geological formations (Kabir et al., 2023). Over the years, the oil industry has effectively utilized this technology, particularly for recovering oil from reservoirs that are approaching their maturity phase. Typically, $CO_2$ is injected using a continuous flooding method, however, the presence of impurities such as nitrogen ($N_2$) in the $CO_2$ can pose challenges, including reduced mobility, viscous fingering, and premature $CO_2$ breakout, particularly in heterogeneous reservoirs. To improve $CO_2$ mobility and enhance oil recovery rates, it is beneficial to adjust the injection strategies. Rezk et al.

(2019) highlight that in addition to aiding in oil recovery, $CO_2$ can also be stored efficiently within reservoirs.

As noted by Rackley (2010), the concentration of carbon dioxide ($CO_2$) in the atmosphere has significantly increased, rising from 280 parts per million in 1750 to 368 parts per million by the year 2000, and reaching 388 parts per million in 2010. Wang et al. (2011) projected that China's annual $CO_2$ emissions would escalate from 5.1 billion tonnes in 2005 to 8.6 billion tonnes by 2020. This represents an average annual increase in emissions of approximately 4.5%. The primary driver behind the rising levels of $CO_2$ is global energy consumption, which is closely linked to climate change and environmental degradation. Hassan et al. (2019) indicate that injecting $CO_2$ is among the most efficient strategies for enhancing recovery rates. Furthermore, $CO_2$ that has been combined with oil can be separated and re-injected, offering a storage solution that can significantly reduce greenhouse gas emissions (McLaughlin, 2016). In addition, studies conducted by Wells et al. (2007), Özkilic and Gumrah (2009), and Yang et al. (2010) propose that depleted or mature oil and gas fields with permeable and porous reservoirs may be suitable locations for $CO_2$ storage.

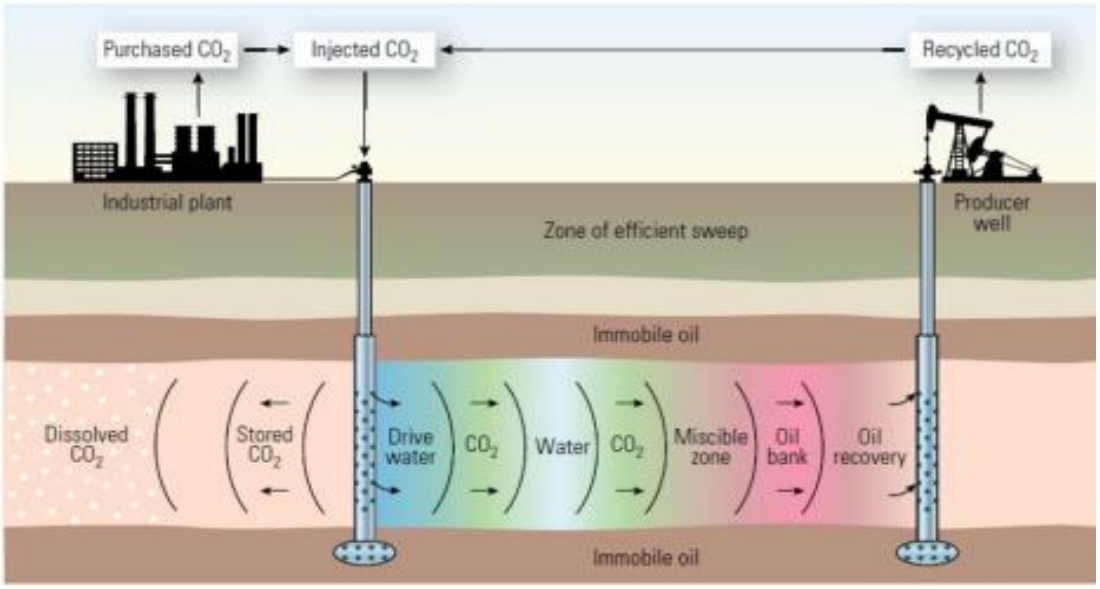


Figure 2.4. $CO_2$ utilization and sequestration (Aroher and Archer, 2010).

**Theoritical Framework**

In our thesis, we will establish a theoretical framework that encompasses all pertinent theories and literature related to our research topic, particularly in relation to CMG software workflows.

**Reservoir Simulation:** The movement and interaction of fluids (oil, water, $N_2$, and $CO_2$) within the reservoir rock are simulated by a reservoir simulation model, which is a mathematical depiction of a subsurface reservoir. To forecast the reservoir's behavior under different circumstances, the model takes into account fluid, geological, and petrophysical characteristics. A simulation model is a simplified representation of a real system that exhibits the key characteristics of the real system or performs aspects that are comparable to it (Jitendra Sangwai & Dandekar, 2022). These computations may be numerical or analytical. By "analytical," we mean that the model's equations could be resolved by mathematical methods similar to those applied to algebraic or differential problems. Analytical solutions are typically defined using "well-known" equations or functions ($x^2$, sin x, $e^x$, etc.) (Heriot-Watt, 1997). A reservoir simulation model serves a variety of functions, such as:

- Production Forecasting: Models aid in the long-term prediction of fluid distributions, reservoir pressure variations, and future rates of oil and gas production.
- Improving Recovery: They support the optimization of recovery strategies, such as $CO_2$ injection and other enhanced oil recovery (EOR) approaches.
- Risk assessment: Models can detect possible risks and uncertainties related to reservoir management by simulating various scenarios.

We have different types of models including:

- Mathematical Model: By Aziz et al. (1979), a suitable set of mathematical equations must be used to express the physical system to be described. Many assumptions are formed during this procedure. For practical reasons, it is necessary to make assumptions to stabilize the situation. For example, we are forced to use the relative permeability concept even though all reservoir engineers are aware of its shortcomings.

- Numerical Model: The reservoir's mathematical model's equations are nearly always intractable using analytical techniques. Approximations must be made to describe the equations in a fashion that digital computers can solve. This type of equational set produces a numerical model (Sangwai et al.,2022).
- Computer Model: A computer model of the reservoir is a computer program or collection of algorithms created to solve the equations of the numerical model (Sangwai et al.,2022).

**GEM Simulator:** GEM is a sophisticated compositional simulator designed by the Computer Modeling Group (CMG) that serves the needs of reservoir simulation and petroleum engineering. This simulator features advanced capabilities such as dual porosity modeling, the ability to handle miscible gas interactions, and intricate phase behavior, which collectively enable engineers to analyze fluid dynamics within reservoirs. GEM makes use of established equations of state, including Peng-Robinson and Soave-Redlich-Kwong, to accurately predict the behavior and properties of different phases. Additionally, it applies the quasi-Newton successive substitution method for its nonlinear calculations. The comprehensive input and output data provided by the simulator allow engineers to effectively refine field development strategies and enhance recovery plans.

## Related Research

Nitrogen ($N_2$) presents an intriguing alternative to carbon dioxide in various applications, particularly in enhanced oil recovery (EOR). Its abundance comprising around 78% of the atmosphere makes it a cost-effective option that is also less corrosive than carbon dioxide (Sheng and Soliman, 2013). However, while nitrogen has potential advantages, its utilization has not reached the same level as $CO_2$ due to specific physicochemical properties. Notably, nitrogen's lower solubility in crude oil complicates its effectiveness in reducing oil viscosity and interfacial tension benefits that carbon dioxide provides more readily.

Prior research illustrates the solubility advantages of carbon dioxide over other gases. For instance, Beecher and Parkhurst (1926) demonstrated that carbon dioxide has significantly greater solubility on a molar basis in 30.2° API oil compared to

natural gas and air. Similarly, Nguyen and Ali (1998) reinforced that carbon dioxide is the most soluble gas in bitumen when compared to methane and nitrogen.

Numerous experimental studies and successful field cases worldwide have showcased nitrogen's potential as an injection gas for enhancing oil recovery. Simulation studies suggest that nitrogen can be effectively employed in regions like Trinidad (Sinanan and Budri, 2012) and southeastern assets (Belhaj et al., 2013). However, it is important to note that the minimum miscibility pressure (MMP) of nitrogen is generally higher than the fracture pressure of the reservoirs, indicating that nitrogen is more suitable for applications at lower pressures where immiscible displacement methods are preferred (Tileuberdi & Gussenov, 2024).

In their exploration of various EOR techniques, Joslin et al. (2017) found that nitrogen flooding is particularly effective for pressure maintenance in reservoirs with permeability lower than 0.03 mD. While there has been significant investigation into nitrogen injection in tight oil reservoirs, research into the feasibility and mechanisms of simultaneous $CO_2/N_2$ injection remains somewhat limited and merits further study.

The work by Fong et al. (2016) highlighted both opportunities and challenges when utilizing nitrogen during vertical core flooding with 21° API oil. Their findings revealed that using flue gas with approximately 80% nitrogen and 20% carbon dioxide led to earlier gas breakthroughs compared to pure $CO_2$ scenarios. This resulted in a recovery of only 23% of oil initially in place (OOIP) with the nitrogen-enriched mixture, while pure $CO_2$ yielded 56% recovery. These insights underline the importance of evaluating optimal gas compositions for enhanced recovery.

Recent research by Lansangan and Smith (2017) on the diffusion characteristics of a 10% nitrogen and 90% carbon dioxide mixture in oil indicated that nitrogen presence decreases the diffusion rate of carbon dioxide by forming a stagnant phase. This phenomenon reduces the interfacial equilibrium concentration of carbon dioxide, hindering mass transfer rates even at lower nitrogen concentrations.

Furthermore, Holm and Josendal (2019) indicated that carbon dioxide alone does not completely displace methane when in contact with oil, while Monger (2019) identified that nitrogen's presence negatively impacts carbon dioxide solubility in oil, unlike sulfur dioxide, which might enhance it.

In a study conducted by Spivak and Chima (2019) on an 82% carbon dioxide and 18% nitrogen mixture, it was found that only a small portion of nitrogen was soluble in Wilmington oil under specific conditions. This reduced the viscosity reduction effectiveness due to diminished carbon dioxide solubility in the presence of nitrogen. Their work also noted earlier gas breakthroughs, lower recovery rates, and a more dispersed compositional front compared to pure carbon dioxide, illustrating the need for continued investigation into the impacts of nitrogen on oil recovery dynamics.

Additionally, Siregar et al. (2020) conducted laboratory experiments assessing nitrogen injection, which revealed that while nitrogen flooding did not lead to substantial increases in oil recovery, other studies indicated that it could yield stable and relatively high production rates. Moreover, Nguyen and Ali (1998) observed that substituting pure carbon dioxide for impure carbon dioxide during the water-alternating-gas (WAG) process adversely affected oil recovery, with higher nitrogen concentrations resulting in losses of up to 10% in recovery rates.

In conclusion, while nitrogen presents distinct advantages as an injection gas for enhanced oil recovery, further research is essential to understand its behavior, optimize its use in conjunction with carbon dioxide, and fully harness its potential in mitigating environmental impacts and improving recovery efficiencies.

**Location of the Study Area**

The Ghawar oil field located in the Al Ahsa Governorate of Saudi Arabia's Eastern Province, stands as the world's largest conventional oil field. With dimensions of approximately 280 kilometers by 30 kilometers (or about 8,400 square kilometers), Ghawar accounted for nearly one-third of Saudi Arabia's total oil output as of 2018 (Simmons, 2013). Exclusively owned and operated by Saudi Aramco, the state-run oil company, the field stretches approximately 280 kilometers in length, is 30 kilometers wide, and has a thickness of about 90 meters. It is situated on the southern part of the En Nala anticline and is composed of six production regions, arranged from north to south: Fazran, Ain Dar, Shedgum, Uthmaniyah, Haradh, and Hawiyah.

Production at Ghawar began in 1951, following the field's discovery by Saudi Aramco in 1948. The record for the highest daily oil production from a single field

occurred in 1981, reaching 5.7 million barrels per day. While the southern areas, Hawiyah and Haradh, were still undergoing development, overall production began to decline for economic reasons after 1981. As of 2019, the Ghawar field had an estimated production capacity of 3.8 million barrels per day, with remaining proven oil reserves estimated at 58.3 billion barrels of oil equivalent (Gbbl). Our thesis will specifically concentrate on the Arab-D reservoir located in the Ain Dar region (Fink, 2015).

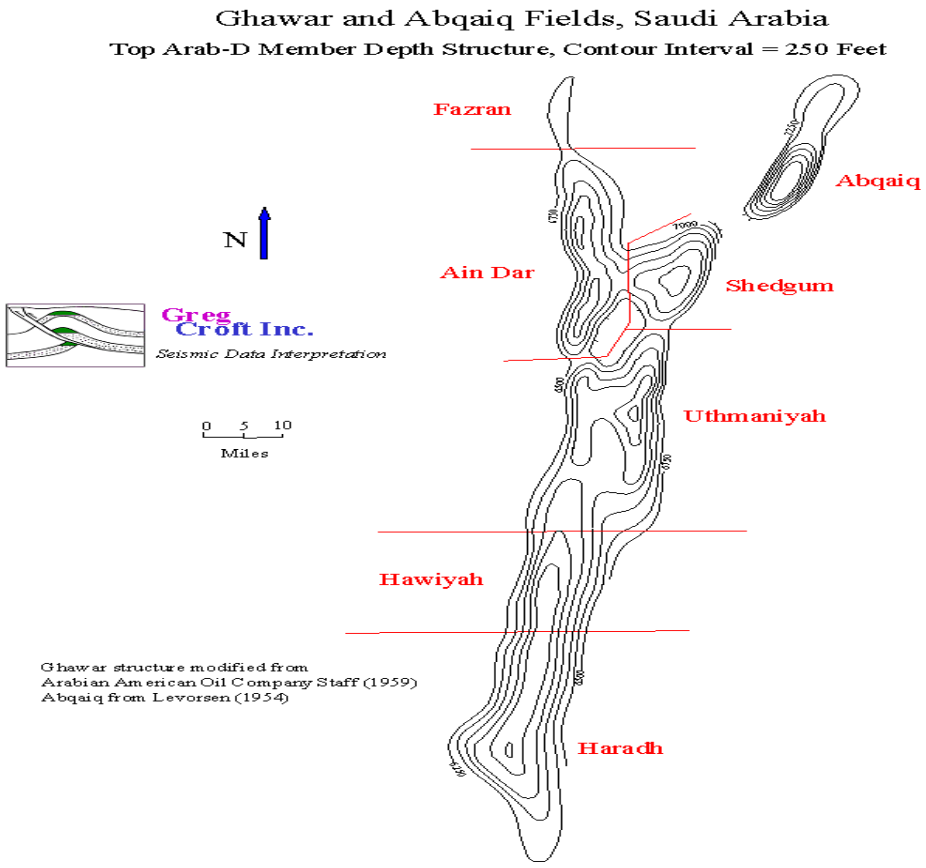


Figure 2.5. Ghawar oil field's map (Saudi Arabia, 2005)

**Geological Background:** The development of oil reservoirs occurs during the late jurassic to early cretaceous periods, with the Arab-D reservoir serving as the primary source of oil extraction from Ghawar. This reservoir consists predominantly of dolomite, comprising approximately 75% of the upper jurassic dolomites and carbonate formations. It is important to note that dolomites and limestones possess distinct reservoir characteristics, largely due to the processes involved in the diagenesis

of limestone. The Arab-D reservoir is capped by the upper jurassic hith anhydrite, which acts as a seal, effectively preventing vertical migration of oil by trapping vapors of the Arab C-D anhydrite above it (Sultan et al., 2019). The Arab-D reservoir is the source of all the oil produced at Ghawar. Dolomite makes up about 75% of the upper jurassic dolomites and carbonate rocks that make up the Arab-D reservoir. Dolomites and limestones have fundamentally different reservoir properties since these rocks are typically generated during the diagenesis of limestones. Upper jurassic anhydrite, known as hith anhydrite, covers the Arab-D reservoir, sealing it with vapors of Arab C-D anhydrite and preventing oil from migrating vertically (Sultan et al., 2019).

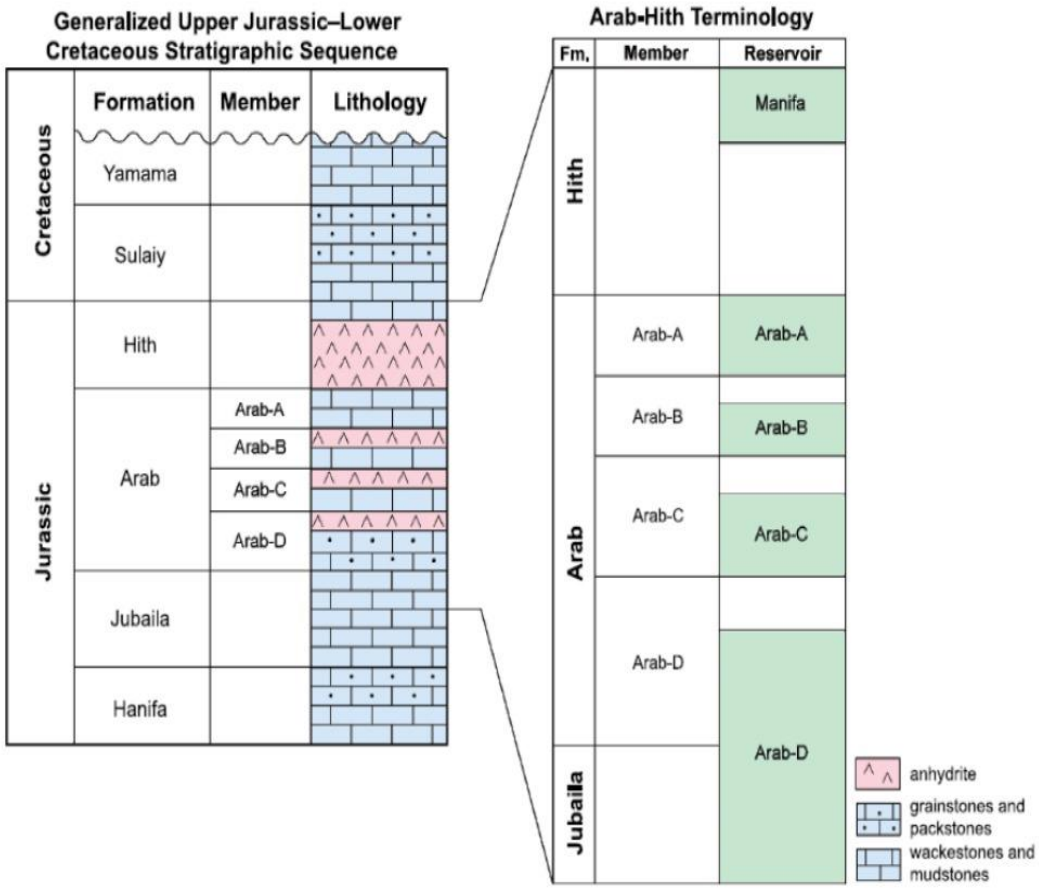


Figure 2.6. General different geological layers, showing in detail the Arab-Hith layers and the location of the simulated Arab-D (Hamimi et al., 2021)

The Arab-D dolomite formation within the Ghawar oil field is responsible for the creation of super-k zones, characterized by exceptionally high permeability. Areas such as Ain Dar qualify as super-k when they exhibit flow rates exceeding 500 barrels per day per vertical foot. The dolomite found in these locales features significant inter-crystalline and moldic porosity. When various porous varieties are combined, flow and

recovery rates are enhanced. Nevertheless, these super-K areas also present challenges; notably, the wells in these areas demonstrate substantial water flow during secondary recovery processes. Furthermore, the quality of the reservoir diminishes from north to south within Ghawar due to lower porosity and permeability in the southern sections. Additionally, the oil found in the southern region tends to have higher density and sulfur content compared to that in the north, leading to a noticeable decrease in oil quality. The Arab-D dolomite of Ghawar is the cause of super-k or extremely high permeability zones. Additionally, compared to oil in the northern region, the density and sulfur content of the oil in the southern region are higher, resulting in a decline in oil quality (Simmons, 2013).

This thesis investigates the enhanced oil recovery process, focusing on the injection of miscible $CO_2$ combined with $N_2$ into the Arab-D reservoir located in the Ghawar oil field through the use of CMG GEM simulation software.

# CHAPTER III
# Methodology

This project employed a compositional simulation modeling approach utilizing CMG-GEM software, specifically designed to simulate composition reservoirs and understand the intricate interactions among various chemical components. This chapter outlines the simulation process of miscible carbon dioxide ($CO_2$) for the Arab-D reservoir, focusing initially on the setup and completion of both production and injection wells. The chapter then elaborates on the reservoir fluid PVT data and the Equation-of-State (EOS) modeling methods implemented in Winprop. Additionally, the minimum miscibility pressure (MMP) between $CO_2$ and the reservoir oil was calculated through the EOS approach. Ultimately, the analysis includes various scenarios of miscible carbon dioxide ($CO_2$) injection, nitrogen ($N_2$) injection, and primary production to identify the optimal strategy for enhancing oil recovery and production.

## Research Design

This research utilizes a comparative design to evaluate the effectiveness of different injection scenarios of carbon dioxide and nitrogen, aiming to determine the most efficient method. The GEM compositional simulator possesses distinct advantages over IMEX and STARS, particularly in modeling the complex interactions among chemical components. GEM provides flexibility in representing a diverse range of components and phases, and it can accurately model advanced processes, including fluid mixing, chemical reactions, and phase changes. In contrast, IMEX prioritizes simplicity and quick execution for black oil reservoirs, while STARS is proficient in thermal simulations but falls short in accurately modeling chemical interactions. Consequently, GEM is recognized for its capability to deliver a thorough and precise understanding of reservoir dynamics, which is critical for enhanced oil recovery efforts (Agarwal & Liu, 2024).

Using the CMG-GEM compositional reservoir simulator, a three-dimensional (3D) vertical reservoir was constructed. The model comprises 25 grid cells in the x-

direction, 20 in the y-direction, and 6 in the z-direction. The CMG-GEM software facilitated various simulation analyses, including:

- Reservoir Data
- Components
- Rock Fluid Characteristics
- Initial Conditions
- Numerical Data
- Tracer Data
- Well and Recurrent Data

**Population of Study/Sample**

The study sample was drawn from a reference article titled "Ghawar Oil Field," which was obtained from the Saudi Arabian Oil Company's Global Medium Term Note Programme (Wald, 2018).

**Data Collection Tools / Methods and Materials**

The primary tool utilized in this study is CMG GEM, which facilitated the development of the simulation model. Numerous iterations were executed through trial and error to identify optimal outcomes. Additionally, Winprop was employed to ascertain the minimum miscibility pressure. To accurately characterize the reservoir fluid sample, the black oil PVT state-based equation was applied. This step is crucial, as incorporating a realistic physical model of the fluid sample into the model is essential before conducting reservoir simulations. Data on compositional characteristics were collected and analyzed in depth to investigate the efficacy of miscible CO2 flooding. An equation of state (EOS) was developed based on information from a traditional pressure-volume-temperature (PVT) study. This study included estimations of fluid properties, two-stage flash experiments, compositional evaluations, differential liberation tests, and separator analyses.

**Reservoir Conditions and Fluid Properties**

The reservoir model was established using a cartesian grid measuring 25×20×6, resulting in 3,000 grid cells. The hydrocarbon-bearing reservoir spans 14062500 square feet, with I-block and J-block dimensions of 3,750 ft and 3,000 ft, respectively. The model incorporates four production wells (P) and a single injection well (I1), where $CO_2$ and $N_2$ are injected under various operational sequences and constraints. This setup is categorized as a standard cuboidal grid model, featuring a five-spot well configuration as depicted in figure 7.

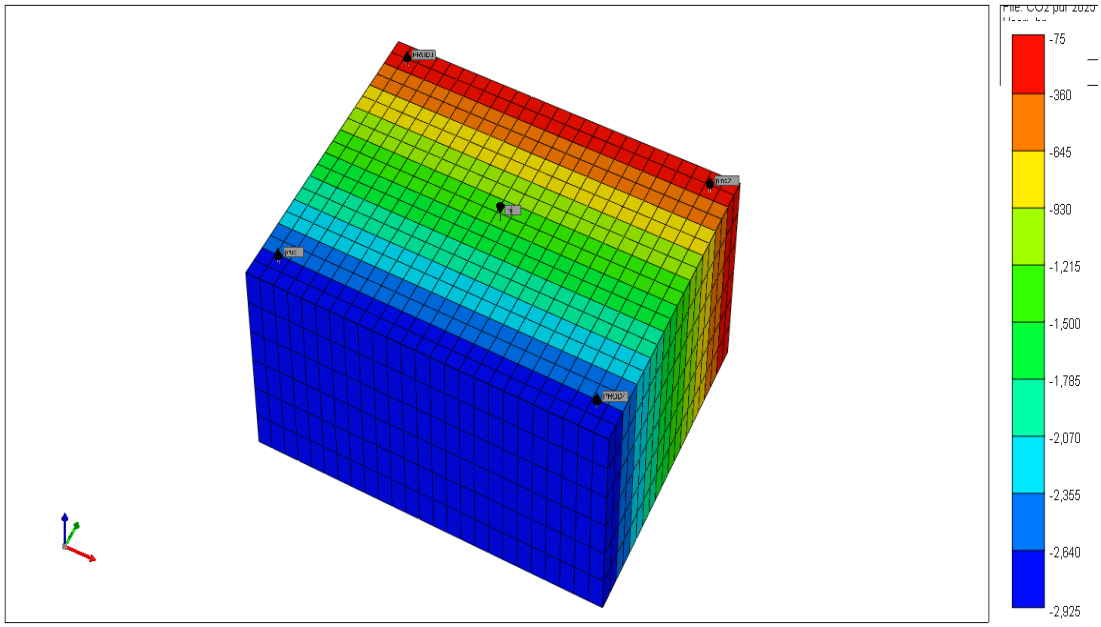


Figure 3.1. Reservoir model (CMG Builder, 2021).

Statistics for the Ain Dar field's Arab-D reservoir fluid indicate an initial gas-to-oil ratio (GOR) of 550 SCF/BBL, an average API gravity of 35°API, a reservoir temperature of 215°F and a bubble point pressure of 1,920 psi. The Arab-D formation within the Ain Dar Field exhibits a formation volume factor of approximately 1.34 RB/STB and depths ranging from 5,500 to 6,500 feet. For this study, the formation depth selected is 6,100 feet, resulting in an initial reservoir pressure of 3,212 psi, with an initial water saturation of 0.11.

Table 3.1. General reservoir conditions and fluid properties (Saudi Arabia, 2005)

| **Properties** | **Values** |
|---|---|
| Reservoir temperature (°F) | 215 |

| | |
|---|---|
| Bubble point pressure (psi) | 1920 |
| Solution gas oil ratio (SCF/BBL) | 550 |
| API gravity (ºAPI) | 35 |
| Depth (ft) | 6100 |
| Oil viscosity (cp) | 0.62 |
| Initial reservoir pressure (psi) | 3212 |
| Initial water saturation (%) | 11 |
| Formation volume factor (RB/STB) | 1.34 |
| Permeability (mD) | 617 |
| Porosity (%) | 19 |
| Injection rate ($ft^3$ /day) | 100000 |

**Compositional Model**

Black-oil models, which are often foundational for many reservoir simulations, illustrate how the properties of reservoir fluids fluctuate with variations in temperature and pressure. While these models may suffice for traditional recovery techniques like primary recovery and waterflooding, they are inadequate for enhanced oil recovery (EOR) methods such as miscible gas injection, where fluid composition also plays a significant role in influencing properties. EOS-based methodologies are widely adopted in compositional simulations to depict the phase behavior of reservoir fluids numerically. Each component of an EOS model necessitates critical parameters, including critical temperature, critical pressure, and acentric factors. Including every reservoir component in the compositional model is often impractical due to challenges in quantifying molar fractions and the extensive computational time required for individual simulations. Consequently, components are frequently aggregated into a limited number of pseudo-components to mitigate simulation complexity. To forecast the MMP and the phase behavior of $CO_2$/$N_2$/oil interactions, the Winprop software is employed to replicate fluid behavior through the following steps:

- Data collection
- Uploading compositional data into WinProp software
- Exporting the developed EOS model for use in reservoir simulation

For effective EOS-based compositional modeling, accurate EOS modeling is essential. In the petroleum industry, four common cubic equations of state (EOS) are employed:

- Van der Waals EOS (Johannes Diderik, 1873)
- Soave-Redlich-Kwong (SRK) EOS (Soave, 1972)
- Peng-Robinson (PR) EOS (Peng & Robinson, 1976)
- Modified Peng-Robinson (PR78) EOS (Peng & Robinson, 1978)

When employing volume translation, both the Peng-Robinson (PR) and Soave-Redlich-Kwong (SRK) equations of state (EOS) yield comparable predictions for vapor-liquid equilibrium (VLE), as well as accurate estimates for the volumes and densities of vapor and liquid phases. This makes them widely used in the oil and gas sector (Whitson, 2000). In this study, the decision to adopt the PR EOS for fluid modeling was largely based on the acentric factor, which suggests that the acentric factors of the reservoir oil are greater than 0.5. Consequently, we will use the PR EOS to assess gas/oil miscibility and to analyze the phase behavior of the oil reservoir.

**PR EOS Development and Modeling:** In reservoir engineering, the equation of State (EOS) is a fundamental approach for defining the properties of reservoir fluids and understanding their phase behavior. To accurately simulate the characteristics of miscible $CO_2$ within a reservoir, it is crucial to mathematically represent these fluid properties. The Peng–Robinson EOS, established by Peng and Robinson in 1976, is widely recognized as the standard in compositional reservoir simulations. This research utilizes the Peng-Robinson EOS to effectively model the fluid properties and phase behavior of the reservoir. The mathematical representation of the Peng-Robinson cubic EOS is detailed in equation 1:

$$P = \frac{RT}{v-b} + \frac{a}{v(v+b)+b(v-b)} \quad (1)$$

Where:

T = temperature, $^{0}R$

v = specific volume, $\frac{ft}{mole}$

R = gas constant, $\frac{ft^3 * psia}{^{0}R * lb-mole}$

a = attraction parameter, $\frac{ft^6 * psi}{lb^2.mol^2}$

P = pressure, psi

b = repulsion parameter, $ft^3/mol$

The parameters associated with attraction, designated as "a" and repulsion referred to as "b," are defined at critical points and depend on both the critical temperature $(T_C)$ and critical pressure $(P_C)$. This relationship is detailed in equations 2 and 3:

$$b(T_C) = \Omega_b \frac{RT_c}{p_c} = 0.07780 \frac{RT_c}{p_c} \quad (2)$$

$$a(T_c) = \Omega_a \frac{R^2 T_c^2}{p_c} = 0.45724 \frac{R^2 T_c^2}{p_c} \quad (3)$$

With the constants $\Omega_b = 0.07780$ and $\Omega_a = 0.45724$

In regions that are not considered critical points, the parameters a and b can be determined using equations 4, 5, and 6, as presented below:

$$b(T) = b(T_c) \quad (4)$$

$$a(T) = b(T_c) * \alpha(T_r, \boldsymbol{\omega}) \quad (5)$$

$$\alpha(T_r, \omega) = 1 + (0.37464 + 1.54226\omega - 0.26992\omega^2)(1 - T_r^{0.5}) \quad (6)$$

Where:

$T_r$= the reduced temperature, $\frac{T}{T_c}$

Here, the acentric factor ω in equation 6 is specific to each pure component, similar to the critical temperature $T_c$ and critical pressure $P_c$. For mixtures, various mixing rules are recommended, as outlined in equations 7, 8, and 9:

$$b = \sum_j (y_j b_j) \quad (7)$$

$$a(T) = \sum_i \sum_j [y_i y_j a(T)_{ij}] \quad (8)$$

$$a(T)_{ij} = (1 - \delta_{ij})[a(T)_i a(T)_j] \quad (9)$$

Where:

$\delta_{ij}$ = binary interaction coefficient.

The impact of polar forces on the interactions among system components is incorporated through the binary interaction coefficient in equation 9, which is considered constant regardless of temperature and pressure variations. The parameters a and b from the Peng-Robinson equation of state (EOS) were selected for this study due to their widespread application in characterizing phase behaviors and the physical properties of reservoir fluids. To accurately model the EOS (Equation of State), a range of PVT (Pressure-Volume-Temperature) data is essential. Key parameters include gas-oil ratios, oil formation volume factors, relative oil volumes, and the viscosities of oil. These data points play a crucial role in the modeling process.

**Compositional Reservoir Simulation**: For the sake of simplification, we will disregard factors such as thermal variations, capillary effects, gravitational forces, and diffusion in the subsequent discussion. The foundational mass conservation equation for component i within the two-phase compositional framework is formulated as follows (Chen & Voskov, 2019):

$$\frac{\partial}{\partial t}(\phi \sum_{j=1}^{2} x_{i,j} \rho_j S_j) + \nabla . \sum_{j=1}^{2} x_{i,j} \rho_j \mathbf{u_j} + \sum_{j=1}^{2} x_{i,j} \rho_j q_j = 0 , \quad i = 1, .., N_c \quad (10)$$

Where:

$S_j$ = phase saturation, %

$\phi$= porosity of the reservoir, %

$N_c$= number of the components

$x_{i,j}$ = the mole fraction of component i in phase j

t = time, seconds (s)

$\rho_j$= molar phase density, $mol/m^3$

$q_j$= is the source or sink term of phase j, $\mathrm{mol/m^3.s}$

The Darcy velocity $\mathbf{u_j}$ is defined as follows (Chen & Voskov, 2019):

$$\mathbf{u_j} = -K\frac{k_{rj}}{\mu_j}.\nabla_p\,, \qquad j = 1,2\,, \tag{11}$$

Where :

$\mathbf{u_j}$ = darcy velocity, m/s

K= absolute permeability, $\mathrm{m^2}$

$k_{rj}$= relative permeability of phase j

$\mu_j$= viscosity of phase j, $P_a.s$

P= pressure, $P_a$

$\nabla_p$ = pressure gradient, $P_a/m$

Compositional reservoir simulators rely on the mass or molar balance equations applicable to each component present. Notably, the water equation remains consistent with the previously established black-oil formulation (E. Shtepani, 2007):

$$\nabla.\left(\frac{\lambda_w}{B_w}\nabla\Phi_w\right) + q_w = \frac{\partial}{\partial x}\left(\frac{\phi S_w}{B_w}\right) \tag{12}$$

Where:

$\lambda_w$= water mobility, darcy (D)

$B_w$= formation volume factor of water, RB/STB

$\nabla\Phi_w$= Gradient of potential for water, $P_a/m$

$q_w$= Source or sink term for water, $\mathrm{m^3/s}$

$S_w$= Water saturation, %

The hydrocarbon equation represents the movement of components i throughout both the oil and gas phases (E. Shtepani, 2007):

$$\nabla . \left(x_i \xi_o \lambda_o \nabla \Phi_o + y_i \xi_g \lambda_g \nabla \Phi_g\right) + q_i = \frac{\partial}{\partial t}[\phi\left(x_i \xi_o S_o + y_i \xi_g S_g\right)] \quad (13)$$

Where: $\lambda_p = kk_{rp}/\mu_p$ , $(p = o, g \text{ or } w)$

$\lambda_p$= phase mobility, darcy (D)

$\nabla\Phi_p$= gradient of potential for the phase, $P_a/m$

$\xi_p$= molar phase density, $mol/m^3$

$\nabla$= gradient operator, 1/m

$\lambda_p$= Mobility of the phase, $m^2/P_a/s$

$x_i$= mole fraction of component i in the oil phase

$S_p$= phase saturation

$y_i$ = mole fraction of component i in the gas phase

$\frac{\partial}{\partial t}$ = partial derivative with respect to time, 1/s.

**Determination of $CO_2$ Minimum Miscibility Pressure (MMP)**

Minimum miscibility pressure (MMP) is defined as the lowest pressure at which multiple contacts between carbon dioxide ($CO_2$) and oil can achieve miscibility, allowing the two fluids to blend in any proportion without creating an interface, forming a single phase that enhances oil recovery and supports an oil sweep efficiency of around 90% (Holm and Josendal, 1974). In the context of $CO_2$ flooding, understanding the minimum miscibility pressure is crucial for both the design and operation of the process.

The efficiency of fluid displacement in enhanced oil recovery is closely tied to the MMP. Accurately identifying this pressure enables operators to optimize injection

conditions and design surface facilities effectively. A reliable assessment of MMP is vital in commercial applications to determine the feasibility of achieving miscibility between gas and oil under specific reservoir conditions. As noted by Orr & Silva (1987), this critical parameter influences the effectiveness of gas in displacing oil and can be affected by several factors, including temperature, pressure and the fluid composition.

Given the variability of reservoir conditions and the characteristics of the fluids involved, MMP is not a static value; it fluctuates based on the composition of both the gas and the oil. Various empirical correlations exist for calculating MMP, as outlined in equations (14), (15), and (16):

- **Alston** (1985):

$$MMP_{CO_{2(pure)}} = 0.000878(1.8T_R + 32)^{1.06} M_{C_{5+}}^{1.78} \left(\frac{X_{vol}}{X_{int}}\right)^{0.136} \quad (14)$$

$$MMP_{CO_{2(impure)}} = MMP_{co2_{(pure)}} . F_{imp} \quad (15)$$

$$F_{imp} = \left(\frac{87.8}{T_{cm}}\right)^{1.935^{\left(\frac{87.8}{T_{cm}}\right)}} \quad (16)$$

Where:

$T_R$ refers to the temperature of the reservoir measured in degrees Fahrenheit (°F).
$M_{C_{5+}}$ denotes the molecular weight associated with the heavier fractions of fluids, $g.mol^{-1}$.
$X_{vol}$ indicates the mole fraction of volatile substances, including nitrogen ($N_2$) and methane ($CH_2$), $mol.mol^{-1}$.
$X_{int}$ represents the mole fraction of intermediate compounds, specifically those within the carbon range of $C_2$-$C_6$.
$T_{cm}$ is the weight-averaged pseudocritical temperature of the mixture, also expressed in degrees Fahrenheit (°F).

- **Glaso** (1980): Glaso undertook both correlational and experimental studies focused on oil reservoirs located in the North Sea. According to the findings by Chen et al. (2020), the study utilized established graphical relationships, which played a crucial role in forecasting minimum miscibility pressure (MMP). The study identified

two distinct types of correlations that were determined by the proportion of the intermediate compounds present.

For intermediate mole fractions of $C_2$-$C_6$ exceeding 18 mol, the MMP can be determined using the following formula:

$$MMP = 5.58657 - 0.02347739 \times M_{C_{7+}} + [1.1725 \times 10^{-11} \times (M_{C_{7+}})^{3.73} \times e^{786.8 * M_{C_{7+}} - 1.058}] \times (1.8T_R + 32) \quad (17)$$

Conversely, for mole fractions of $C_2$ to $C_6$ less than 18 mol, the MMP is given by:

$$MMP = 20.33 - 0.02347739 \times M_{C_{7+}} + [1.1725 \times 10^{-11} \times (M_{C_{7+}})^{3.73} \times e^{786.8 * M_{C_{7+}} - 1.058}] \times (1.8T_R + 32) - 0.836 \times F_R \quad (18)$$

$F_R$ indicates the mole percentage of intermediate components (%).

In our research, we employed compositional simulation techniques to ascertain the MMP. The PR EOS has shown to be highly effective for modeling reservoir fluids and is compatible with the CMG software, specifically Winprop, which facilitates the calculation of minimum miscibility pressure (MMP). Winprop utilizes three distinct methods to accurately assess MMP:

- **Multiple Mixing Cell** (Ahmadi & Johns, 2011): This method simulates a series of mixing cells where various proportions of oil and injected gas are mixed. By examining the phase behavior at different pressures and compositional variations within each cell, we can pinpoint the pressure at which the oil and gas become miscible. One key advantage of this approach is the comprehensive phase behavior data it yields, making it particularly effective for complex mixtures.

- **Tie Line** (Chen & Cheung, 1983): The Tie Line method employs a ternary diagram to visualize the equilibrium compositions of the oil and gas phases. Drawing a tie line on this diagram allows us to find the intersection with the phase envelope, which indicates the pressure at which miscibility occurs. This method is appreciated for its simplicity and speed, making it suitable for systems with clear phase behavior.

- **Cell-to-Cell Simulation** (Dipesh Niraula et al., 2024): This technique simulates the interactions between adjacent cells in a reservoir model. By assessing phase behavior at the interfaces of these cells under various pressure conditions, we

can ascertain miscibility. While this method offers a realistic depiction of reservoir dynamics and fluid flow, it demands considerable computational resources.

## Ternary Diagram

To determine phase equilibrium within a pressure-volume cell, we carry out calculations following several contacts between gas and oil. Research by Zick (1986), Johns et al. (1993), and Cook et al. (1969) suggest that multiple contacts may be required to generate phase equilibrium data, from which a pseudo-ternary diagram is created. According to Kanatbayev et al. (2015), both forward and backward contact processes can be analyzed at specific temperatures and compositions across a defined pressure range. Figure 8 illustrates a typical ternary diagram, which, as described, represents three components. The points on this diagram correspond to 100% composition of each constituent, typically including heavier compounds ($C_{7+}$) and intermediates ($C_2$-$C_6$), with the injection gas represented at the apex. The plait point, marked as point P, is where the dew and bubble point curves intersect, providing insights into composition enrichment conditions, as noted by Mihçakan et al. (1993). The ternary diagram displays several lines and points that convey critical information.

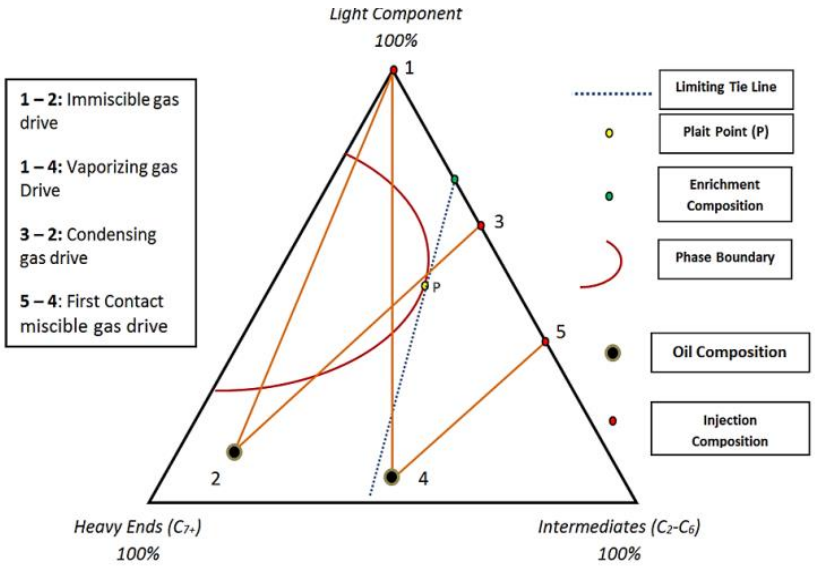


Figure 3.2. A typical representation of a ternary diagram (Adekunle, 2007).

The envelope depicted in the diagram outlines a two-phase zone, where the sample composition is illustrated as a single point. If any line crosses the two-phase envelope, it indicates immiscibility between gas and oil. On the other hand, if the lines stay outside the phase envelope, it implies complete miscibility between gas and oil.

**Reservoir Components**

To establish the pressure, volume, and temperature properties of the system, we identified ten components within the reservoir. Each component is characterized by its critical molecular weight, critical temperature, and critical pressure. The viscosities of these components, along with the densities of oil and water, were assessed using Winprop software.

Table 3.2. components properties (generated by CMG WINPROP, 2021).

| No. | Component | HC | Pc (Atm) | Tc (°K) | Acentric fact. | MW |
|---|---|---|---|---|---|---|
| 1 | $CO_2$ | 3 | 72.8 | 304.2 | 0.225 | 44.01 |
| 2 | $CH_4$ | 1 | 45.4 | 190.6 | 0.008 | 16.043 |
| 3 | $C_2H_6$ | 1 | 48.2 | 305.4 | 0.098 | 30.07 |
| 4 | $C_3H_8$ | 1 | 41.9 | 369.8 | 0.152 | 44.097 |
| 5 | $IC_4$ | 1 | 36 | 408.1 | 0.176 | 58.124 |
| 6 | $NC_4$ | 1 | 37.5 | 425.2 | 0.193 | 58.124 |
| 7 | $IC_5$ | 1 | 33.4 | 460.4 | 0.227 | 72.151 |
| 8 | $NC_5$ | 1 | 33.3 | 469.6 | 0.251 | 72.151 |
| 9 | $FC_6$ | 1 | 32.46 | 507.5 | 0.27504 | 86 |
| 10 | $C_{7+}$ | 1 | 15.284 | 723.823 | 0.6609 | 215 |

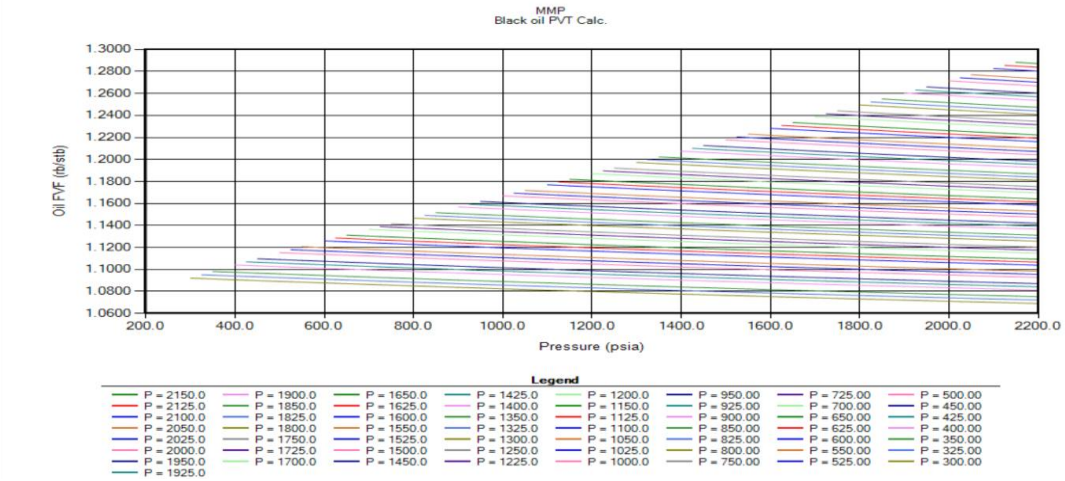


Figure 3.3. The relationship between the oil Formation Volume Factor (FVF) and pressure (CMG Builder, 2021).

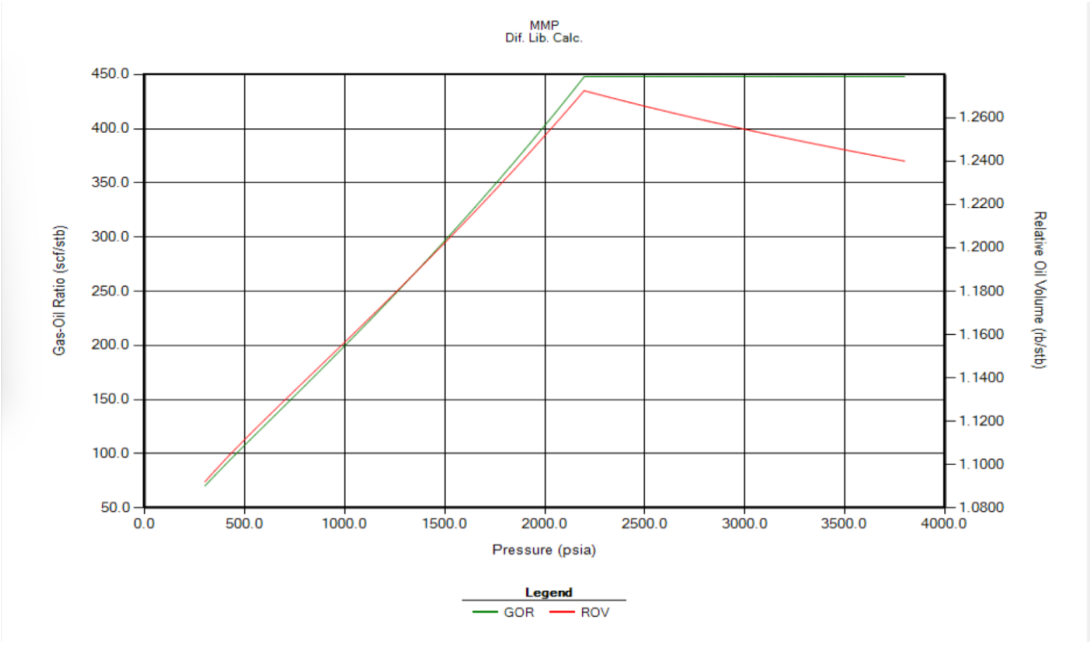


Figure 3.4. The correlation of Gas Oil Ratio (GOR) and Relative Oil Volume (ROV) with Pressure (CMG Builder, 2021).

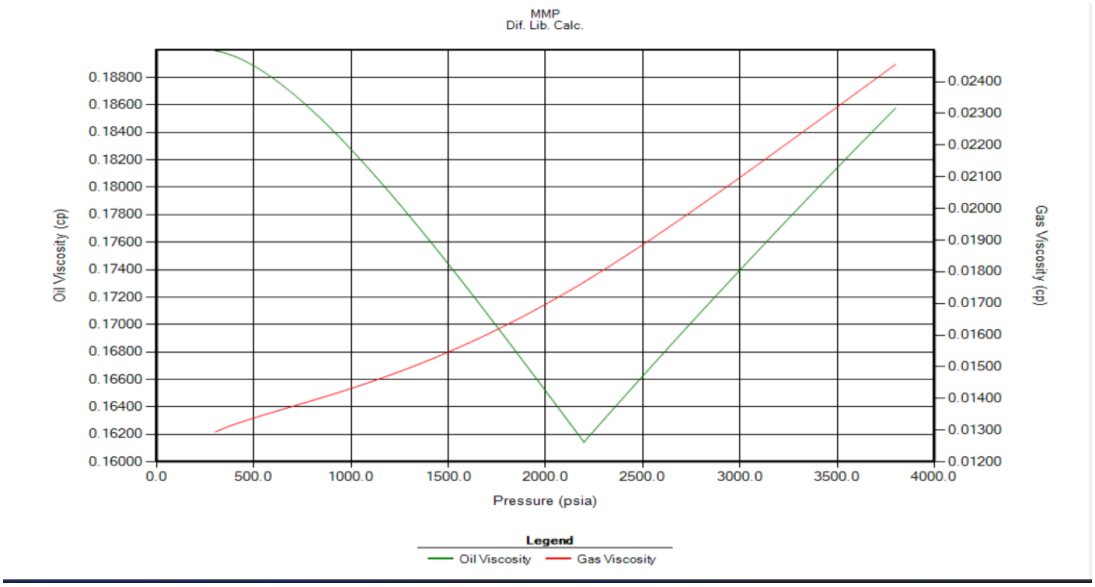


Figure 3.5. The dependence of oil and gas viscosity on pressure (CMG Builder, 2021).

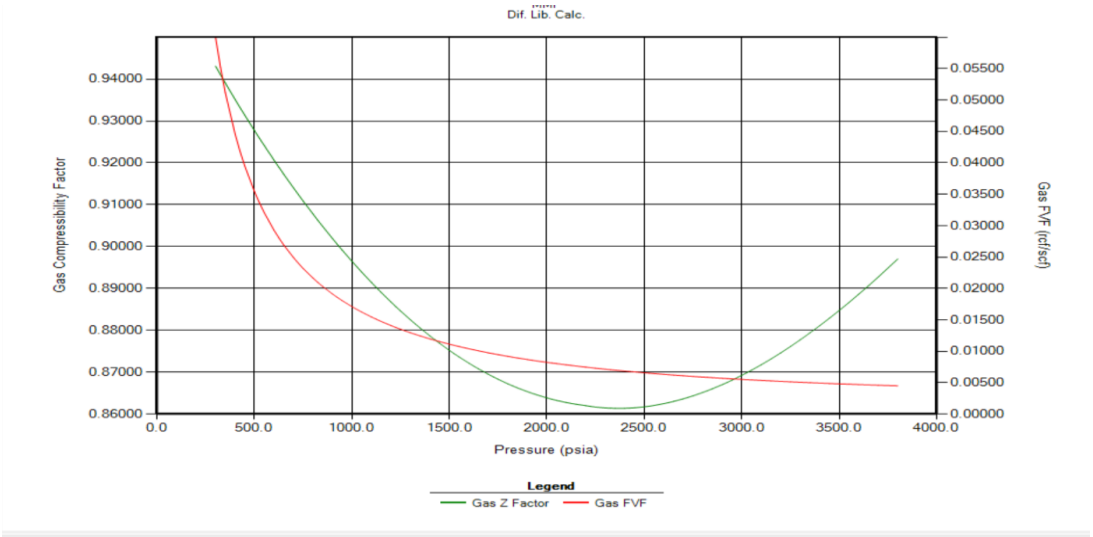


Figure 3.6. The gas FVF and the gas compressibility factor in relation to Pressure (developed using CMG Builder, 2021).

## Rock Fluid

In this study, the PVT module of the Winprop software was utilized to determine fluid properties at a temperature of 215°F and a reservoir pressure of 3212 psi. Subsequently, the pressure-temperature phase diagram was generated, illustrated in Figure 14, which depicts the bubble point pressure and the phase behavior of the reservoir oil.

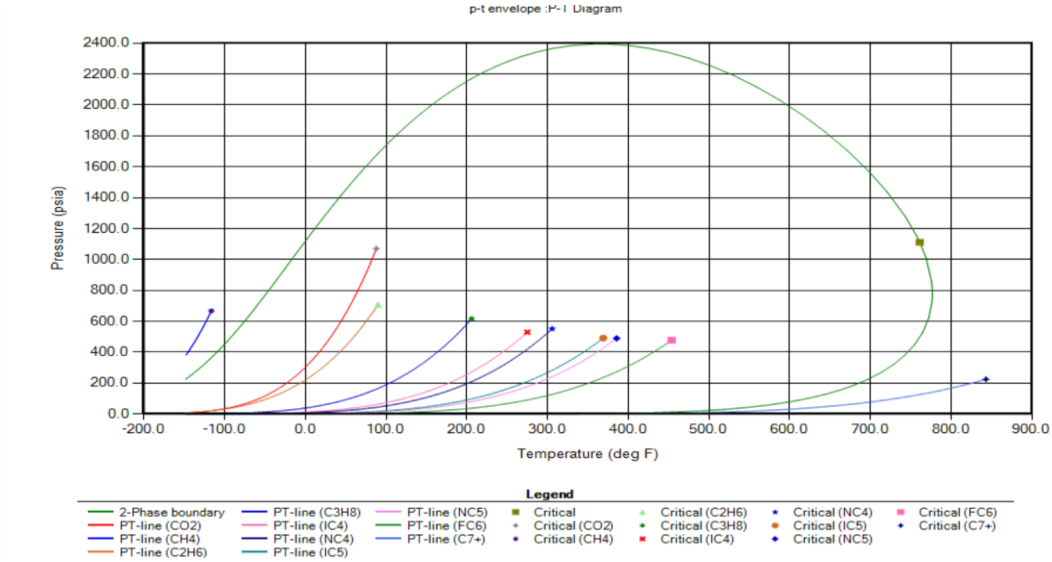


Figure 3.7. Schematic two-phase diagrams of the oil composition used in this study (CMG Builder, 2021).

By utilizing a suitable scaling factor, it is possible to obtain representative values for capillary pressure and relative permeability corresponding to specific pressure and composition conditions. Generally, the miscible displacement for a specific rock section will fall within these established ranges. It is important to note that the phase potential and mobility outlined in equation (13) are not influenced by interfacial tension. There are multiple methods to utilize interfacial tension as a scaling factor for capillary pressure and relative permeability during miscible displacements:

- Relative permeability to gas and oil phase:

$$k_{rg} = \sigma^* k_{rg}|_{\sigma_{max}} + (1 - \sigma^*) k_{rg}|_{\sigma_{min}} \quad (19)$$

$$k_{rog} = \sigma^* k_{rog}|_{\sigma_{max}} + (1 - \sigma^*) k_{rog}|_{\sigma_{min}} \quad (20)$$

Where:

$k_{rog}$= oil and gas phase relative permeability, mD

$S_{or}$= residual oil saturation, %

- Capillary pressure:

$$P_c = \sigma^* P_c|_{\sigma_{max}} + (1 - \sigma^*) P_c|_{\sigma_{min}} \quad (21)$$

Where $\sigma^* = \frac{\sigma - \sigma_{min}}{\sigma_{max} - \sigma_{min}}$ (21.1)

This dimensionless parameter is used to adjust the empirical bounding values. The interfacial tension $\sigma$ can be determined by employing the modified Macleod-Sugden correlation for multi-component mixtures, a method originally suggested by Weinaug and Katz in 1943:

$$\sigma = [\sum_i P_i (x_i \frac{\rho_o}{M_o} - y_i \frac{\rho_g}{M_g})]^\theta \quad (22)$$

In this context, $\sigma$ represents surface tension measured in dynes/cm, while $\rho$ denotes the phase density expressed in g/cm. The molecular weight of the phase is given by M, and the mole fraction of component i in the liquid phase is indicated as $x_i$, with $y_i$ representing the mole fraction of the same component in the gas phase. The pressure of component i, $P_i$, can be determined using established correlations. The exponent $\theta$, which is slightly less than 4, was initially introduced by Macleod and Sugden.

In order to accurately model fluid movement in reservoirs, it is essential to comprehend the relative permeability curves that correspond to the equilibrium state of fluids at both high and low interfacial tension during displacement processes. These graphs can serve as the defining bounding relative permeability curves in the simulation model.

At a water saturation of 0.25, the relative permeability of water ($k_{rw}$) starts to increase in the oil-water phase, as seen in Figure 14, represented by the red line. Conversely, the relative permeability of oil-water ($k_{row}$) diminishes, ultimately reaching zero at a saturation level of 0.58, as shown by the blue line. Figure 15 depicts the relationship between relative permeability and liquid saturation. This plot indicates that the relative permeability of gas decreases over time, achieving zero at a liquid saturation of 0.86. In contrast, the relative permeability of oil-gas ($K_{rog}$) shows a declining trend from its initial saturation level until it reaches 0.45.

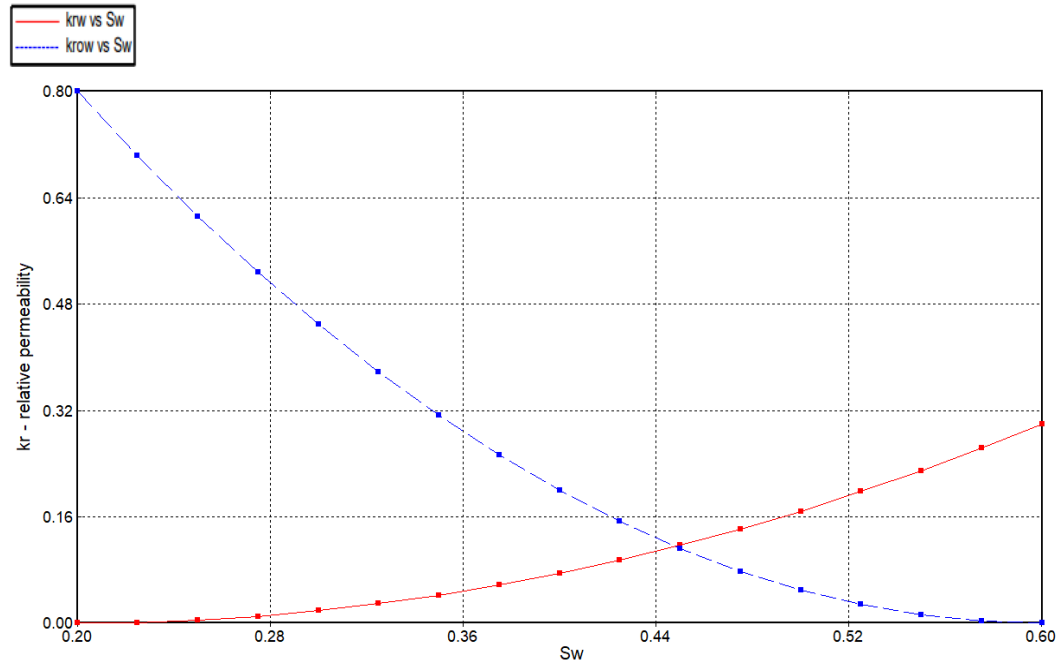


Figure 3.8. Relative permeability versus water saturation (CMG Builder, 2021).

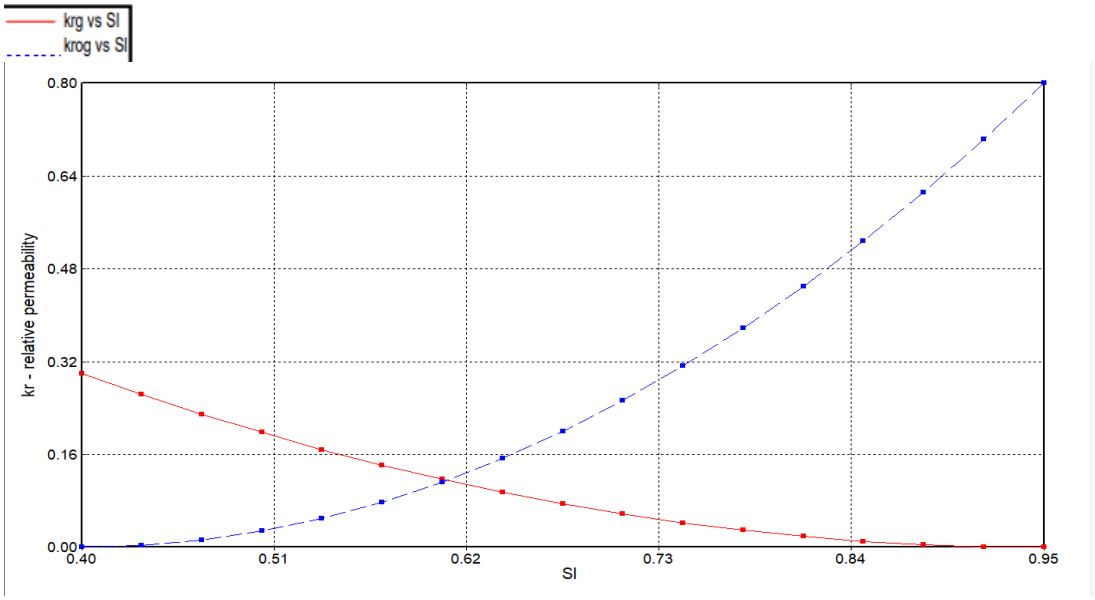


Figure 3.9. Relative permeability versus liquid saturation (CMG Builder, 2021).

## Fluid Contacts and Initialization

To accurately validate the simulation, it is essential to establish the initial conditions, which include the depths of fluid contacts (referred to as the oil-water contact depth), as well as the reference depth, pressure, and phase saturation of the grid cells. In this study, we input the oil-water contact (OWC) depth, the water-oil

contact (WOC) depth, the pressure at the reservoir's reference depth, and the reference depth itself to ascertain the initial state of the reservoir model. The initial pressure was set at 3212 psi, with a reference depth of 6100 feet and an initial WOC depth of 6600 feet. For numerical controls, the standard temperature variation was fixed at 18 °F, while pressure variation was set at 145 psi.

**Production and Injection Well Constraints**

For the simulation constraints, the producing well was limited to a minimum bottom-hole pressure (BHP) of 28 psi and a maximum surface oil rate of 15000 bbl/day. The injectors were constrained at a maximum surface gas rate of 100,000 SCF/day and a bottom-hole pressure of 2000 psi. Each layer was perforated, enabling various solvents to be injected along the model's flank, while producers were strategically positioned around the injectors to optimize the oil transfer process. The CMG-GEM 2021 simulator completed the initial simulation utilizing the natural depletion of the Arab-D reservoir, along with various scenarios involving different injected fluids, to maximize recovery. The comparison case includes:

- Case 1: Natural depletion
- Case 2: 100% pure $CO_2$
- Case 3: Impure $CO_2$ , which included
    - 75% $CO_2$ + 25% $N_2$
    - 50% $CO_2$ + 50% $N_2$
    - 75% $N_2$ + 25% $CO_2$
- Case 4: 100% pure $N_2$

**Data Collection Procedures**

To thoroughly analyze the findings, it is crucial to consider several factors, including the study duration, oil production rates, cumulative oil output, overall field recovery, and the total amounts of $CO_2$ and $N_2$ captured. Further details on these aspects will be discussed in the next chapter.

**Data Analysis Plan**

The research study will follow a structured approach, outlined in the following steps:

A. Initially, we will compile data from multiple sources related to the Ghawar oil field to establish a thorough dataset that enables detailed investigation.
B. Utilizing CMG GEM software, a compositional reservoir simulation model will be developed, while CMG Winprop will be employed to determine the MMP by evaluating the miscibility levels between $CO_2/N_2$ gas and oil through established correlations.
C. A range of simulation scenarios will be developed to evaluate the impacts of injecting pure miscible fluids as compared to alternative mixtures of $N_2$. This comparative analysis will assist in identifying the most effective strategy for enhancing oil recovery significantly.
D. Finally, an assessment will be conducted regarding the potential environmental implications of $CO_2$ injection, focusing on issues such as groundwater contamination, risks associated with leakage, and the overall capacity for $CO_2$ storage.

# CHAPTER IV

## Findings and Discussion

This chapter outlines the findings derived from the collected data. After incorporating the reservoir data into the CMG GEM software, we executed the simulation, which yielded significant results. Our research initially aimed to evaluate the efficacy of miscible carbon dioxide ($CO_2$) injection to enhance oil recovery. The outcomes from the miscible $CO_2$ injection were scrutinized and compared to those obtained from a mixture with nitrogen ($N_2$), allowing us to assess the influence of impurities on key performance metrics. These include the average reservoir pressure, oil recovery factor, cumulative oil production, oil production rate, and carbon capture.

### Case 1: Natural Depletion

In this scenario, we examined how the reservoir behaves under natural depletion alongside projected recovery rates, utilizing the GEM software for simulation. The model parameters included a maximum flowing bottom hole pressure of 2000 psi, establishing this case as the base case scenario. Without an injection well and supported solely by four production wells located at the reservoir's periphery, this scenario exemplifies natural production.

The simulation results, spanning a period from 2000 to 2025 (25 years), indicated that the oil recovery factor was 27.3% of the original oil in place (OOIP). By the end of 20 years, cumulative oil production reached 10 million barrels. During the first year, the reservoir exhibited an oil production rate of 8,745.14 barrels per day, alongside a decline in reservoir pressure to 172.5 psi. The graphical representations of the discussed outcomes are displayed in the following figures:

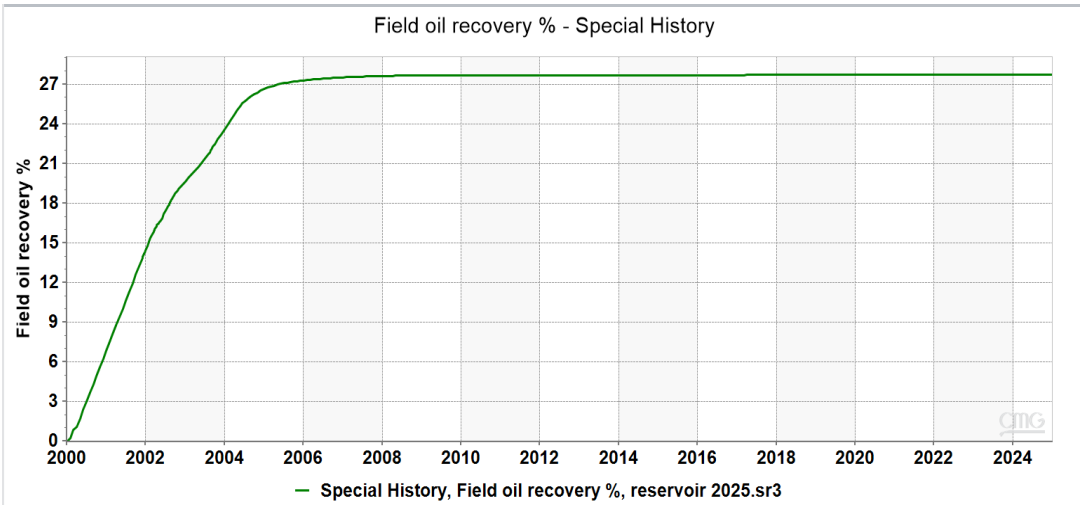


Figure 4.1. Oil recovery factor vs time for base case scenario (generated by CMG Results, 2021).

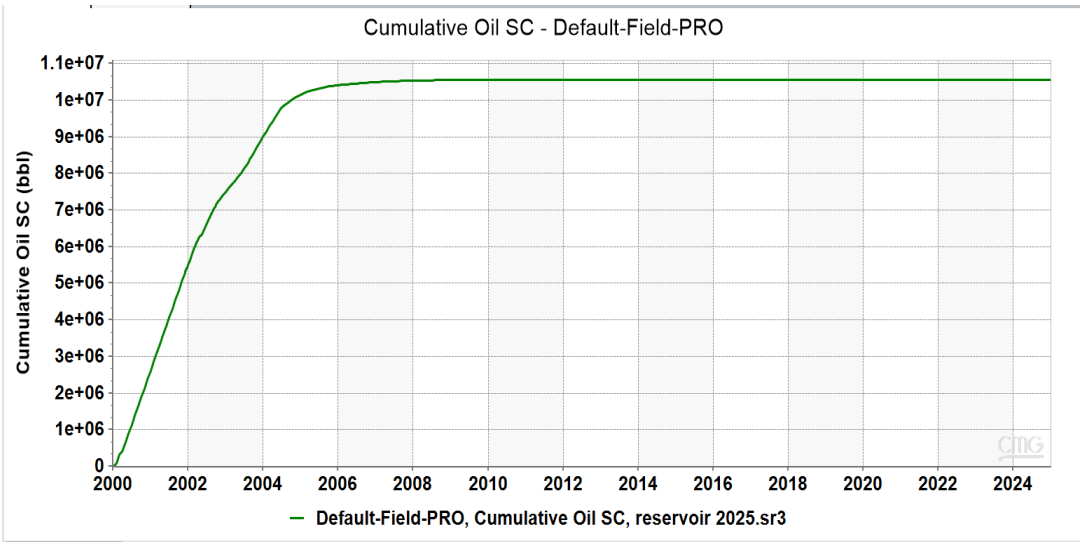


Figure 4.2. Cumulative oil vs time for base case scenario (generated by CMG Results, 2021).

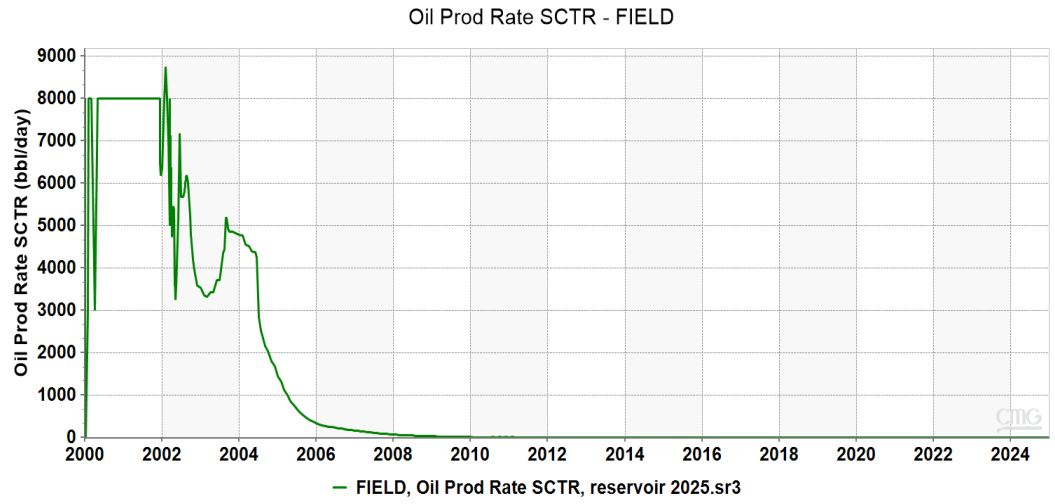


Figure 4.3. Oil production rate vs time for base case scenario (generated by CMG Results, 2021).

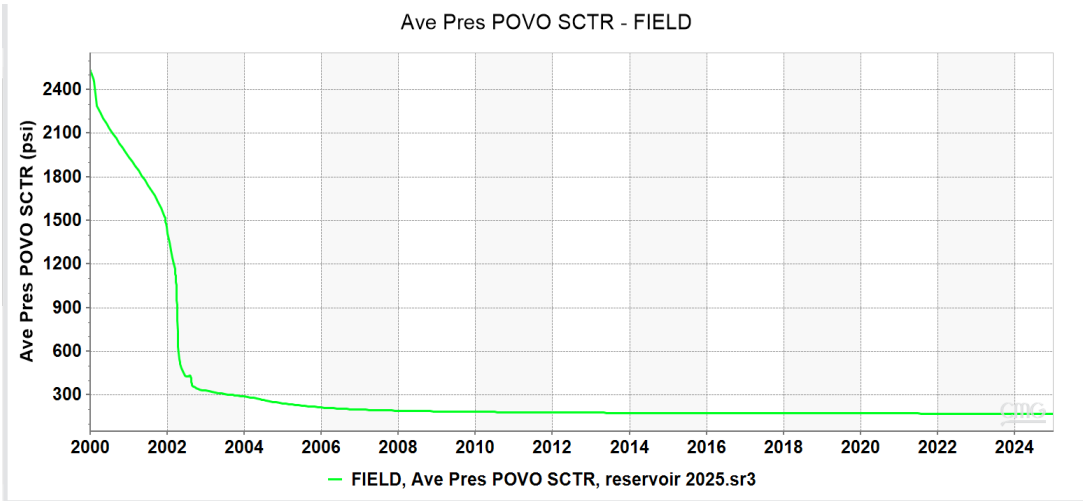


Figure 4.4. Average pressure povo SCTR vs time for base case scenario (generated by CMG Results, 2021).

### Case 2: Miscible Pure $CO_2$ Flooding

In this case, we examined the injection of 100% $CO_2$ into the reservoir. The method of miscible gas injection involves introducing gas into the reservoir at pressures above the miscibility pressure to enhance oil recovery (El-Hoshoudy & Desouky, 2018; Fath & Pouranfard, 2014). For this scenario, 100% pure $CO_2$ was injected, and simulations were conducted using a compositional model in CMG GEM 2021. The correlations employed, including multiple mixing, cell-to-cell, and tie lines,

are summarized in the table below, which displays the various pressure values at FCM and MCM for the miscibility of carbon dioxide with oil, given an initial reservoir pressure of 3212 psi.

Table 4.1. MMP for pure $CO_2$ (generated by CMG Winprop, 2021).

| Case | Cell to Cell | Tie Lines | Multiple Mixing |
|---|---|---|---|
| Pure $CO_2$ | 2575 psi | 1950 psi | 2623 psi |

This reservoir is modeled as a standard cuboidal grid with five spot wells. The process operated at a rate of 100,000 ft³/day, utilizing four producing wells (P) and one $CO_2$ injection well (I1). The miscible gas injection commenced with a maximum bottom hole pressure constraint of 2000 psi. Compared to the base case, the pure $CO_2$ injection achieved a higher oil recovery factor of 73.8% and a cumulative oil production of 38 million barrels. Additionally, the reservoir pressure decreased to 1000 psi, and the maximum oil production rate at the end of the 25 years was determined to be 60,000 bbl/day. These results were facilitated by the implementation of an injector well with the optimal bottom-hole pressure and gas injection rates, or the surface gas rate (STG), using pure $CO_2$ as the component fluid. The subsequent figures illustrate the oil recovery factor, cumulative oil production, oil production rate, and average pressure pore volume.

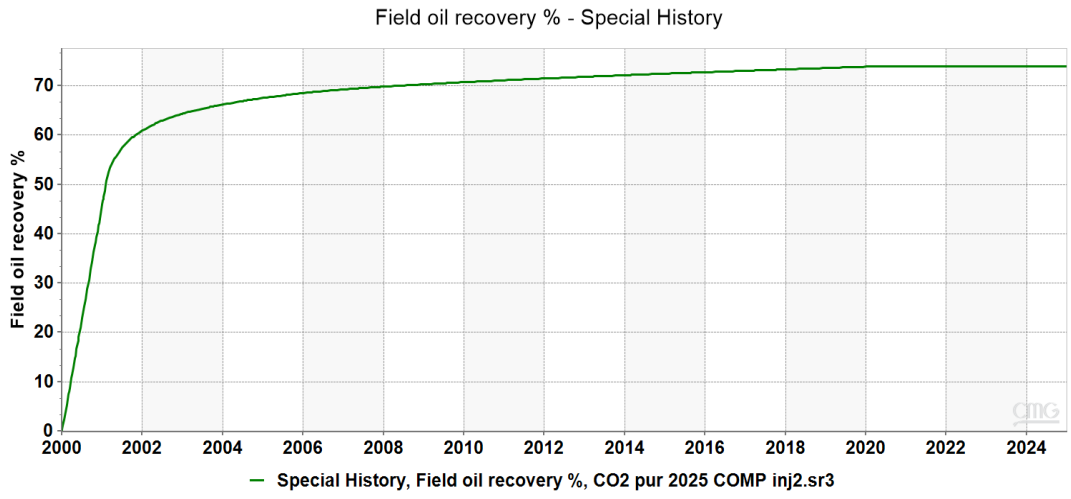


Figure 4.5. Oil recovery factor vs time for 100% $CO_2$ injection (generated by CMG Results, 2021).

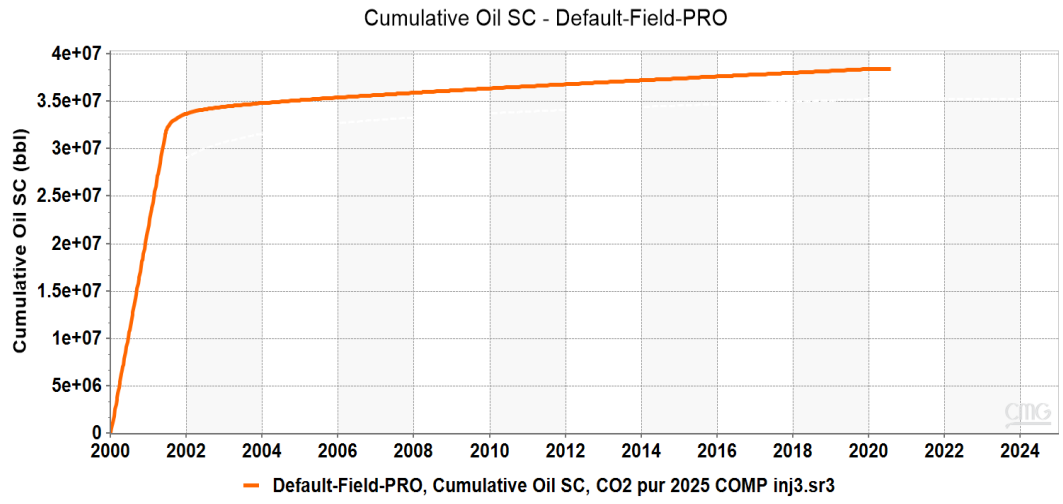


Figure 4.6. Cumulative oil production vs time for 100% $CO_2$ injection (generated by CMG Results, 2021).

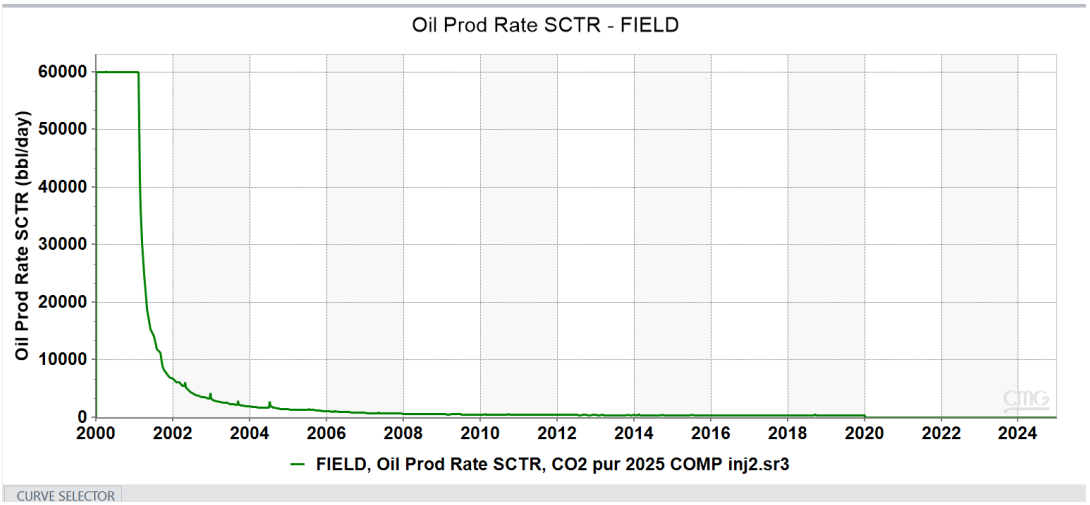


Figure 4.7. Oil production rate vs time for 100% $CO_2$ injection (generated by CMG Results, 2021).

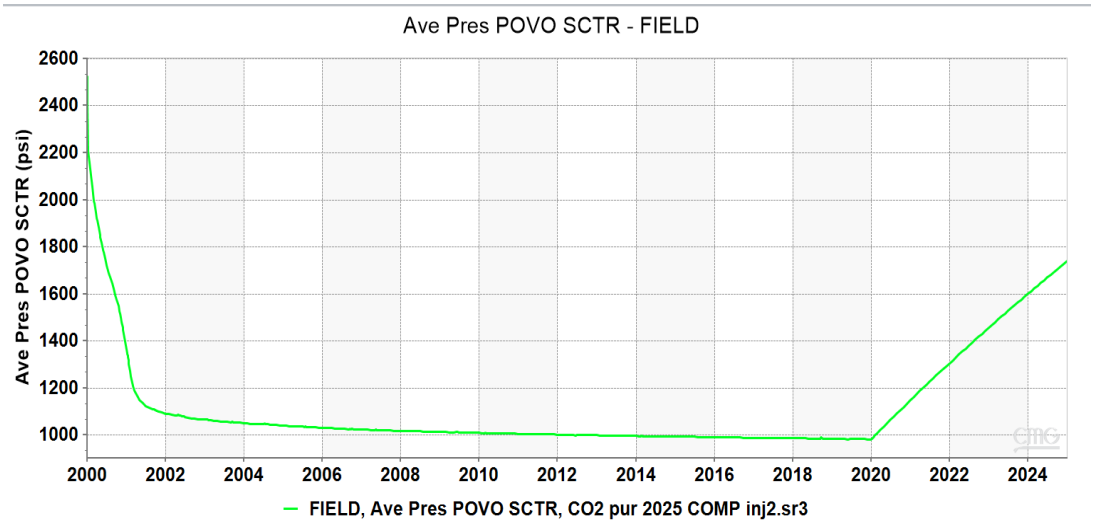


Figure 4.8. Average pressure povo SCTR vs time for 100% $CO_2$ injection (generated by CMG Results, 2021).

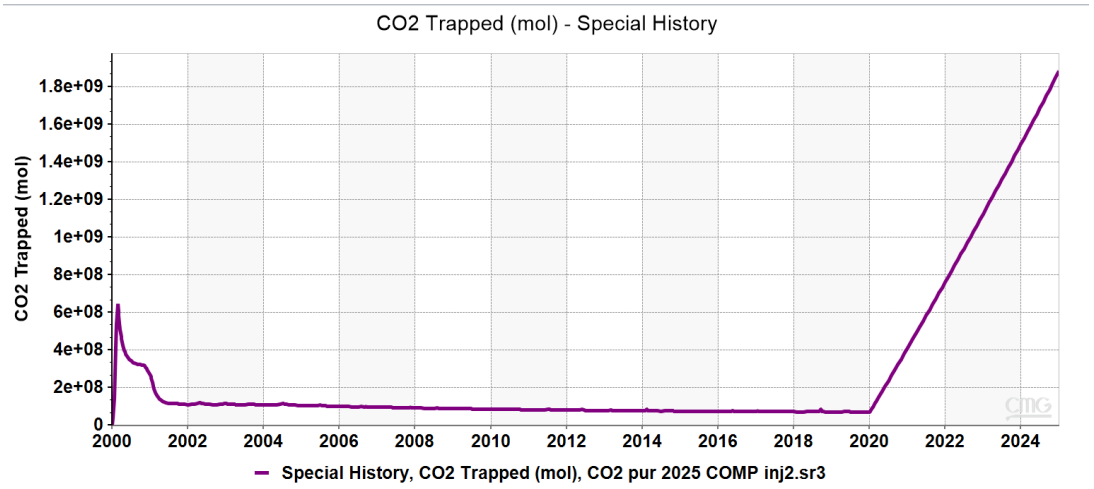


Figure 4.9. Cumulative $CO_2$ trapped vs time for 100% $CO_2$ injection (generated by CMG Results, 2021).

### Case 3: Impure $CO_2$ Flooding

Carbon dioxide ($CO_2$) can be captured from a variety of origins using different technologies. However, these $CO_2$ streams often contain several impurities, including nitrogen ($N_2$), methane ($CH_4$), hydrogen sulfide ($H_2S$), and argon ($A_r$). The concentration of these impurities in $CO_2$ is influenced by the extent of fuel oxidation as well as the specific characteristics of the fuel utilized. Among the prevalent carbon capture techniques: pre-combustion, post-combustion, and oxy-fuel combustion; the

oxy-fuel combustion process results in the highest concentration of impurities within the $CO_2$ output.

In addition to these major contaminants, minor constituents like water vapor ($H_2O$), nitrogen oxides ($NO_X$), and sulfur oxides ($SO_X$) are also present. For this study, we will focus specifically on the effect of nitrogen ($N_2$) on the miscibility of $CO_2$ during enhanced oil recovery processes. The following table illustrates the minimum miscibility pressures (MMP) for various blends of $CO_2$ and $N_2$, calculated using three different correlations: multiple mixing, cell to cell, and tie lines.

Table 4.2. MMP for impure $CO_2$ (generated by CMG Winprop, 2021).

| Case | Cell to Cell | Tie Lines | Multiple Mixing |
|---|---|---|---|
| 25% $N_2$ + 75% $CO_2$ | 2700 psi | 2210 psi | 2900 psi |
| 50% $N_2$ + 50% $CO_2$ | 2920 psi | 2500 psi | 3200 psi |
| 75% $N_2$ + 25% $CO_2$ | 3080 psi | 2820 psi | 3600 psi |

The data indicates that the miscibility characteristics are significantly influenced by the gas composition, particularly the presence of $N_2$, which elevates the minimum miscibility pressure required. As seen below, this scenario contains varying proportions of nitrogen and carbon dioxide:

- **25% $N_2$ + 75% $CO_2$:** An examination of a mixture comprising 25% $N_2$ and 75% $CO_2$ reveals that this injection scenario achieved an oil recovery rate of 69%, resulting in a cumulative production of 36.4 million barrels. This performance is notably lower than that observed in scenarios using 100% $CO_2$ injection. Below, we present the metrics for oil recovery factors, cumulative oil produced, and related production rates.

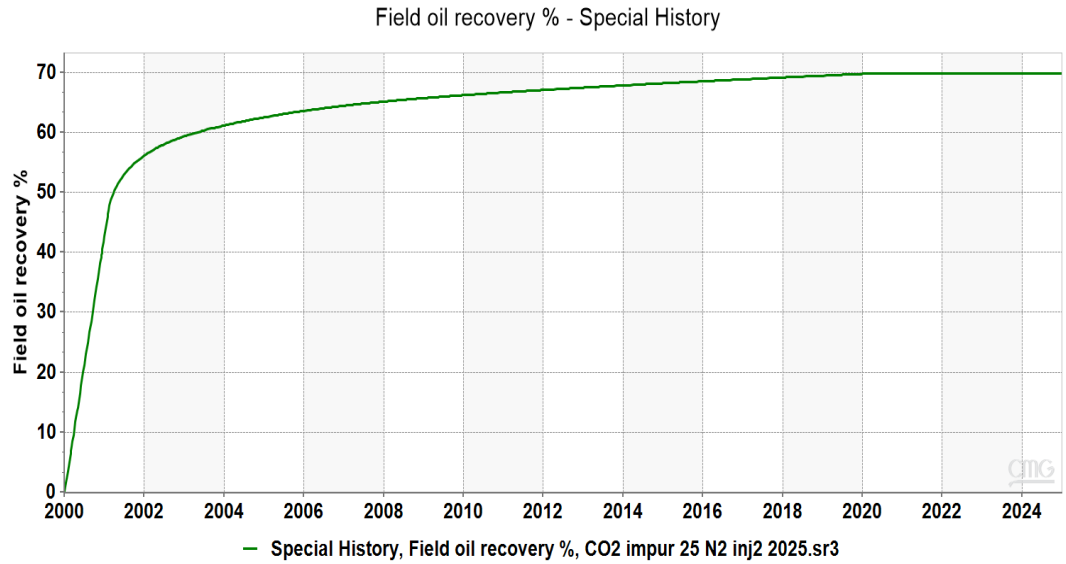


Figure 4.10. Oil recovery factor vs time for 25% $N_2$ + 75% $CO_2$ (generated by CMG Results, 2021).

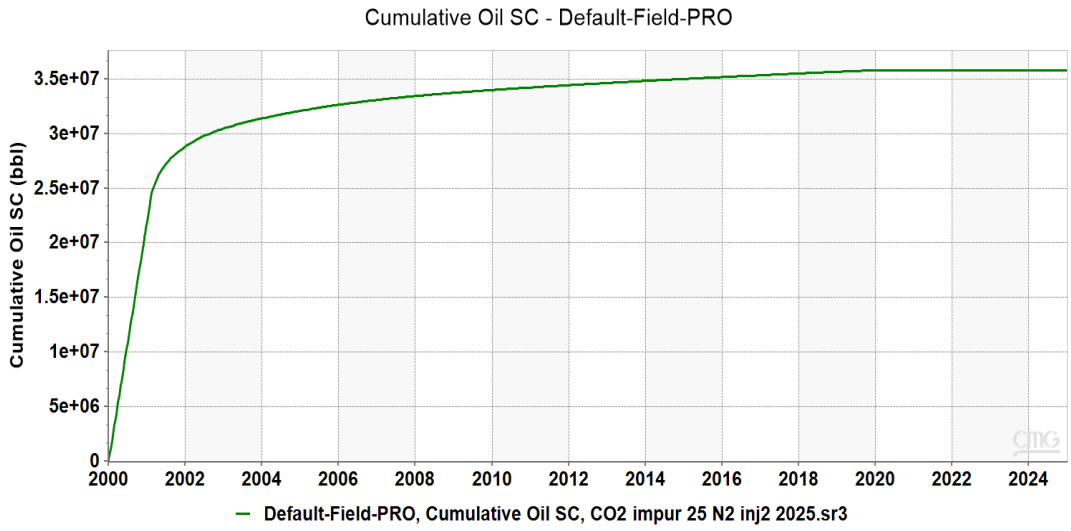


Figure 4.11. Cumulative oil production vs time for 25%$N_2$ + 75% $CO_2$ (generated by CMG Results, 2021).

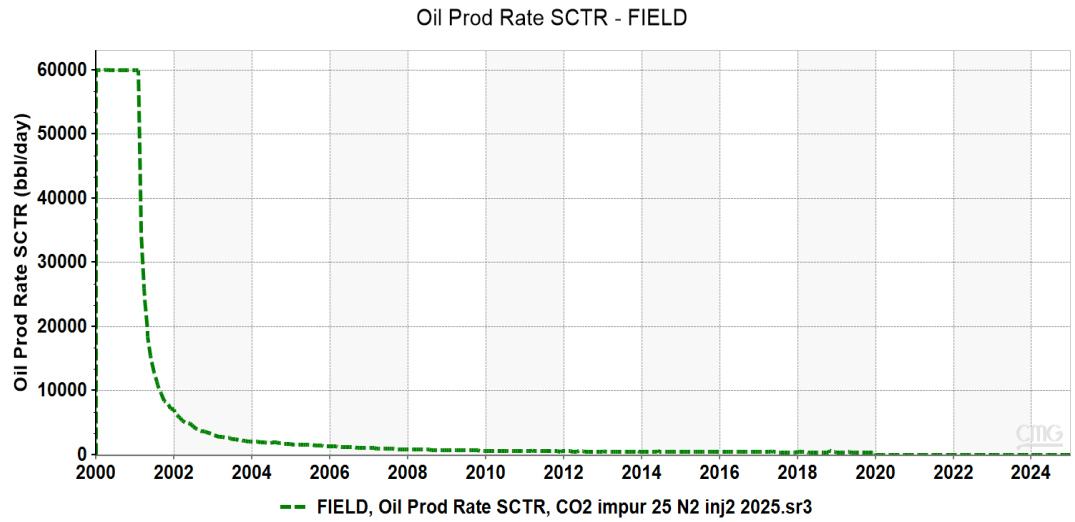


Figure 4.12. Oil production rate vs time for 25% $N_2$ + 75% $CO_2$ (generated by CMG Results, 2021).

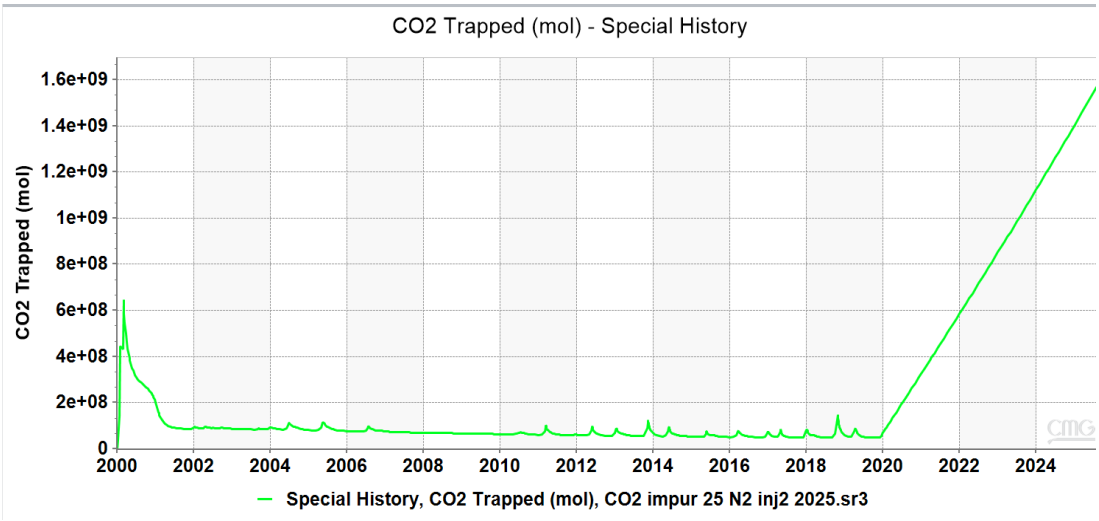


Figure 4.13. Cumulative $CO_2$ trapped vs time for 25% $N_2$ + 75% $CO_2$ (generated by CMG Results, 2021).

- **50% $N_2$ + 50% $CO_2$:** In contrast to the earlier injection scenario, the current injection process has resulted in a total oil production of 36.1 million barrels, achieving an oil recovery rate of 65%. The accompanying figures illustrate the rates of oil production, the cumulative amount of oil produced, and the recovery factor of the oil.

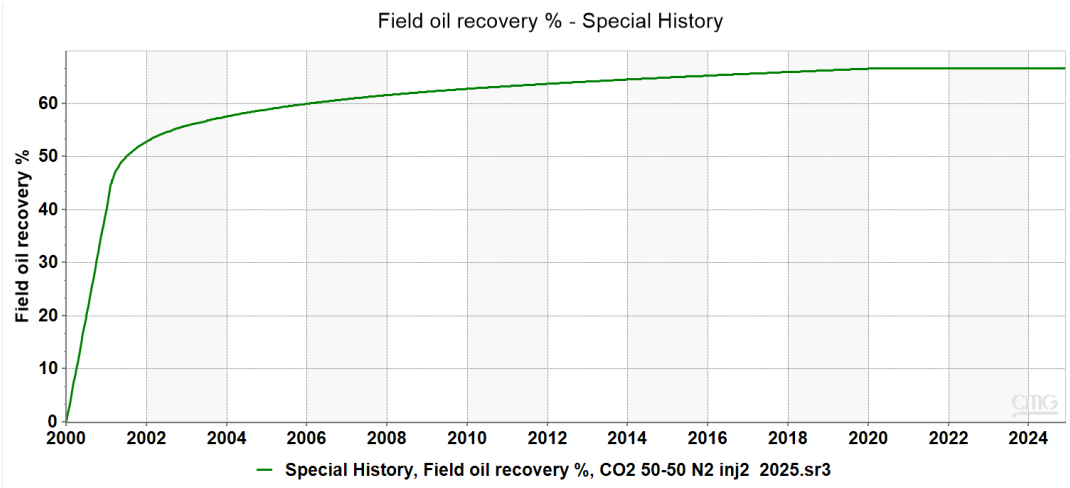


Figure 4.14 Oil recovery factor vs time for 50%$N_2$ + 50% $CO_2$ (generated by CMG Results, 2021).

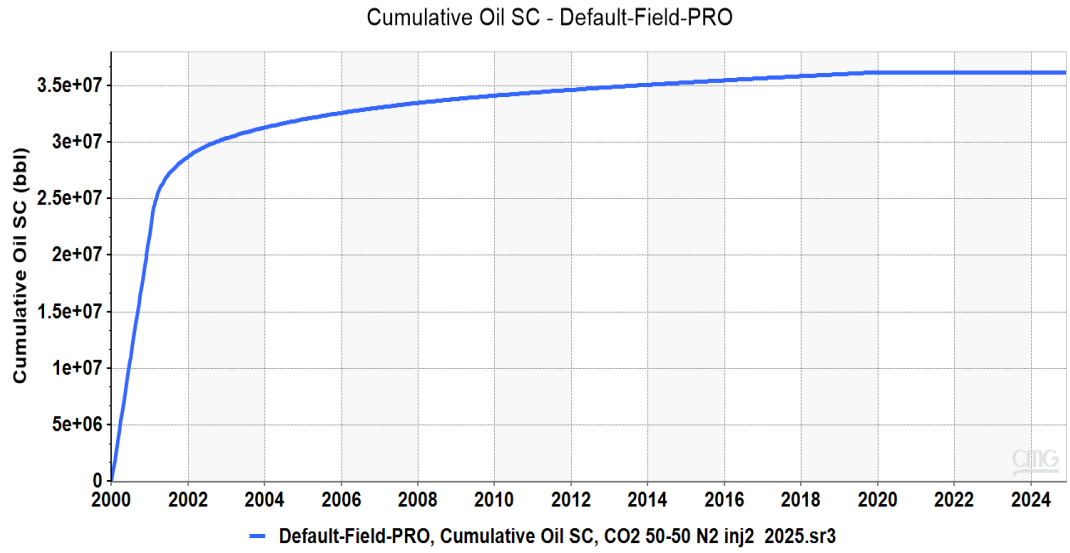


Figure 4.15. Cumulative oil production vs time for 50%$N_2$ + 50%$CO_2$ (generated by CMG Results, 2021).

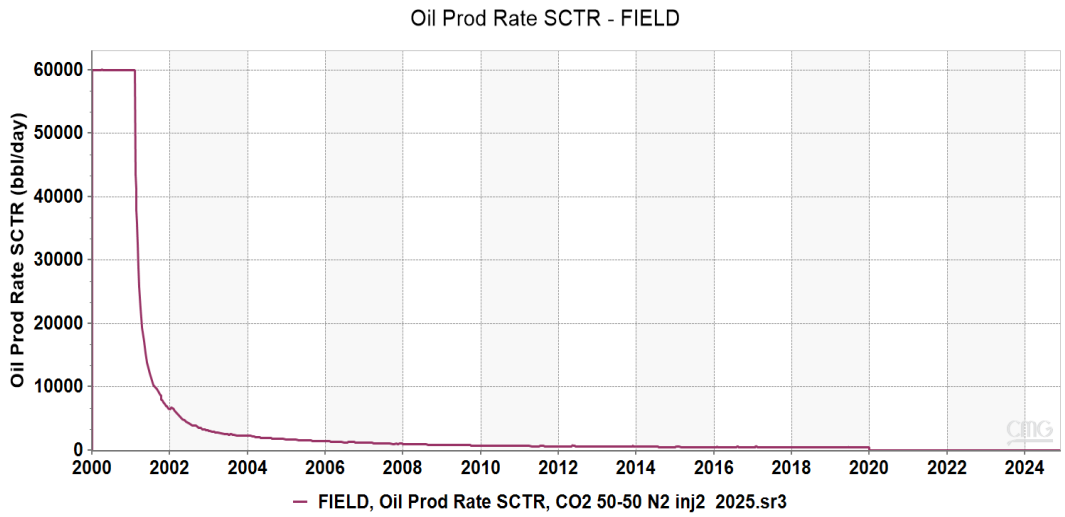


Figure 4.16. Oil production rate vs time for 50%$N_2$ + 50% $CO_2$ (generated by CMG Results, 2021).

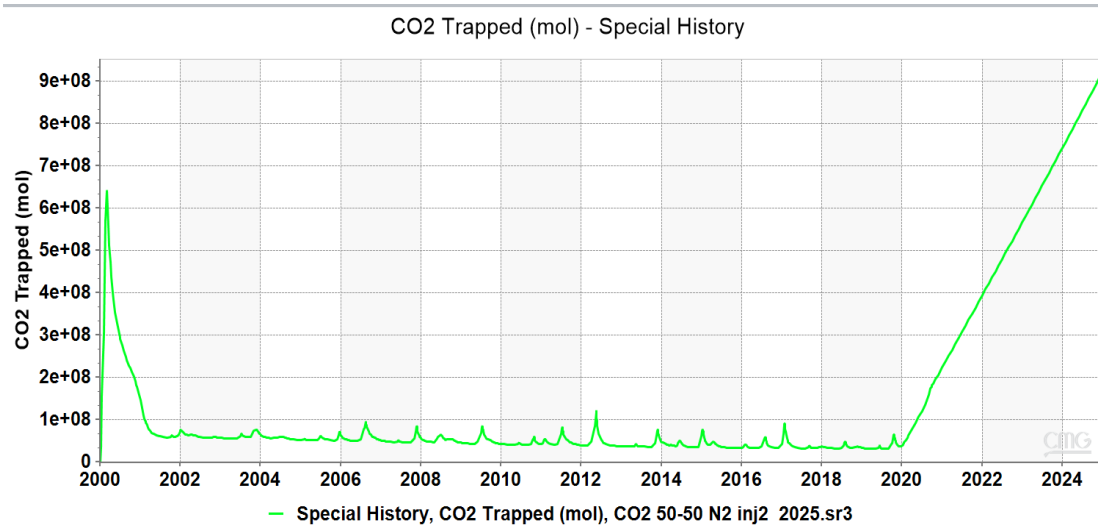


Figure 4.17. Cumulative $CO_2$ trapped vs time for 50% $N_2$ + 50% $CO_2$ (generated by CMG Results, 2021).

- **75% $N_2$ + 25% $CO_2$:** Compared to the earlier injection scenario, the recent injection has resulted in a cumulative production of 35.6 million barrels of oil, with an overall recovery rate of 65%. The figures below depict the oil production rate, the total cumulative oil produced, and the oil recovery factor.

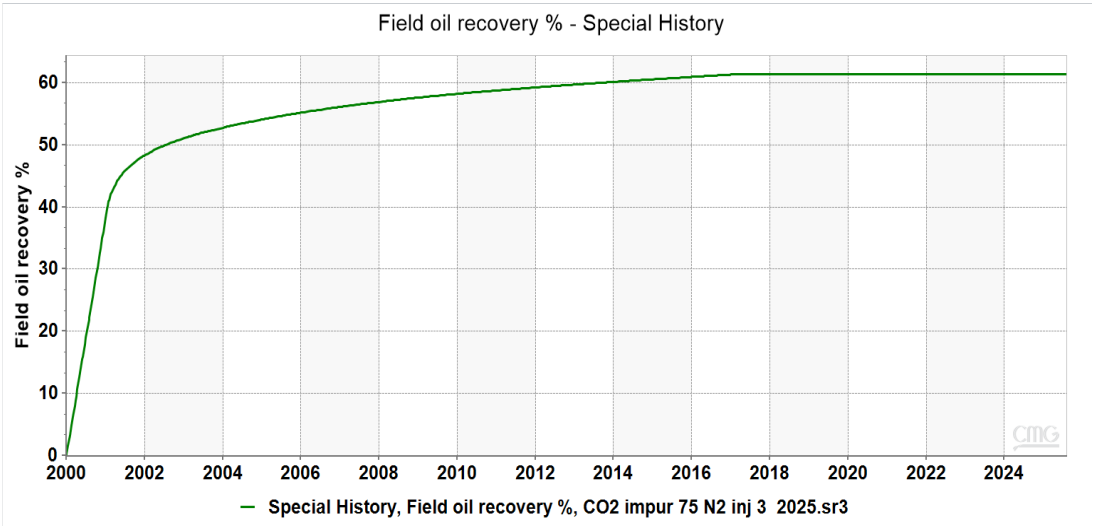


Figure 4.18. Oil recovery factor vs time for 75%$N_2$ + 25% $CO_2$ (generated by CMG Results, 2021).

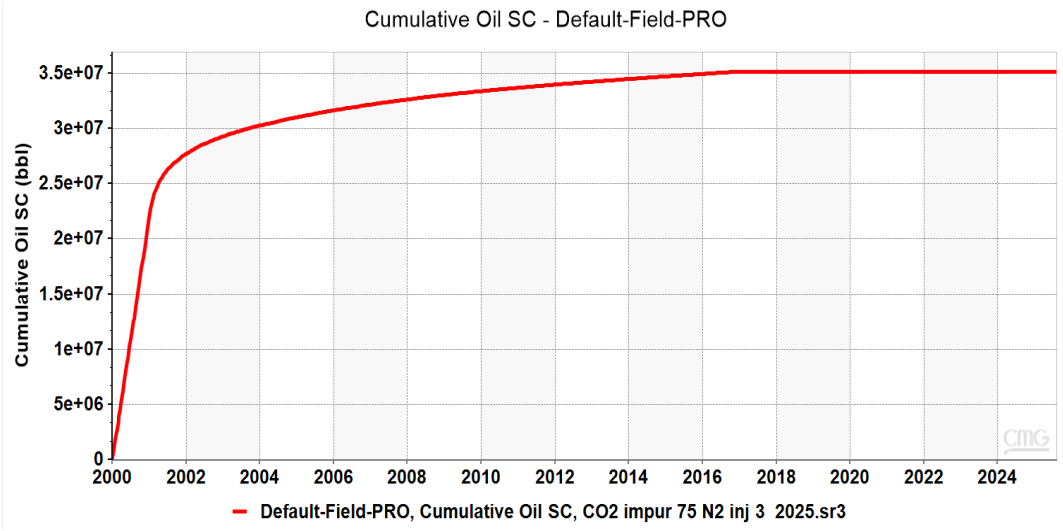


Figure 4.19. Cumulative oil vs time for 75%$N_2$ + 25%$CO_2$ (generated by CMG Results, 2021).

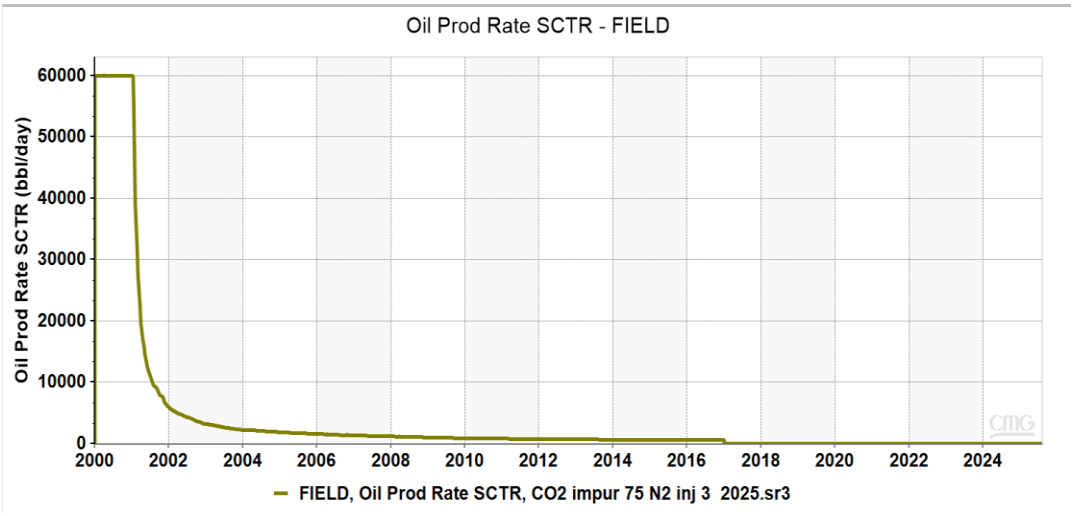


Figure 4.20. Oil production rate vs time for 75%$N_2$ + 25%$CO_2$ (generated by CMG Results, 2021).

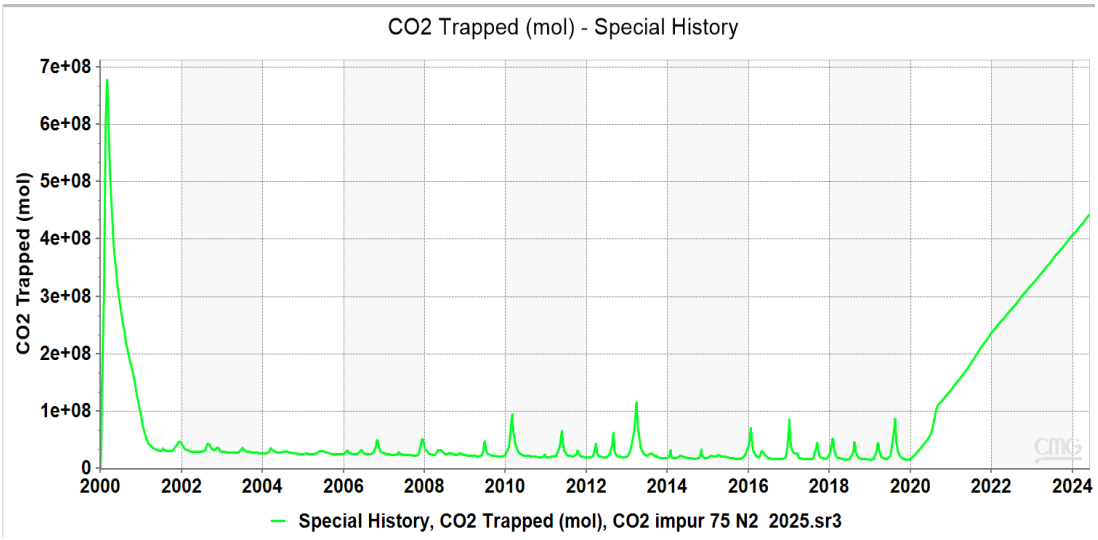


Figure 4.21. Cumulative $CO_2$ trapped vs time for 75%$N_2$ + 25% $CO_2$ (generated by CMG Results, 2021).

**Case 4: 100% $N_2$**

The following table will show the different values of pressure at FCM and MCM of the miscibility of carbon dioxide and nitrogen with oil using the following correlations: multiple mixing, cell to cell, and tie lines.

Table 4.3. MMP for pure $N_2$ (generated by CMG Winprop, 2021).

| Case | Cell to Cell | Tie Lines | Multiple Mixing |
|---|---|---|---|
| 100% $N_2$ | 3150 psi | 3000 psi | 4187 psi |

Compared to the previous injection scenario, the injection has yielded a reduced cumulative oil production of 35 million barrels and a 58% oil recovery. Figures presented below display the oil production rate, cumulative oil production, and oil recovery factor.

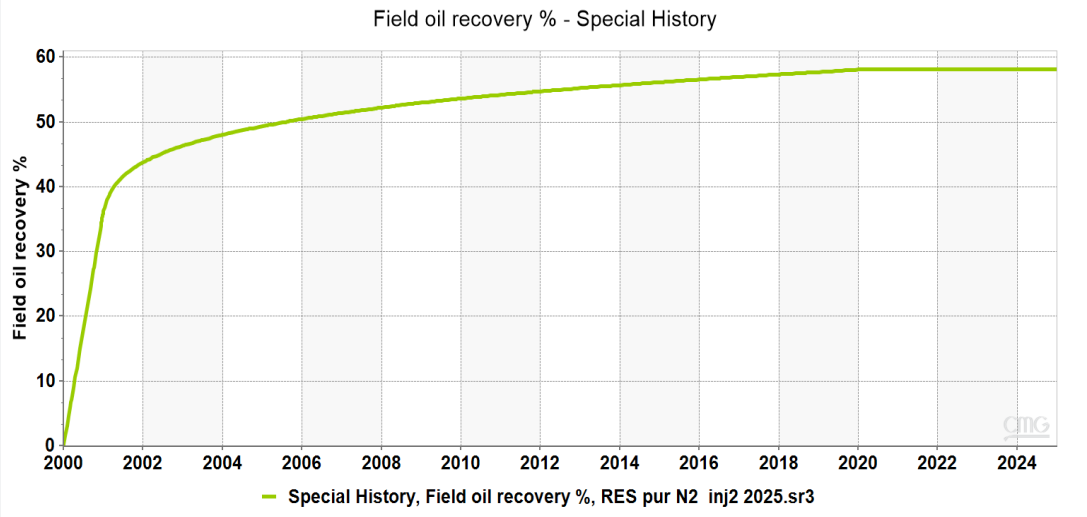


Figure 4.22. Oil recovery factor vs time for 100%$N_2$ (generated by CMG Results, 2021).

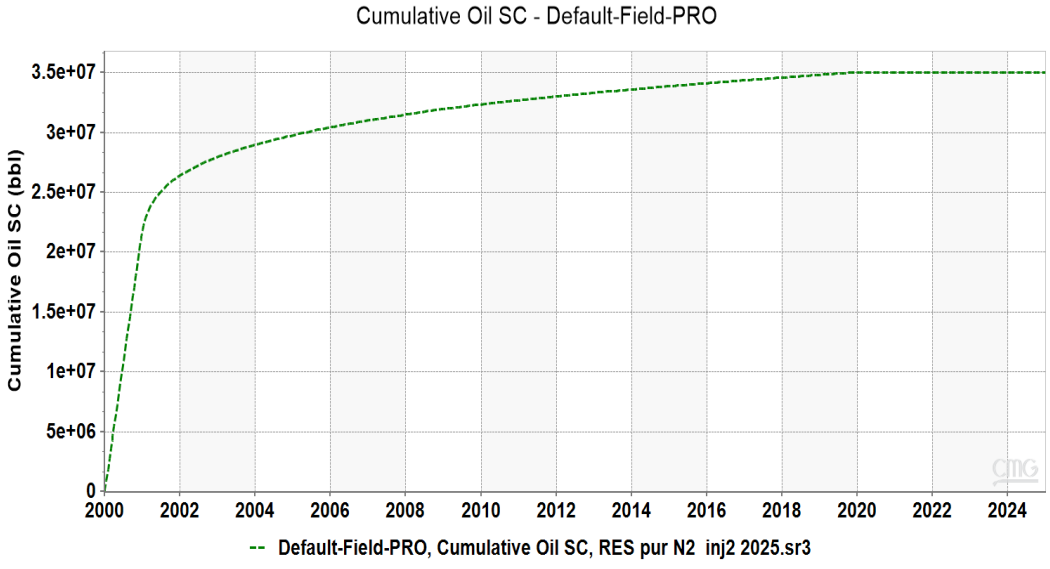

Figure 4.23. Cumulative oil vs time for 100%$N_2$ (generated by CMG Results, 2021).

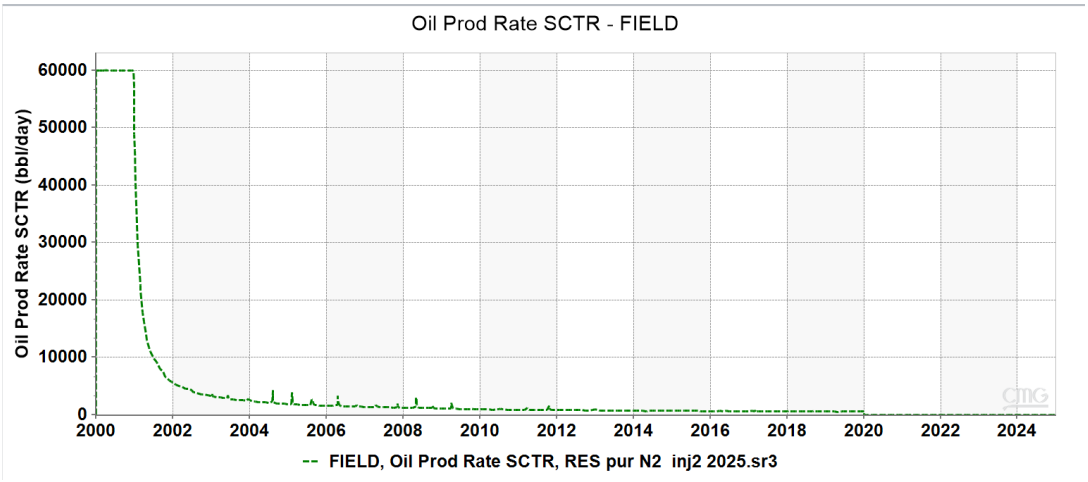


Figure 4.24. Oil production rate vs time for 100%$N_2$ (generated by CMG Results, 2021).

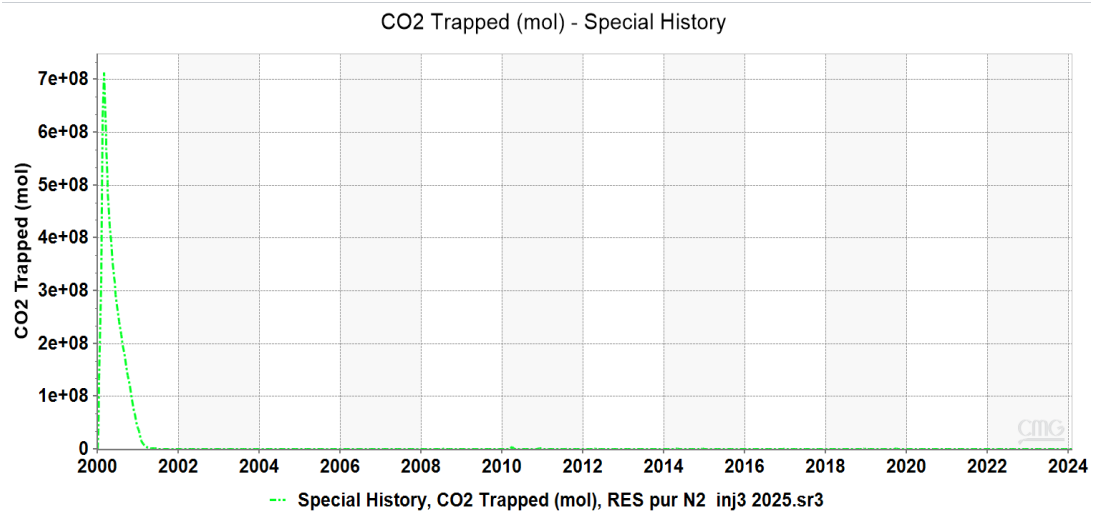


Figure 4.25. Cumulative mole trapped vs time for 100%$N_2$ (generated by CMG Results, 2021).

## Comparison of Injection Scenarios With The Base Base

**Oil Recovery:** The main objective of this research is to enhance the oil recovery factor, quantified as the percentage of natural oil extracted from the original volume of oil in place (OOIP). Cumulative oil production refers to the total quantity of hydrocarbons recovered from the reservoir. Previous studies, including those by Khan et al. (2001, 2003), investigated a miscible $CO_2$ injection scenario, achieving an

oil recovery factor of 32% after 20 years. In contrast, the optimal scenario explored in this project, which entailed 25 years of miscible $CO_2$ injection, realized a significantly higher oil recovery rate of 73.8%, surpassing the outcomes noted in prior literature. The graphical data demonstrate that using pure miscible $CO_2$ yields the highest oil recovery factor when compared to $CO_2$ mixed with nitrogen ($N_2$).

Table 4.4. Recovery factor and cumulative oil results of natural depletion, miscible pure $CO_2$, impure $CO_2$ and pure $N_2$.

| **Case** | **Natural depletion** | **100% $CO_2$** | **25% $N_2$+ 75%$CO_2$** | **50% $N_2$+ 50%$CO_2$** | **75% $N_2$+ 25%$CO_2$** | **100% $N_2$** |
|---|---|---|---|---|---|---|
| Recovery factor% | 27.3% | 73.8% | 69% | 65% | 62% | 58% |
| Cumulative oil | 10 MMbbl | 38 MMbbl | 36.4 MMbbl | 36.1 MMbbl | 35.6 MMbbl | 35 MMbbl |

The scenario involving the injection of pure $CO_2$ demonstrates a significant enhancement in both oil recovery and total cumulative oil production when compared to the baseline case. Over a period of 25 years, the pure $CO_2$ injection achieved an oil recovery factor of 73.8% and a cumulative oil production of 38 million barrels, as indicated in table 6. In contrast, the natural depletion process resulted in only 27.3% oil recovery with total cumulative production reaching 10 million barrels, also outlined in table 6.

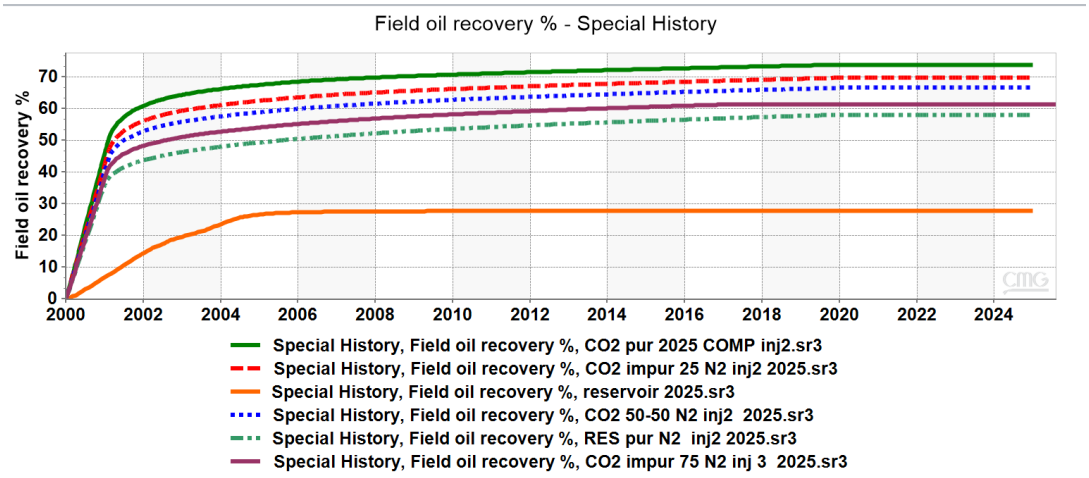


Figure 4.26. Comparison of field oil recovery values in natural depletion, pure $CO_2$, impure $CO_2$, and pure $N_2$ injection scenarios vs time (generated by CMG Results, 2021).

**Cumulative Oil**

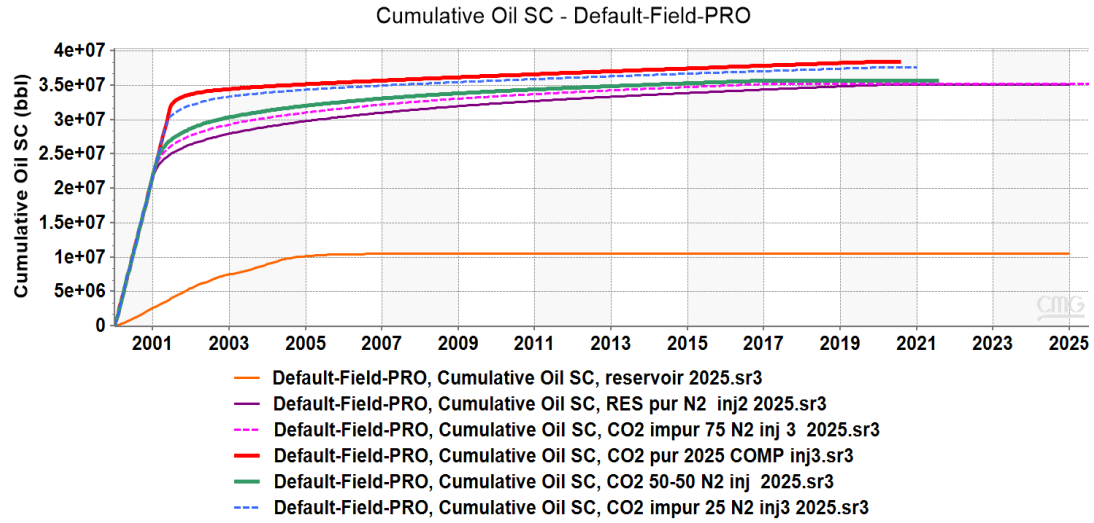


Figure 4.27. Comparison of cumulative oil values in natural depletion, pure $CO_2$, impure $CO_2$ and pure $N_2$ injection scenarios vs time (generated by CMG Results, 2021).

Similarly, Figure 24 illustrates the comparison of cumulative oil production across these scenarios versus time. It is noteworthy that certain scenarios terminate in 2021 while others extend until 2025. This discrepancy is attributed to specific constraints applied to the producers in 2021. Production was halted while injection into the reservoir continued until the bottom hole pressure was achieved.

**Production Rate**

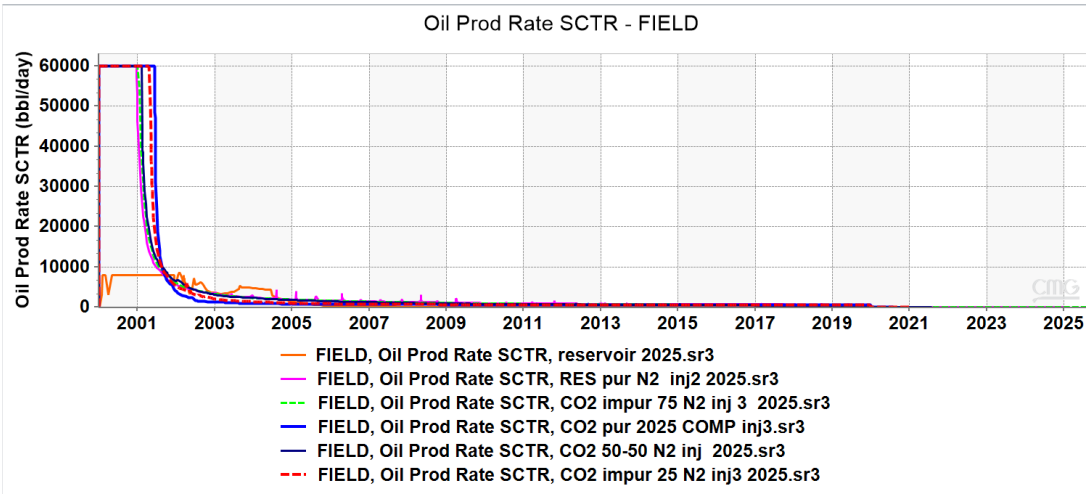


Figure 4.28. Comparison of production oil rate values in natural depletion, pure $CO_2$, impure $CO_2$, and pure $N_2$ injection scenarios vs time.

**Average Reservoir Pressure:** Average reservoir pressure serves as a significant indicator of the remaining fluid (gas, oil, or water) in a reservoir at any given moment. It reflects the potential force available to extract the remaining fluid during the simulation. The presence of $N_2$ occupies additional pore space and consequently increases the average reservoir pressure due to their lower compressibility compared to $CO_2$. However, in pure $CO_2$ scenarios, a greater flow pressure is required to maintain the same bottom hole pressure, as impurities decrease the density of the injected fluid. The ensuing figure demonstrates that contaminants diminish vertical sweep and displacement efficiency, leading to an increase in average reservoir pressure and a corresponding reduction in oil recovery. Specifically, pure nitrogen injection decrease oil recovery by 25.8% compared to pure carbon dioxide.

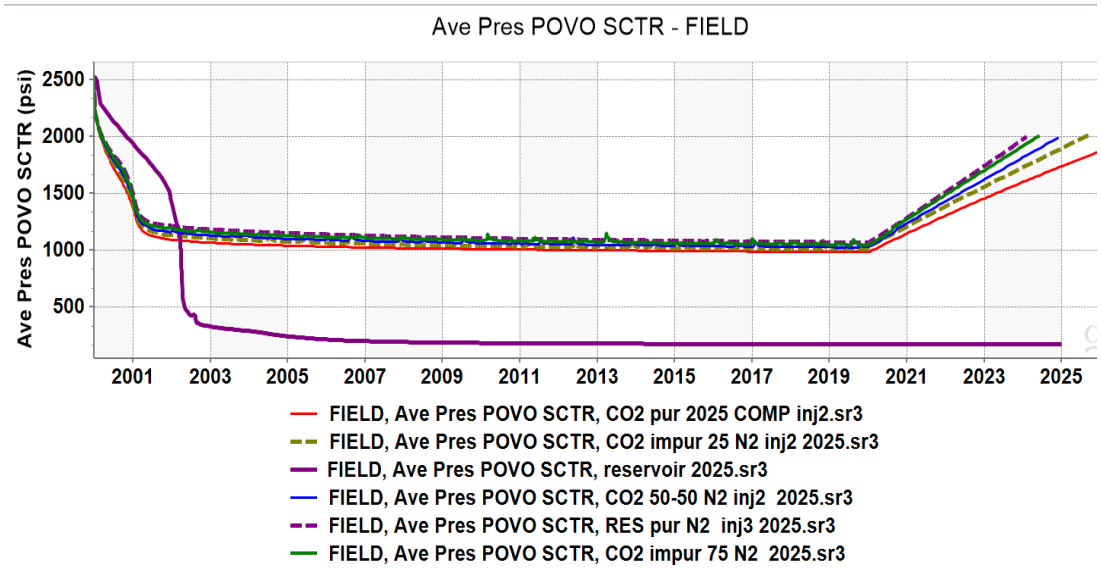


Figure 4.29. Comparison of average reservoir pressure values in natural depletion, pure $CO_2$, impure $CO_2$, and pure $N_2$ injection scenarios vs time (generated by CMG Results, 2021).

### $CO_2$ Trapped

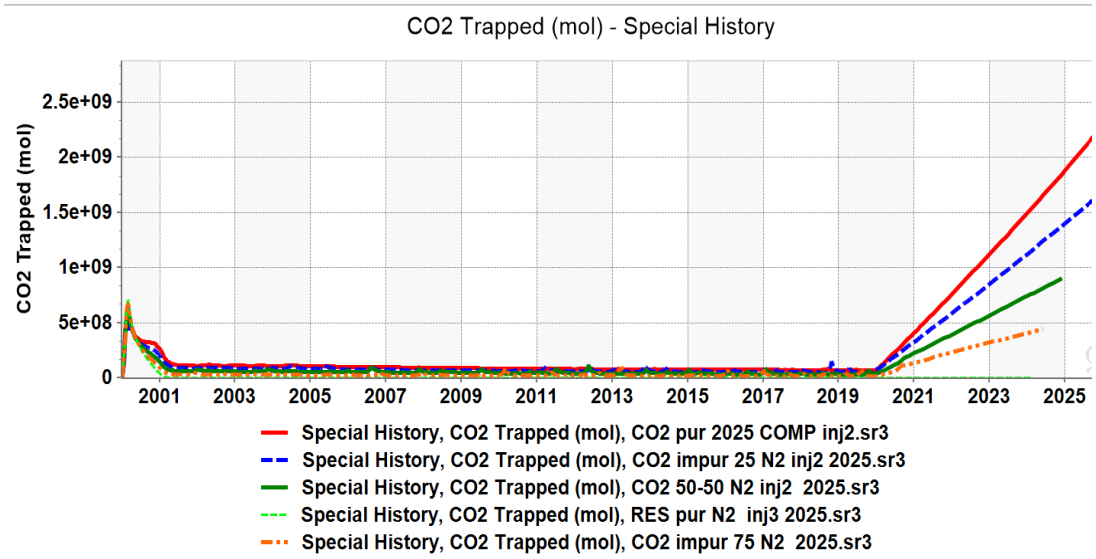


Figure 4.30. Comparison of $CO_2$ trapped for pure $CO_2$, impure $CO_2$, and pure $N_2$ injection scenarios vs time (generated by CMG Results, 2021).

**Sweep Efficiency:** The decline in sweep efficiency associated with contaminants in the $CO_2$ can be attributed to the viscosity of the oil. $N_2$ in the $CO_2$ stream hinder its ability to reduce the oil's viscosity, resulting in a faster migration of the injected gas. Consequently, the presence of $N_2$ leads to an increase in both viscosity

and interfacial tension of the oil, suggesting that reduced solvent capacity exists for the injected gas to lower the viscosity after multiple interactions. The subsequent figure reveals that an injection of 50% $N_2$ + 50%$CO_2$ results in higher oil saturation and, consequently, decreased the displacement sweep efficiency inside the reservoir.

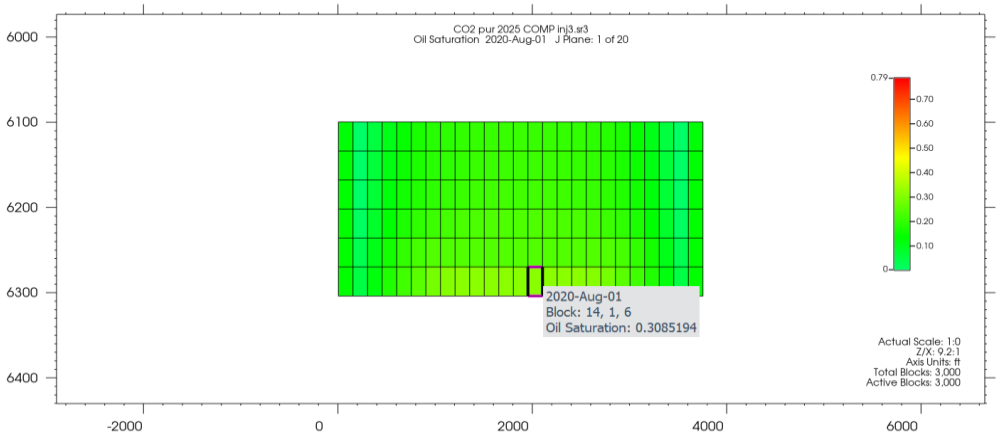


Figure 4.31. 2D aerial view of oil saturation for miscible pure $CO_2$ (generated by CMG Results, 2021).

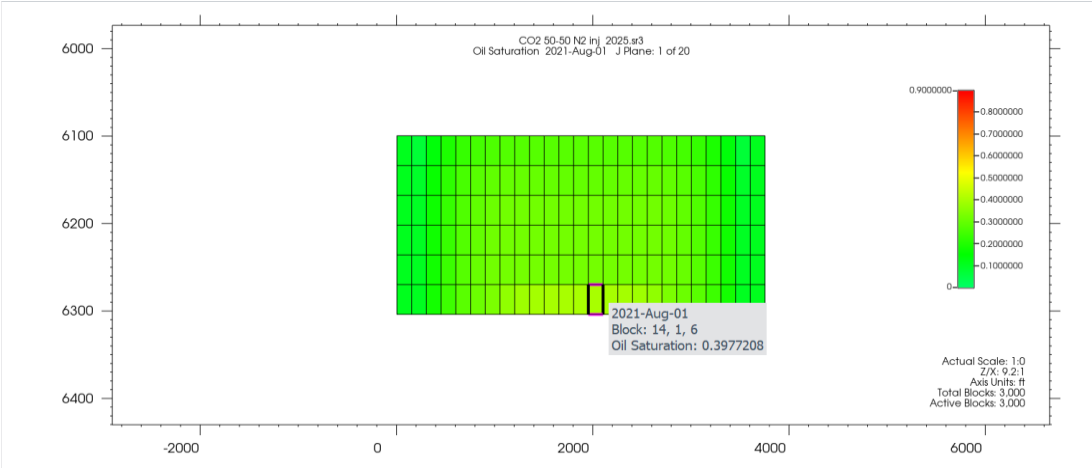


Figure 4.32. 2D aerial view of oil saturation for 50% $N_2$+ 50% $CO_2$ (generated by CMG Results, 2021).

**MMP:** The physical properties of gas can significantly influence both displacement and efficiency. In this study, the minimum miscibility pressure (MMP) of $CO_2$ with the reservoir fluid was determined using Winprop software and juxtaposed with the results obtained from the simulations. It is established that the purity level of $CO_2$ plays a crucial role in determining the MMP between oil and the injected solvent. Typically, the presence of nitrogen ($N_2$) within the $CO_2$ stream leads to an elevation

in the MMP. The outcomes from the MMP simulations with varying correlations of $CO_2$ and $N_2$ are presented in table 7. The inclusion of $N_2$ impurities correspondingly resulted in higher MMP values. Hence, any alterations in the gas's physical characteristics are likely to impact both the displacement efficiency and overall effectiveness of the process.

Table 4.5. MMP values from different correlations.

| Case | Cell to Cell | Tie Lines | Multiple Mixing |
|---|---|---|---|
| Pure $CO_2$ | 2575 psi | 1950 psi | 2623 psi |
| 75% $CO_2$ + 25% $N_2$ | 2700 psi | 2210 psi | 2900 psi |
| 50% $CO_2$ + 50% $N_2$ | 2920 psi | 2500 psi | 3200 psi |
| 25% $CO_2$ + 75% $N_2$ | 3080 psi | 2820 psi | 3600 psi |
| 100% $N_2$ | 3150 psi | 3000 psi | 4187 psi |

This table outlines an overview of three different techniques for multi-phase mixing in reservoirs. The multiple mixing cell method allows for an in-depth analysis of miscibility development through sequential contacts, making it ideal for detailed investigations where ample computational resources are accessible. On the other hand, the tie line method provides a simple and swift evaluation, although it may compromise accuracy when dealing with intricate mixtures. Lastly, the cell-to-cell simulation method portrays more realistic conditions within the reservoir but requires significant computational resources to implement effectively.

**Environmental Impacts of $CO_2$-EOR**

A lifecycle analysis of enhanced oil recovery indicates that $CO_2$ EOR approaches carbon neutrality, possesses a significant capacity for $CO_2$ storage, and

generates minimal process emissions. By mitigating risks associated with global warming, acidification, human toxicity, and eutrophication, as well as reducing waste and resource consumption, $CO_2$-EOR presents substantial environmental benefits compared to traditional oil extraction methods. Notably, one of the key advantages of sequestering $CO_2$ in oil reservoirs is their considerable storage capacity. Our research has revealed that the Arab-D reservoir can store approximately 2.4 x 10^9 moles of $CO_2$ , which is a highly significant. Furthermore, oil reservoirs also have the ability to capture impurities found in carbon dioxide. The data illustrate that a significant quantity of nitrogen ($N_2$) is sequestered within these oil reservoir, which positively influences the environment, as nitrogen is classified as one of the greenhouse gases. This sequestration plays a role in lessening greenhouse gas emissions that can deteriorate the ozone layer, with about 6.4 accounted for. Since oil reservoirs have been effectively retaining oil for millions of years, they also serve as efficient "traps" for $CO_2$ and $N_2$, offering a long operational lifespan that enhances safety considerations.

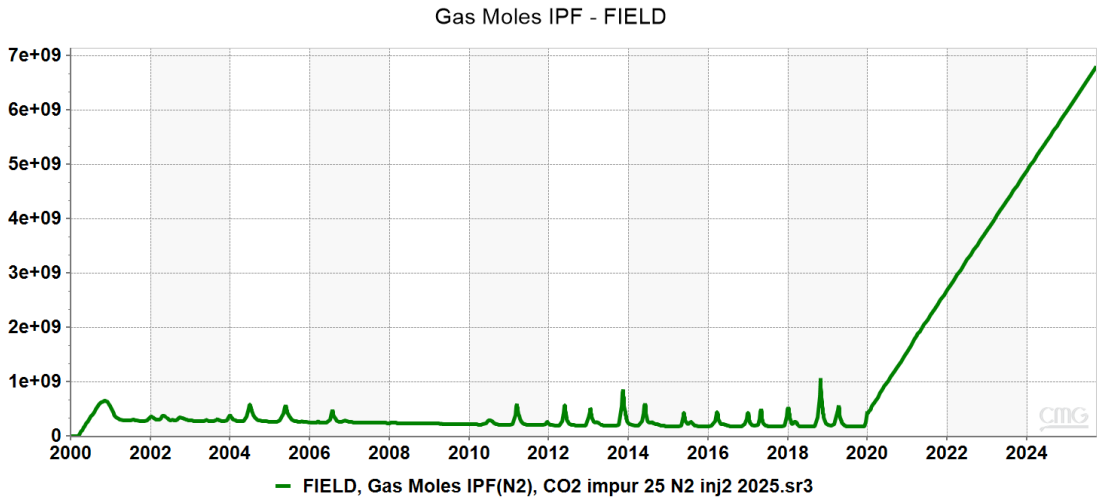


Figure 4.33. Cumulative $N_2$ trapped vs time for 25% $N_2$ + 75% $CO_2$ (generated by CMG Results, 2021).

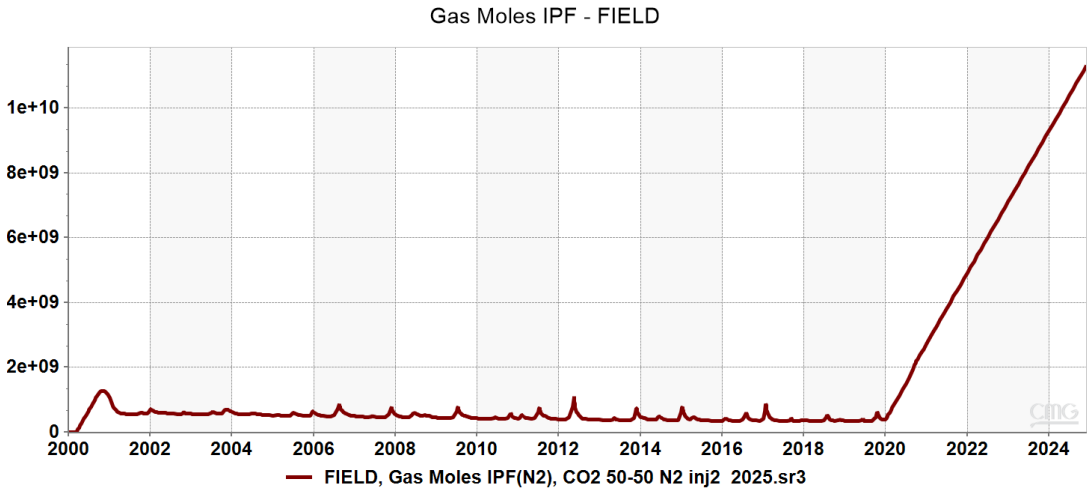


Figure 4.34. Cumulative $N_2$ trapped vs time for 50% $N_2$ + 50% $CO_2$ (generated by CMG Results, 2021).

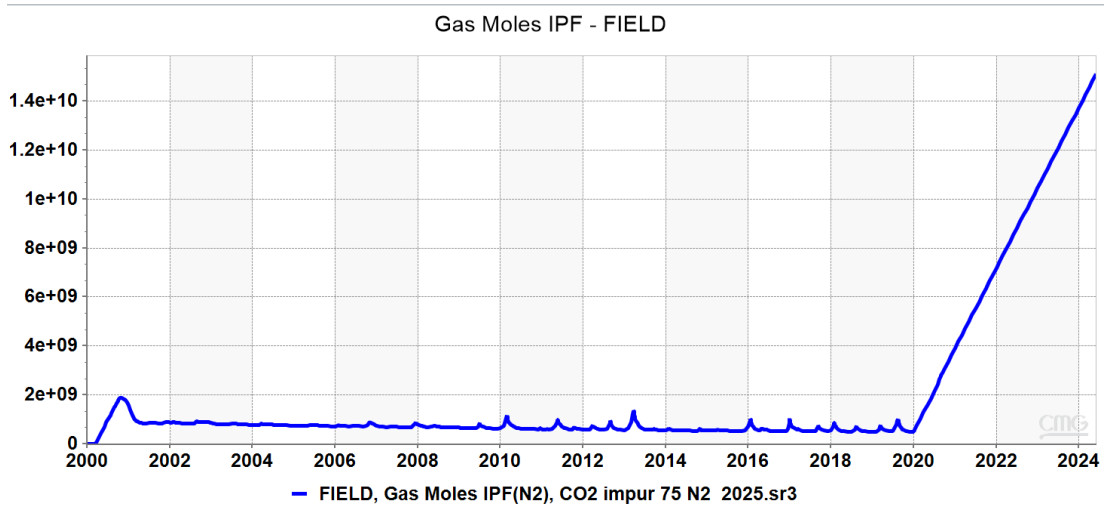


Figure 4.35. Cumulative $N_2$ trapped vs time for 75% $N_2$ + 25% $CO_2$ (generated by CMG Results, 2021).

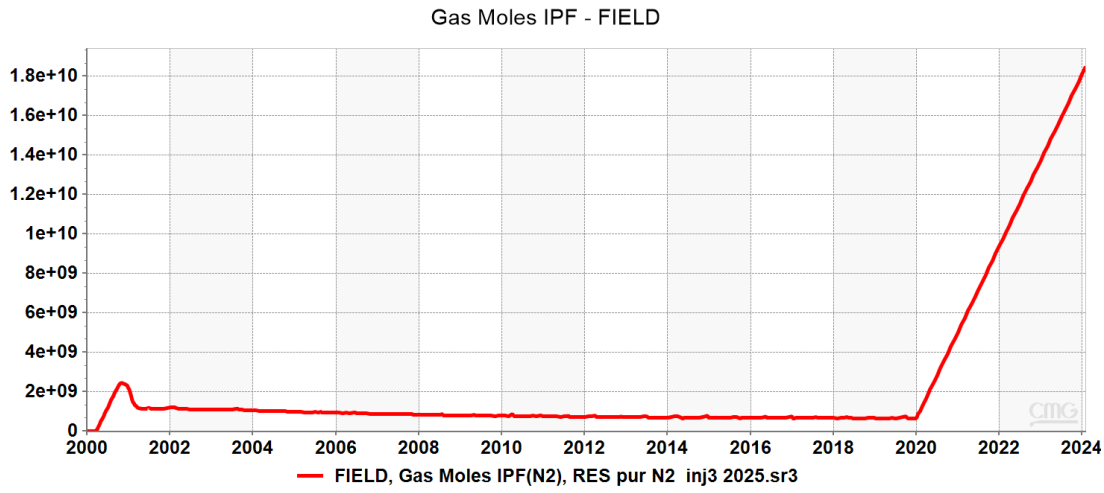


Figure 4.36 Cumulative $N_2$ trapped vs time for 100% $N_2$ (generated by CMG Results, 2021).

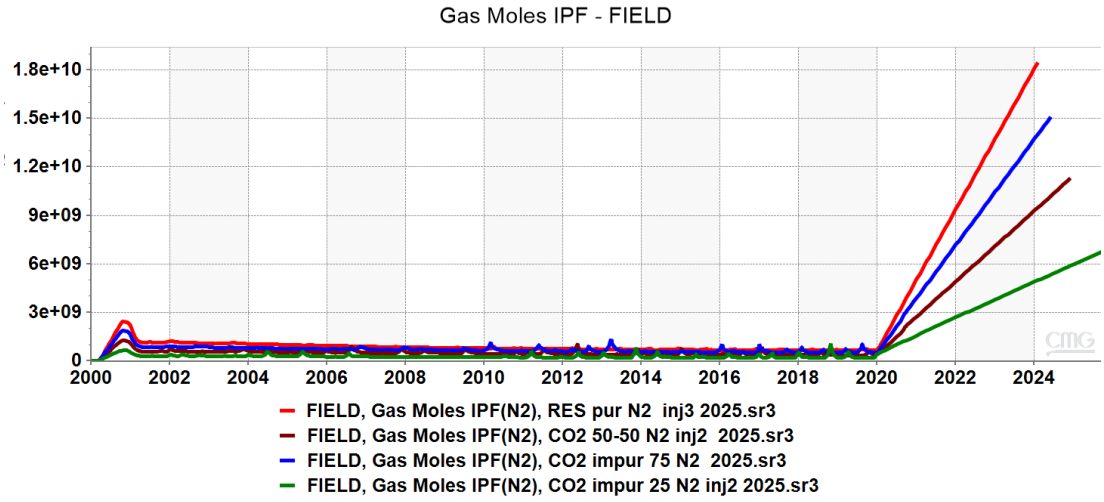


Figure 4.37. Comparison of $N_2$ trapped for injection scenarios vs time (generated by CMG Results, 2021).

The table below provides a detailed summary of the specific volumes of carbon dioxide and nitrogen that were effectively captured in the Arab-D reservoir during our research. This information not only demonstrates the high efficiency of our production rate but also highlights the reservoir's considerable storage capacity. Such capacity is essential as it plays a critical role in advancing environmental sustainability and supporting a healthier ecosystem. The subsequent table outlines the different volumes of carbon dioxide and nitrogen ($CO_2/N_2$) captured in the Arab-D reservoir throughout our modeling. This information showcases the notable production rate we achieved

while also emphasizing the reservoir's significant storage capability, which is instrumental in fostering a sustainable environment.

Table 4.6. Volume of $CO_2$/$N_2$ trapped for different scenarios.

| **Case** | **$CO_2$ trapped(mol)** | **$N_2$ trapped(mol)** |
|---|---|---|
| Pure $CO_2$ | $2.7*10^9$ | 0 |
| 75% $CO_2$ + 25% $N_2$ | $1.6*10^9$ | $6.8*10^9$ |
| 50% $CO_2$ + 50% $N_2$ | $9*10^8$ | $1.1*10^{10}$ |
| 25% $CO_2$ + 75% $N_2$ | $4.4*10^8$ | $1.5*10^{10}$ |
| 100% $N_2$ | 0 | $1.8*10^{10}$ |

# CHAPTER V
## Discussion

In reservoirs when natural energy is exhausted and only a tiny amount of economically viable oil can be produced, enhanced oil recovery is used. Injecting $CO_2$ helps to dissolve oil, reduce viscosity, and increase flow properties including surface area, wettability, etc. However, the miscibility and consequently the performance of the $CO_2$ are affected by the fluid composition, reservoir parameters, and pollutants present in the captured liquid. By storing $CO_2$ in subterranean reservoirs, EOR technology can help reduce rising carbon emissions and global warming. The findings of this study demonstrate that, in comparison to natural depletion, miscible flooding of pure $CO_2$ results in a very high oil recovery of 73.8%. Depending on the quantity of impurities in the $CO_2$, the impure $CO_2$ flood in the alternative model receives a lower overall recovery, ranging from 65 to 62%. This is because the presence of contaminants in the injected solvent causes the flooding process to have a poor mobility ratio, which raises the oil's viscosity. Nitrogen reduces displacement sweep efficiency and raises oil viscosity in the EOR process, which explains why $N_2$ injection has a 58% oil recovery in contrast.

In terms of cumulative oil produced, which is another crucial element to take into account when assessing the overall effectiveness of an EOR operation, pure $CO_2$ injection generated 38 MMbbl of cumulative oil. In contrast, the injection of impure $CO_2$ resulted in a total oil production of 35.6–36.4 MMbbbl respectively in descending order of nitrogen injection throughout the simulated years, while the injection of $N_2$ pure produced an oil of 35 MMbbl. Because of the miscibility of the gas injected with the reservoir oil, the pure $CO_2$ performance clearly shows the increased cumulative oil produced. Lastly, the impure $CO_2$ flood had an oil displacement sweeping efficiency of roughly 40–50%. However, the removal of contaminants from $CO_2$ will result in a 70–75% increase in oil displacement sweeping efficiency. Finally, our results demonstrated that miscible pure $CO_2$ injection performed better than impure $CO_2$ injection.

In their research, Fong et al. (2016) investigated how various gas mixtures influence oil recovery, focusing on a blend comprising 80% nitrogen and 20% carbon

dioxide. Their results showed a significant reduction in recovery efficiency, with merely 23% of the oil initially in place (OOIP) being extracted, compared to a much higher 56% recovery rate achieved using pure carbon dioxide. This outcome aligns with the trends observed in our research, as the early breakthrough of gas in nitrogen-rich mixtures underscores the considerable challenges and inefficiencies related to nitrogen's role in oil recovery processes.

In a similar vein, Spivak and Chima (2019) analyzed a mixture of 82% carbon dioxide and 18% nitrogen. Their findings revealed that this combination also resulted in lower recovery rates and earlier gas breakthroughs than those achieved with pure carbon dioxide. The limited ability of nitrogen to dissolve in Wilmington oil further compromised the overall efficiency of carbon dioxide solubility, leading to reduced performance which are therefore compatibles with the results of our investigation.

Additionally, Nguyen and Ali (1998) looked into the effects of replacing pure carbon dioxide with an impure version in the water-alternating-gas (WAG) method. Their study indicated that such a substitution could cause oil recovery losses of up to 10% due to a high concentration of nitrogen. In contrast, our findings show a loss of 25.8% when comparing pure nitrogen to pure carbon dioxide. This highlights the detrimental effects that elevated nitrogen levels and impurities within gas mixtures have on recovery efficiency, further demonstrating that scenarios utilizing pure carbon dioxide yield significantly improved results in oil extraction processes.

In summary, the collective evidence from these studies illustrates that the incorporation of nitrogen and other impurities in gas mixtures consistently leads to reduced oil recovery rates and operational difficulties when compared to scenarios involving pure carbon dioxide.

To produce high purity $CO_2$, impurities collected with it undergo a purification step, which raises the capture cost considerably. Injecting the $CO_2$ and impurities together is hence economical. On the other hand, impure $CO_2$ has a negative impact on $CO_2$-EOR performance, which leads to less oil recovery. The variation in oil recovery based on the degree of purity will be managed and taken into account. Even though it was not taken into account in this study, it is crucial to create an economic model that uses economic factors like capital expenditures (CAPEX), operating expenditures (OPEX), tax credits, oil price, and $CO_2$ price depending on the purity

level, sources, and technology in order to estimate the proper purity level of the $CO_2$ stream. Field applications need the development of a design for each site, including various injection scenarios, based on economic analysis because the best operating conditions to boost CCS-EOR performance rely on the reservoir's features.

# CHAPTER VI
## Conclusion and Recommendations

This thesis's numerous investigations have illustrated how various parameters affect the use of miscible $\mathbf{CO_2}$ flooding as an EOR method in addition to other CCS strategies. The primary findings of this study are presented in this chapter. Furthermore, some suggestions are made for further research so that the scientists can better understand how to predict the injection of $\mathbf{CO_2}$ miscible gas to enhance oil recovery.

## Conclusion

For the purpose of addressing the world's energy shortfall, the petroleum and natural gas industries' adoption of improved oil recovery has greatly boosted the production of hydrocarbons. Injecting chemicals to enhance oil recovery or storing $CO_2$ underground to lower carbon emissions into the atmosphere are only two of the methods. The purpose of the simulation was to predict the oil recovery, production rates, and pressure in the Ghawar oil field under miscible gas injection. A model may be constructed or run many times at low cost in a short amount of time, but the field can only be produced once at high cost. In order to draw a conclusion following successful simulations, it was determined that miscible pure $CO_2$ injection has significantly increased oil recovery based on the various scenarios used for this project, ranging from the no injection scenario to the $N_2$ flooding scenarios. As a result, this strengthens the reservoir and delays its early depletion.

- In addition to the oil recovery of 73.8% and cumulative oil production of 38 MMbbl, the pure miscible $CO_2$ model appears to be substantially larger than the basic model and the various injections of impure $CO_2$.
- In contrast to the 73.8% OOIP recovery attained during our investigation, a study using 100% pure carbon dioxide revealed that 56% OOIP was recovered (Fong et al., 2000).
- At the same injection pressure of 3212 psi, the gas with the highest oil recovery factor was $CO_2$, whereas the gas with the lowest oil recovery factor was $N_2$.

Furthermore, compared to $CO_2$, which had the longest breakthrough time and the lowest MMP, $N_2$ had the quickest breakthrough time and the highest MMP. This is because $CO_2$ has a greater absorptive capacity and is hence condensable, whereas $N_2$ has a very low adsorptive capacity and is consequently a non-condensable gas.

- The injection of pure nitrogen lowered the overall CCS performance by 38% compared to pure carbon dioxide injection. The Arab-D reservoir has also caught $2.7 * 10^9$ mol of $CO_2$ and $1.8*10^{10}$ mol of $N_2$ corresponding respectively to $1.1 * 10^5$ tonnes and $5.04 * 10^5$ tonnes, in addition to producing a very high oil recovery after the injection of pure $CO_2$.

## Recommendations

### Recommendations According to Findings

- Additionally, a global opportunity for carbon capture and sequestration (CCS) is offered by the injection of miscible gas ($CO_2$). This CCS approach can be further modeled by adopting and improving the model.
- Adequate field data and laboratory work are necessary to effectively model EOR projects using CMG software, particularly as it entails the use of solvents and other chemicals and nanomaterials.

### Recommendations for Further Research

- Even though miscible pure $CO_2$ injection produced the highest oil recovery, it is still advantageous to do an economic analysis to determine the cost per barrel of purification in order to assess the investment's viability. Future studies may focus on this topic.

## References

Abbasi, S., Tavakkolian, M., & Shahrabadi, A. (2010). Investigation of Effect of Gas Injection Pressure on Oil Recovery Accompanying CO2 Increasing in Injection Gas Composition. Nigeria Annual International Conference and Exhibition. Nigeria Annual International Conference and Exhibition, Calabar, Nigeria. https://doi.org/10.2118/140749-ms

Abdullah, N., & Hasan, N. (2021). Effects of miscible CO2 injection on production recovery. Journal of Petroleum Exploration and Production Technology, 11(9), 3543–3557. https://doi.org/10.1007/s13202-021-01223-0

Adekunle, O., & Hoffman, B. T. (2016). Experimental and analytical methods to determine minimum miscibility pressure (MMP) for Bakken formation crude oil. Journal of Petroleum Science and Engineering, 146, 170–182. https://doi.org/10.1016/j.petrol.2016.04.013

Agarwal, R., & Liu, D. (2024). Introduction to modeling, simulation and optimization of CO2 sequestration in various types of reservoirs. Elsevier.

Ahmadi, K., & Johns, R. T. (2011). Multiple-Mixing-Cell method for MMP calculations. SPE Journal, 16(04), 733–742. https://doi.org/10.2118/116823-pa

Alston, R. B., Kokolis, G. P., & James, C. F. (1985). CO2 Minimum Miscibility Pressure: A Correlation for Impure CO2 Streams and Live Oil Systems. Society of Petroleum Engineers Journal, 25(02), 268–274. https://doi.org/10.2118/11959-pa

Bachu, S. (2016). Identification of oil reservoirs suitable for CO 2 -EOR and CO 2 storage (CCUS) using reserves databases, with application to Alberta, Canada. International Journal of Greenhouse Gas Control, 44, 152–165. https://doi.org/10.1016/j.ijggc.2015.11.013

Benham, A. L., Dowden, W. E., & Kunzman, W. J. (1960). Miscible Fluid Displacement - Prediction of Miscibility. Transactions of the AIME, 219(01), 229–237. https://doi.org/10.2118/1484-g

Bon, J., Sarma, H. K., & Theophilos, A. M. (2005). An investigation of minimum miscibility pressure for CO2 - rich injection gases with pentanes-plus fraction. All Days. https://doi.org/10.2118/97536-ms

Chen, G., Gao, H., Fu, K., Zhang, H., Liang, Z., & Paitoon Tontiwachwuthikul. (2020). An improved correlation to determine minimum miscibility pressure

of CO2–oil system. Green Energy & Environment, 5(1), 97–104. https://doi.org/10.1016/j.gee.2018.12.003

Chen, S. M., & Cheung, V. (1983). Ternary diagram plotting software design using the “Tie-Line slope” method. Journal of Canadian Petroleum Technology, 22(01). https://doi.org/10.2118/83-01-03

Chen, Y., & Voskov, D. (2019). Optimization of CO2 injection using multi-scale reconstruction of composition transport. Computational Geosciences, 24(2), 819–835. https://doi.org/10.1007/s10596-019-09841-8

Chequer, L., Al-Shuaili, K., Genolet, L., Behr, A., Kowollik, P., Zeinijahromi, A., & Bedrikovetsky, P. (2019). Optimal slug size for enhanced recovery by low-salinity waterflooding due to fines migration. Journal of Petroleum Science and Engineering, 177, 766–785. https://doi.org/10.1016/j.petrol.2019.02.079

Dai, Z., Middleton, R., Viswanathan, H., Fessenden-Rahn, J., Bauman, J., Pawar, R., Lee, S.-Y., & McPherson, B. (2013). An integrated framework for optimizing CO2 sequestration and enhanced oil recovery. Environmental Science & Technology Letters, 1(1), 49–54. https://doi.org/10.1021/ez4001033

Dicharry, R. M., Perryman, T. L., & Ronquille, J. D. (1973). Evaluation and Design of a CO2 Miscible Flood Project-SACROC Unit, Kelly-Snyder Field. Journal of Petroleum Technology, 25(11), 1309–1318. https://doi.org/10.2118/4083-pa

Dipesh Niraula, Issam El Naqa, Jack Adam Tuszynski, & Gatenby, R. A. (2024). Modeling non-genetic information dynamics in cells using reservoir computing. IScience, 27(4), 109614–109614. https://doi.org/10.1016/j.isci.2024.109614

E. Shtepani. (2007). Experimental and modeling requirements for compositional simulation of miscible CO2-EOR processes. All Days. https://doi.org/10.2118/111290-ms

Filonchyk, M., Peterson, M. P., Zhang, L., Hurynovich, V., & He, Y. (2024). Greenhouse gases emissions and global climate change: Examining the influence of CO2, CH4, and N2O. Science of the Total Environment, 935, 173359–173359. https://doi.org/10.1016/j.scitotenv.2024.173359

Haddadnia, A., Zirrahi, M., Hassanzadeh, H., & Abedi, J. (2017). Solubility and thermo-physical properties measurement of CO 2 - and N 2 -Athabasca

bitumen systems. Journal of Petroleum Science and Engineering, 154, 277–283. https://doi.org/10.1016/j.petrol.2017.04.035

Hamimi, Z., Fowler, A.-R., LiégeoisJ.-P., Collins, A., Abdelsalam, M. G., & Abd EI-Wahed, M. (2021). The geology of the Arabian-Nubian Shield. Springer.

Hassan, A., Elkatatny, S., & Abdulraheem, A. (2019). Intelligent Prediction of Minimum Miscibility Pressure (MMP) During CO2 Flooding Using Artificial Intelligence Techniques. Sustainability, 11(24), 7020. https://doi.org/10.3390/su11247020

Holm, L. W. (1959). Carbon dioxide solvent flooding for increased oil recovery. Transactions of the AIME, 216(01), 225–231. https://doi.org/10.2118/1250-g

Hu, Y., Hao, M., Chen, G., Sun, R., & Li, S. (2019). Technologies and practice of CO2 flooding and sequestration in China. Petroleum Exploration and Development, 46(4), 753–766. https://doi.org/10.1016/S1876-3804(19)60233-8

Joslin, K., Ghedan, S. G., Abraham, A., & Pathak, V. (2017). EOR in tight reservoirs, technical and economical feasibility. https://doi.org/10.2118/185037-ms

Kabir, M., Habiba, U. E., Khan, W., Shah, A., Rahim, S., Farooqi, Z.-U.-R., Muhammad Zafar Iqbal, & Shafiq, M. (2023). Climate change due to increasing concentration of carbon dioxide and its impacts on environment in 21st century; a mini review. Journal of King Saud University - Science, 35(5), 102693–102693. https://doi.org/10.1016/j.jksus.2023.102693

Klins, M. A. (1984). CO2 — heavy oil flooding — economic design. Heavy Crude Oil Recovery, 211–272. https://doi.org/10.1007/978-94-009-6140-1_7

Leslie, J. D. (1943). Graphical interconversions for multicomponent systems. Industrial & Engineering Chemistry, 35(4), 495–496. https://doi.org/10.1021/ie50400a023

Massarweh, O., & Abushaikha, A. S. (2021). A review of recent developments in CO2 mobility control in enhanced oil recovery. Petroleum. https://doi.org/10.1016/j.petlm.2021.05.002

Nguyen, T. A., & Ali, S. M. F. (1998). Effect of nitrogen on the solubility and diffusivity of carbon dioxide into oil and oil recovery by the immiscible WAG process. Journal of canadian petroleum technology, 37(02). https://doi.org/10.2118/98-02-02

Ren, B., & Duncan, I. J. (2019). Reservoir simulation of carbon storage associated with CO2 EOR in residual oil zones, San Andres formation of West Texas, permian basin, USA. Energy, 167, 391–401. https://doi.org/10.1016/j.energy.2018.11.007

Rezk, M. G., Foroozesh, J., Zivar, D., & Mumtaz, M. (2019). CO2 storage potential during CO2 enhanced oil recovery in sandstone reservoirs. Journal of Natural Gas Science and Engineering, 66, 233–243. https://doi.org/10.1016/j.jngse.2019.04.002

Saner, S., Al-Hinai, K., & Perincek, D. (2005). Surface expressions of the Ghawar structure, Saudi Arabia. Marine and Petroleum Geology, 22(5), 657–670. https://doi.org/10.1016/j.marpetgeo.2004.12.006

Simon, R. (1981). Enhanced oil recovery: Definitions, fundamentals, applications, and research frontiers. Physics and Chemistry of the Earth, 13-14, 447–460. https://doi.org/10.1016/0079-1946(81)90022-7

Siregar, S., Hidayaturobbi, A. D., Wijaya, B. A., Listiani, S. N., T. Adiningrum, Irwan Irwan, & Pratomo, A. I. (2007). Laboratory experiments on enhanced oil recovery with nitrogen injection. ITB Journal of Engineering Science, 39(1), 20–27. https://doi.org/10.5614/itbj.eng.sci.2007.39.1.2

Sultan, M., Sturchio, N. C., Alsefry, S., Emil, M. K., Ahmed, M., Abdelmohsen, K., AbuAbdullah, M. M., Yan, E., Save, H., Alharbi, T., Othman, A., & Chouinard, K. (2019). Assessment of age, origin, and sustainability of fossil aquifers: A geochemical and remote sensing-based approach. Journal of Hydrology, 576, 325–341. https://doi.org/10.1016/j.jhydrol.2019.06.017

Thomas, S. (2007). Enhanced oil recovery - an overview. Oil & Gas Science and Technology - Revue de L'IFP, 63(1), 9–19. https://doi.org/10.2516/ogst:2007060

Tileuberdi, N., & Gussenov, I. (2024). Review on miscible, immiscible, and progressive nitrogen injection for enhanced oil recovery. Energy Reports, 12, 360–367. https://doi.org/10.1016/j.egyr.2024.06.004

Wald, E. R. (2018). Saudi, Inc.: The Arabian Kingdom's Pursuit of Profit and Power. Simon and Schuster.

Yu, Y., & Sheng, J. J. (2016). Experimental evaluation of shale oil recovery from eagle ford core samples by nitrogen gas flooding. All Days. https://doi.org/10.2118/179547-ms

Zhang, N., Yin, M., Wei, M., & Bai, B. (2019). Identification of CO2 sequestration opportunities: CO2 miscible flooding guidelines. Fuel, 241, 459–467. https://doi.org/10.1016/j.fuel.2018.12.072

Zhao, Y., Fan, G., Song, K., Li, Y., Chen, H., & Sun, H. (2021). The experimental research for reducing the minimum miscibility pressure of carbon dioxide miscible flooding. Renewable & Sustainable Energy Reviews, 145, 111091–111091. https://doi.org/10.1016/j.rser.2021.111091

Zick, A. A. (1986, October 5). A combined condensing/vaporizing mechanism in the displacement of oil by enriched gases. Onepetro.org; OnePetro. https://doi.org/10.2118/15493-MS

# Appendices

## Appendix A

**Modeling Miscible $CO_2/N_2$ Injection for Enhanced Oil Recovery CMG GEM Data**

INUNIT FIELD

WSRF WELL 1

WSRF GRID TIME

OUTSRF GRID PRES SG SIG SO SW VISO

OUTSRF RES NONE

OUTSRF WELL GHGSOL

GHGTHY

PAVG

RECG

RECO

WPRN GRID 0

OUTPRN GRID NONE

OUTPRN RES NONE

Definition of fundamental cartesian grid

**GRID VARI 25 20 6**

KDIR DOWN

DI IVAR

25*150

DJ JVAR

20*150

DK ALL

3000*34

DTOP

500*6100

XOFFSET 0.0000

YOFFSET 0.0000

ROTATION 0.0000

AXES-DIRECTIONS 1.0 -1.0 1.0

NULL CON 1

POR CON 0.19

PERMI CON 617

PERMJ CON 617

PERMK CON 61

PINCHOUTARRAY CON 1

PRPOR 2500

CPOR 0.000004

The following is the fluid component

property data in GEM format.

The unit system and fluid compositions should

be specified in the I/O control section.

The units and compositions specified in WinProp

are included here as comments for informational purposes.

PVT UNITS CONSISTENT WITH *INUNIT *FIELD

COMPOSITION PRIMARY

0.01590000 0.34280000 0.07520000 0.05640000 0.00970000

0.02490000 0.01100000 0.01410000 0.01970000 0.43030000

COMPOSITION *SECOND

1.00000000 0.00000000 0.00000000 0.00000000 0.00000000

0.00000000 0.00000000 0.00000000 0.00000000 0.00000000

Model and number of components

**MODEL PR**

NC 10 10

COMPNAME 'CO2' 'CH4' 'C2H6' 'C3H8' 'IC4' 'NC4' 'IC5' 'NC5' 'FC6' 'C7+'

The Hydrocarbon component flag values: 1 - Hydro-Carbon, 0 - non Hydro-Carbon

The read-in HC-HC BIN values will be overwritten by the internal GEM calculated

values for these HC-HC pairs, if the original *HCFLAG values are used.

This is fine if there is only 1 HC-HC group defined in the original WinProp

data set. Otherwise, all-zero *HCFLAG will be output here in order to use the

full read-in BIN values.

The original WinProp HC-flags:

HCFLAG 3 1 1 1 1 1 1 1 1 1

HCFLAG

0 1 1 1 1 1 1 1 1 1

TRES 215.00000

PVC3 1.20000000E+00

VISCOR HZYT

MIXVC 1.0000000E+00

VISCOEFF

1.0230000E-01 2.3364000E-02 5.8533000E-02 -4.0758000E-02 9.3324000E-03

MW

4.4010000E+01 1.6043000E+01 3.0070000E+01 4.4097000E+01 5.8124000E+01
5.8124000E+01 7.2151000E+01 7.2151000E+01 8.6000000E+01 2.1500000E+02

AC

2.2500000E-01 8.0000000E-03 9.8000000E-02 1.5200000E-01 1.7600000E-01 1.9300000E-
01 2.2700000E-01 2.5100000E-01 2.7504000E-01 6.6096582E-01

PCRIT

7.2800000E+01 4.5400000E+01 4.8200000E+01 4.1900000E+01 3.6000000E+01
3.7500000E+01 3.3400000E+01 3.3300000E+01 3.2460000E+01 1.5284295E+01

VCRIT

9.4000000E-02 9.9000000E-02 1.4800000E-01 2.0300000E-01 2.6300000E-01 2.5500000E-01 3.0600000E-01 3.0400000E-01 3.4400000E-01 8.9560826E-01

TCRIT

3.0420000E+02 1.9060000E+02 3.0540000E+02 3.6980000E+02 4.0810000E+02 4.2520000E+02 4.6040000E+02 4.6960000E+02 5.0750000E+02 7.2382387E+02

PCHOR

7.8000000E+01 7.7000000E+01 1.0800000E+02 1.5030000E+02 1.8150000E+02 1.8990000E+02 2.2500000E+02 2.3150000E+02 2.5010880E+02 5.8135500E+02

SG

8.1800000E-01 3.0000000E-01 3.5600000E-01 5.0700000E-01 5.6300000E-01 5.8400000E-01 6.2500000E-01 6.3100000E-01 6.9000000E-01 8.0000000E-01

TB

-1.0921000E+02 -2.5861000E+02 -1.2757000E+02 -4.3690000E+01 1.0670000E+01 3.1190000E+01 8.2130000E+01 9.6890000E+01 1.4693000E+02 5.3421523E+02

OMEGA

4.5723553E-01 4.5723553E-01 4.5723553E-01 4.5723553E-01 4.5723553E-01 4.5723553E-01 4.5723553E-01 4.5723553E-01 4.5723553E-01 4.5723553E-01

OMEGB

7.7796074E-02 7.7796074E-02 7.7796074E-02 7.7796074E-02 7.7796074E-02 7.7796074E-02 7.7796074E-02 7.7796074E-02 7.7796074E-02 7.7796074E-02

VSHIFT

0.0000000E+00 0.0000000E+00 0.0000000E+00 0.0000000E+00 0.0000000E+00 0.0000000E+00 0.0000000E+00 0.0000000E+00 0.0000000E+00 0.0000000E+00

HEATING_VALUES

0.0000000E+00 8.4429001E+02 1.4784600E+03 2.1051600E+03 2.7115400E+03 2.7115400E+03 3.3536600E+03 3.3536600E+03 3.9759100E+03 0.0000000E+00

VISVC

9.4000000E-02 9.9000000E-02 1.4800000E-01 2.0300000E-01 2.6300000E-01 2.5500000E-01 3.0600000E-01 3.0400000E-01 3.4400000E-01 8.9560826E-01

BIN

1.0500000E-01

1.3000000E-01 2.6890022E-03

1.2500000E-01 8.5370405E-03 1.6620489E-03

1.2000000E-01 1.5715316E-02 5.4857876E-03 1.1165976E-03

1.1500000E-01 1.4748531E-02 4.9143360E-03 8.6625350E-04 1.5903506E-05

1.1500000E-01 2.0878892E-02 8.7338646E-03 2.8007353E-03 3.8207590E-04 5.5378054E-04

1.1500000E-01 2.0640839E-02 8.5779330E-03 2.7121325E-03 3.4971119E-04 5.1467786E-04 7.1665797E-07

1.1500000E-01 2.5345101E-02 1.1747825E-02 4.6198099E-03 1.2003051E-03 1.4920539E-03 2.2833006E-04 2.5462307E-04

0.0000000E+00 7.6042151E-02 5.1834174E-02 3.5697700E-02 2.4546345E-02 2.5774365E-02 1.8938276E-02 1.9166794E-02 1.5080614E-02

ENTHCOEF

9.6880000E-02 1.5884300E-01 -3.3712000E-05 1.4810500E-07 -9.6620300E-11 2.0738320E-14

-2.8385700E+00 5.3828500E-01 -2.1140900E-04 3.3927600E-07 -1.1643220E-10 1.3896120E-14

-1.4220000E-02 2.6461200E-01 -2.4568000E-05 2.9140200E-07 -1.2810330E-10 1.8134820E-14

6.8715000E-01 1.6030400E-01 1.2608400E-04 1.8143000E-07 -9.1891300E-11 1.3548500E-14

1.4595600E+00 9.9070000E-02 2.3873600E-04 9.1593000E-08 -5.9405000E-11 9.0964500E-15

7.2281400E+00 9.9687000E-02 2.6654800E-04 5.4073000E-08 -4.2926900E-11 6.6958000E-15

1.7694120E+01 1.5946000E-02 3.8244900E-04 -2.7557000E-08 -1.4303500E-11 2.9567700E-15

9.0420900E+00 1.1182900E-01 2.2851500E-04 8.6331000E-08 -5.4464900E-11 8.1845000E-15

0.0000000E+00 -1.6543463E-02 4.1169069E-04 -5.7742757E-08 0.0000000E+00 0.0000000E+00

0.0000000E+00 2.2135278E-03 3.9756979E-04 -5.3302731E-08 0.0000000E+00
0.0000000E+00

CW 0.000004

REFPW 2500

SOLUBILITY HENRY

TRACE-COMP 2

** HENRYC calculated at 215.00 deg F

HENRYC

8.4206782E+04 0 1.2941741E+06 1.8308289E+06 2.1086164E+06 2.1088205E+06
4.8095508E+06 4.8677661E+06 1.4695949E+21 1.4695949E+21

REFPH

2.1960000E+03 2.1960000E+03 2.1960000E+03 2.1960000E+03 2.1960000E+03
2.1960000E+03 2.1960000E+03 2.1960000E+03 2.1960000E+03 2.1960000E+03

VINFINITY

3.5668181E-02 0 5.2487562E-02 7.1896258E-02 9.1466009E-02 9.1485931E-02
1.1055231E-01 1.1302877E-01 1.2497583E-01 3.7227583E-01

HENRY-MOD1-CO2

BIN-TDEP-CO2

AQUEOUS-DENSITY *LINEAR

**ROCKFLUID**

HYS_MODEL LINEAR

RPT 1

Sw krw krow

SWT

0.21 0 0.8

0.225 0.00117187 0.703125

0.25 0.0046875 0.6125

0.275 0.0105469 0.528125

0.3 0.01875 0.45

0.325 0.0292969 0.378125

0.35 0.0421875 0.3125

0.375 0.0574219 0.253125

0.4 0.075 0.2

0.425 0.0949219 0.153125

0.45 0.117187 0.1125

0.475 0.141797 0.078125

0.5 0.16875 0.05

0.525 0.198047 0.028125

0.55 0.229688 0.0125

0.575 0.263672 0.003125

0.6 0.3 0

** Sl krg krog

SLT

0.4 0.3 0

0.434375 0.263672 0.003125

0.46875 0.229688 0.0125

0.503125 0.198047 0.028125

0.5375 0.16875 0.05

0.571875 0.141797 0.078125

0.60625 0.117188 0.1125

0.640625 0.0949219 0.153125

0.675 0.075 0.2

0.709375 0.0574219 0.253125

0.74375 0.0421875 0.3125

0.778125 0.0292969 0.378125

0.8125 0.01875 0.45

0.846875 0.0105469 0.528125

0.88125 0.0046875 0.6125

0.915625 0.00117188 0.703125

0.95 0 0.8

HYSKRG

**INITIAL**

VERTICAL BLOCK_CENTER WATER_OIL_GAS

ZOIL

0.0159 0.3428 0.0752 0.0564 0.0097 0.0249 0.011 0.0141 0.0197 0.4303

ZGAS

0 0.3 0.07 0.06 0.0093 0.02 0.011 0.01 0.0197 0.5

REFPRES

2500

REFDEPTH

6100

DWOC

6600

DGOC

6000

**NUMERICAL**

DTMAX 1000000

DTMIN 0.000001

NORM UNKNOWN

MAXCHANGE TEMP 15

CONVERGE PRESS 0.01

**RUN**

```
DATE 2000 1 1

WELL  'inj'

INJECTOR 'inj'

INCOMP  SOLVENT  1.0  0.0  0.0  0.0  0.0  0.0  0.0  0.0  0.0  0.0

OPERATE  MAX  STG  10000000.0  CONT REPEAT

OPERATE  MAX  BHP  2000.0  CONT REPEAT

 rad  geofac  wfrac  skin

GEOMETRY  K  0.25  0.37  1.0  0.0

PERF     GEOA  'inj'

UBA            ff        Status  Connection

13 10 1        1.0  OPEN    FLOW-FROM  'SURFACE'  REFLAYER

13 10 2        1.0  OPEN    FLOW-FROM  1

13 10 3        1.0  OPEN    FLOW-FROM  2

13 10 4        1.0  OPEN    FLOW-FROM  3

13 10 5        1.0  OPEN    FLOW-FROM  4

13 10 6        1.0  OPEN    FLOW-FROM  5

LAYERXYZ  'inj'

perf geometric data: UBA, block entry(x,y,z) block exit(x,y,z), length

13 10 1  1875.000000  1425.000000  6100.000000  1875.000000  1425.000000
6134.000000  34.000000

13 10 2  1875.000000  1425.000000  6134.000000  1875.000000  1425.000000
6168.000000  34.000000

13 10 3  1875.000000  1425.000000  6168.000000  1875.000000  1425.000000
6202.000000  34.000000

13 10 4  1875.000000  1425.000000  6202.000000  1875.000000  1425.000000
6236.000000  34.000000

13 10 5  1875.000000  1425.000000  6236.000000  1875.000000  1425.000000
6270.000000  34.000000

13 10 6  1875.000000  1425.000000  6270.000000  1875.000000  1425.000000
6304.000000  34.000000
```

OPEN 'inj'

WELL 'prod'

PRODUCER 'prod'

OPERATE MAX STO 15000.0 CONT

OPERATE MIN BHP 28.0 CONT

rad geofac wfrac skin

GEOMETRY K 0.25 0.37 1.0 0.0

PERF GEOA 'prod'

UBA ff Status Connection

2 19 1 1.0 OPEN FLOW-TO 'SURFACE' REFLAYER

2 19 2 1.0 OPEN FLOW-TO 1

2 19 3 1.0 OPEN FLOW-TO 2

2 19 4 1.0 OPEN FLOW-TO 3

2 19 5 1.0 OPEN FLOW-TO 4

2 19 6 1.0 OPEN FLOW-TO 5

LAYERXYZ 'prod'

perf geometric data: UBA, block entry(x,y,z) block exit(x,y,z), length

2 19 1 225.000000 2775.000000 6100.000000 225.000000 2775.000000 6134.000000 34.000000

2 19 2 225.000000 2775.000000 6134.000000 225.000000 2775.000000 6168.000000 34.000000

2 19 3 225.000000 2775.000000 6168.000000 225.000000 2775.000000 6202.000000 34.000000

2 19 4 225.000000 2775.000000 6202.000000 225.000000 2775.000000 6236.000000 34.000000

2 19 5 225.000000 2775.000000 6236.000000 225.000000 2775.000000 6270.000000 34.000000

2 19 6 225.000000 2775.000000 6270.000000 225.000000 2775.000000 6304.000000 34.000000

OPEN 'prod'

```
WELL  'prod2'

PRODUCER 'prod2'

OPERATE  MAX  STO  15000.0  CONT

OPERATE  MIN  BHP  28.0  CONT

 rad  geofac  wfrac  skin

GEOMETRY  K  0.25  0.37  1.0  0.0

PERF     GEOA  'prod2'

UBA           ff        Status  Connection

24 2 1       1.0  OPEN    FLOW-TO  'SURFACE'  REFLAYER

24 2 2       1.0  OPEN    FLOW-TO  1

24 2 3       1.0  OPEN    FLOW-TO  2

24 2 4       1.0  OPEN    FLOW-TO  3

24 2 5       1.0  OPEN    FLOW-TO  4

24 2 6       1.0  OPEN    FLOW-TO  5

LAYERXYZ  'prod2'

perf geometric data: UBA, block entry(x,y,z) block exit(x,y,z), length

24 2 1  3525.000000  225.000000  6100.000000  3525.000000  225.000000  6134.000000
34.000000

24 2 2  3525.000000  225.000000  6134.000000  3525.000000  225.000000  6168.000000
34.000000

24 2 3  3525.000000  225.000000  6168.000000  3525.000000  225.000000  6202.000000
34.000000

24 2 4  3525.000000  225.000000  6202.000000  3525.000000  225.000000  6236.000000
34.000000

24 2 5  3525.000000  225.000000  6236.000000  3525.000000  225.000000  6270.000000
34.000000

24 2 6  3525.000000  225.000000  6270.000000  3525.000000  225.000000  6304.000000
34.000000

OPEN 'prod2'

WELL  'PROD3'
```

PRODUCER 'PROD3'

OPERATE MAX STO 15000.0 CONT

OPERATE MIN BHP 28.0 CONT

rad geofac wfrac skin

GEOMETRY K 0.25 0.37 1.0 0.0

PERF GEOA 'PROD3'

UBA ff Status Connection

2 2 1 1.0 OPEN FLOW-TO 'SURFACE' REFLAYER

2 2 2 1.0 OPEN FLOW-TO 1

2 2 3 1.0 OPEN FLOW-TO 2

2 2 4 1.0 OPEN FLOW-TO 3

2 2 5 1.0 OPEN FLOW-TO 4

2 2 6 1.0 OPEN FLOW-TO 5

LAYERXYZ 'PROD3'

perf geometric data: UBA, block entry(x,y,z) block exit(x,y,z), length

2 2 1 225.000000 225.000000 6100.000000 225.000000 225.000000 6134.000000 34.000000

2 2 2 225.000000 225.000000 6134.000000 225.000000 225.000000 6168.000000 34.000000

2 2 3 225.000000 225.000000 6168.000000 225.000000 225.000000 6202.000000 34.000000

2 2 4 225.000000 225.000000 6202.000000 225.000000 225.000000 6236.000000 34.000000

2 2 5 225.000000 225.000000 6236.000000 225.000000 225.000000 6270.000000 34.000000

2 2 6 225.000000 225.000000 6270.000000 225.000000 225.000000 6304.000000 34.000000

OPEN 'PROD3'

WELL 'PROD4'

PRODUCER 'PROD4'

```
OPERATE  MAX  STO  15000.0  CONT

OPERATE  MIN  BHP  28.0  CONT

rad  geofac  wfrac  skin

GEOMETRY  K  0.25  0.37  1.0  0.0

PERF     GEOA  'PROD4'

UBA            ff        Status  Connection

24 19 1        1.0  OPEN    FLOW-TO  'SURFACE'  REFLAYER

24 19 2        1.0  OPEN    FLOW-TO  1

24 19 3        1.0  OPEN    FLOW-TO  2

24 19 4        1.0  OPEN    FLOW-TO  3

24 19 5        1.0  OPEN    FLOW-TO  4

24 19 6        1.0  OPEN    FLOW-TO  5

LAYERXYZ  'PROD4'

perf geometric data: UBA, block entry(x,y,z) block exit(x,y,z), length

24 19 1  3525.000000  2775.000000  6100.000000  3525.000000  2775.000000
6134.000000  34.000000

24 19 2  3525.000000  2775.000000  6134.000000  3525.000000  2775.000000
6168.000000  34.000000

24 19 3  3525.000000  2775.000000  6168.000000  3525.000000  2775.000000
6202.000000  34.000000

24 19 4  3525.000000  2775.000000  6202.000000  3525.000000  2775.000000
6236.000000  34.000000

24 19 5  3525.000000  2775.000000  6236.000000  3525.000000  2775.000000
6270.000000  34.000000

24 19 6  3525.000000  2775.000000  6270.000000  3525.000000  2775.000000
6304.000000  34.000000

OPEN 'PROD4'

GUIDEI  STG  'inj'

1e+07

*MXCNRPT  100
```

DATE 2000 2  1.00000

DATE 2000 3  1.00000

DATE 2000 4  1.00000

DATE 2000 5  1.00000

DATE 2000 6  1.00000

DATE 2000 7  1.00000

DATE 2000 8  1.00000

DATE 2000 9  1.00000

DATE 2000 10  1.00000

DATE 2000 11  1.00000

DATE 2000 12  1.00000

DATE 2001 1  1.00000

DATE 2001 2  1.00000

DATE 2001 3  1.00000

DATE 2001 4  1.00000

DATE 2001 5  1.00000

DATE 2001 6  1.00000

DATE 2001 7  1.00000

DATE 2001 8  1.00000

DATE 2001 9  1.00000

DATE 2001 10  1.00000

DATE 2001 11  1.00000

DATE 2001 12  1.00000

DATE 2002 1  1.00000

DATE 2002 2  1.00000

DATE 2002 3  1.00000

DATE 2002 4  1.00000

DATE 2002 5  1.00000

DATE 2002 6  1.00000

DATE 2002 7  1.00000

DATE 2002 8  1.00000

DATE 2002 9  1.00000

DATE 2002 10  1.00000

DATE 2002 11  1.00000

DATE 2002 12  1.00000

DATE 2003 1  1.00000

DATE 2003 2  1.00000

DATE 2003 3  1.00000

DATE 2003 4  1.00000

DATE 2003 5  1.00000

DATE 2003 6  1.00000

DATE 2003 7  1.00000

DATE 2003 8  1.00000

DATE 2003 9  1.00000

DATE 2003 10  1.00000

DATE 2003 11  1.00000

DATE 2003 12  1.00000

DATE 2004 1  1.00000

DATE 2004 2  1.00000

DATE 2004 3  1.00000

DATE 2004 4  1.00000

DATE 2004 5  1.00000

DATE 2004 6  1.00000

DATE 2004 7  1.00000

DATE 2004 8  1.00000

DATE 2004 9  1.00000

DATE 2004 10  1.00000

DATE 2004 11  1.00000

DATE 2004 12  1.00000

DATE 2005 1  1.00000

DATE 2005 2  1.00000

DATE 2005 3  1.00000

DATE 2005 4  1.00000

DATE 2005 5  1.00000

DATE 2005 6  1.00000

DATE 2005 7  1.00000

DATE 2005 8  1.00000

DATE 2005 9  1.00000

DATE 2005 10  1.00000

DATE 2005 11  1.00000

DATE 2005 12  1.00000

DATE 2006 1  1.00000

DATE 2006 2  1.00000

DATE 2006 3  1.00000

DATE 2006 4  1.00000

DATE 2006 5  1.00000

DATE 2006 6  1.00000

DATE 2006 7  1.00000

DATE 2006 8  1.00000

DATE 2006 9  1.00000

DATE 2006 10  1.00000

DATE 2006 11  1.00000

DATE 2006 12  1.00000

DATE 2007 1  1.00000

DATE 2007 2  1.00000

DATE 2007 3  1.00000

DATE 2007 4  1.00000

DATE 2007 5  1.00000

DATE 2007 6  1.00000

DATE 2007 7  1.00000

DATE 2007 8  1.00000

DATE 2007 9  1.00000

DATE 2007 10  1.00000

DATE 2007 11  1.00000

DATE 2007 12  1.00000

DATE 2008 1  1.00000

DATE 2008 2  1.00000

DATE 2008 3  1.00000

DATE 2008 4  1.00000

DATE 2008 5  1.00000

DATE 2008 6  1.00000

DATE 2008 7  1.00000

DATE 2008 8  1.00000

DATE 2008 9  1.00000

DATE 2008 10  1.00000

DATE 2008 11  1.00000

DATE 2008 12  1.00000

DATE 2009 1  1.00000

DATE 2009 2  1.00000

DATE 2009 3  1.00000

DATE 2009 4  1.00000

DATE 2009 5  1.00000

DATE 2009 6  1.00000

DATE 2009 7  1.00000

DATE 2009 8  1.00000

DATE 2009 9  1.00000

DATE 2009 10  1.00000

DATE 2009 11  1.00000

DATE 2009 12  1.00000

DATE 2010 1  1.00000

DATE 2010 2  1.00000

DATE 2010 3  1.00000

DATE 2010 4  1.00000

DATE 2010 5  1.00000

DATE 2010 6  1.00000

DATE 2010 7  1.00000

DATE 2010 8  1.00000

DATE 2010 9  1.00000

DATE 2010 10  1.00000

DATE 2010 11  1.00000

DATE 2010 12  1.00000

DATE 2011 1  1.00000

DATE 2011 2  1.00000

DATE 2011 3  1.00000

DATE 2011 4  1.00000

DATE 2011 5  1.00000

DATE 2011 6  1.00000

DATE 2011 7  1.00000

DATE 2011 8  1.00000

DATE 2011 9  1.00000

DATE 2011 10  1.00000

DATE 2011 11  1.00000

DATE 2011 12  1.00000

DATE 2012 1  1.00000

*MXCNRPT  100

DATE 2012 2  1.00000

DATE 2012 3  1.00000

DATE 2012 4  1.00000

DATE 2012 5  1.00000

DATE 2012 6  1.00000

DATE 2012 7  1.00000

DATE 2012 8  1.00000

DATE 2012 9  1.00000

DATE 2012 10  1.00000

DATE 2012 11  1.00000

DATE 2012 12  1.00000

DATE 2013 1  1.00000

DATE 2013 2  1.00000

DATE 2013 3  1.00000

DATE 2013 4  1.00000

DATE 2013 5  1.00000

DATE 2013 6  1.00000

DATE 2013 7  1.00000

DATE 2013 8  1.00000

DATE 2013 9  1.00000

DATE 2013 10  1.00000

DATE 2013 11  1.00000

DATE 2013 12  1.00000

DATE 2014 1  1.00000

DATE 2014 2  1.00000

DATE 2014 3  1.00000

DATE 2014 4  1.00000

DATE 2014 5  1.00000

DATE 2014 6  1.00000

DATE 2014 7  1.00000

DATE 2014 8  1.00000

DATE 2014 9  1.00000

DATE 2014 10  1.00000

DATE 2014 11  1.00000

DATE 2014 12  1.00000

DATE 2015 1  1.00000

DATE 2015 2  1.00000

DATE 2015 3  1.00000

DATE 2015 4  1.00000

DATE 2015 5  1.00000

DATE 2015 6  1.00000

DATE 2015 7  1.00000

DATE 2015 8  1.00000

DATE 2015 9  1.00000

DATE 2015 10  1.00000

DATE 2015 11  1.00000

DATE 2015 12  1.00000

DATE 2016 1  1.00000

DATE 2016 2  1.00000

DATE 2016 3  1.00000

DATE 2016 4  1.00000

DATE 2016 5  1.00000

DATE 2016 6  1.00000

DATE 2016 7  1.00000

DATE 2016 8  1.00000

DATE 2016 9  1.00000

DATE 2016 10  1.00000

DATE 2016 11  1.00000

DATE 2016 12  1.00000

DATE 2017 1  1.00000

DATE 2017 2  1.00000

DATE 2017 3  1.00000

DATE 2017 4  1.00000

DATE 2017 5  1.00000

DATE 2017 6  1.00000

DATE 2017 7  1.00000

DATE 2017 8  1.00000

DATE 2017 9  1.00000

DATE 2017 10  1.00000

DATE 2017 11  1.00000

DATE 2017 12  1.00000

DATE 2018 1  1.00000

DATE 2018 2  1.00000

DATE 2018 3  1.00000

DATE 2018 4  1.00000

DATE 2018 5  1.00000

DATE 2018 6  1.00000

DATE 2018 7  1.00000

DATE 2018 8  1.00000

DATE 2018 9  1.00000

DATE 2018 10  1.00000

DATE 2018 11  1.00000

DATE 2018 12  1.00000

DATE 2019 1  1.00000

DATE 2019 2  1.00000

DATE 2019 3  1.00000

DATE 2019 4  1.00000

DATE 2019 5  1.00000

DATE 2019 6  1.00000

DATE 2019 7  1.00000

DATE 2019 8  1.00000

DATE 2019 9  1.00000

DATE 2019 10  1.00000

DATE 2019 11  1.00000

DATE 2019 12  1.00000

DATE 2020 1  1.00000

PRODUCER 'PROD3'

OPERATE  MAX  STG  0.0  CONT REPEAT

```
OPERATE  MIN  BHP  28.0  CONT

SHUTIN 'PROD3'

PRODUCER 'PROD4'

OPERATE  MAX  STG  0.0  CONT REPEAT

OPERATE  MIN  BHP  28.0  CONT

SHUTIN 'PROD4'

PRODUCER 'prod'

OPERATE  MAX  STG  0.0  CONT REPEAT

OPERATE  MIN  BHP  28.0  CONT

SHUTIN 'prod'

PRODUCER 'prod2'

OPERATE  MAX  STG  0.0  CONT REPEAT

OPERATE  MIN  BHP  28.0  CONT

SHUTIN 'prod2'

DATE 2020 1  4.00000

INJECTOR 'inj'

INCOMP  SOLVENT  1.0  0.0  0.0  0.0  0.0  0.0  0.0  0.0  0.0  0.0

OPERATE  MAX  STG  10000000.0  CONT REPEAT

OPERATE  MAX  BHP  2000.0  STOP

OPEN 'inj'

DATE 2020 2  1.00000

DATE 2020 3  1.00000

DATE 2020 4  1.00000

DATE 2020 5  1.00000

DATE 2020 6  1.00000

DATE 2020 7  1.00000

DATE 2020 8  1.00000
```

DATE 2020 9  1.00000

DATE 2020 10  1.00000

DATE 2020 11  1.00000

DATE 2020 12  1.00000

DATE 2021 1  1.00000

DATE 2021 2  1.00000

DATE 2021 3  1.00000

DATE 2021 4  1.00000

DATE 2021 5  1.00000

DATE 2021 6  1.00000

DATE 2021 7  1.00000

DATE 2021 8  1.00000

DATE 2021 9  1.00000

DATE 2021 10  1.00000

DATE 2021 11  1.00000

DATE 2021 12  1.00000

DATE 2022 1  1.00000

DATE 2022 2  1.00000

DATE 2022 3  1.00000

DATE 2022 4  1.00000

DATE 2022 5  1.00000

DATE 2022 6  1.00000

DATE 2022 7  1.00000

DATE 2022 8  1.00000

DATE 2022 9  1.00000

DATE 2022 10  1.00000

DATE 2022 11  1.00000

DATE 2022 12  1.00000

DATE 2023 1  1.00000

DATE 2023 2  1.00000

DATE 2023 3  1.00000

DATE 2023 4  1.00000

DATE 2023 5  1.00000

DATE 2023 6  1.00000

DATE 2023 7  1.00000

DATE 2023 8  1.00000

DATE 2023 9  1.00000

DATE 2023 10  1.00000

DATE 2023 11  1.00000

DATE 2023 12  1.00000

DATE 2024 1  1.00000

DATE 2024 2  1.00000

DATE 2024 3  1.00000

DATE 2024 4  1.00000

DATE 2024 5  1.00000

DATE 2024 6  1.00000

DATE 2024 7  1.00000

DATE 2024 8  1.00000

DATE 2024 9  1.00000

DATE 2024 10  1.00000

DATE 2024 11  1.00000

DATE 2024 12  1.00000

DATE 2025 1  1.00000

# Appendix B

## Similarity Report

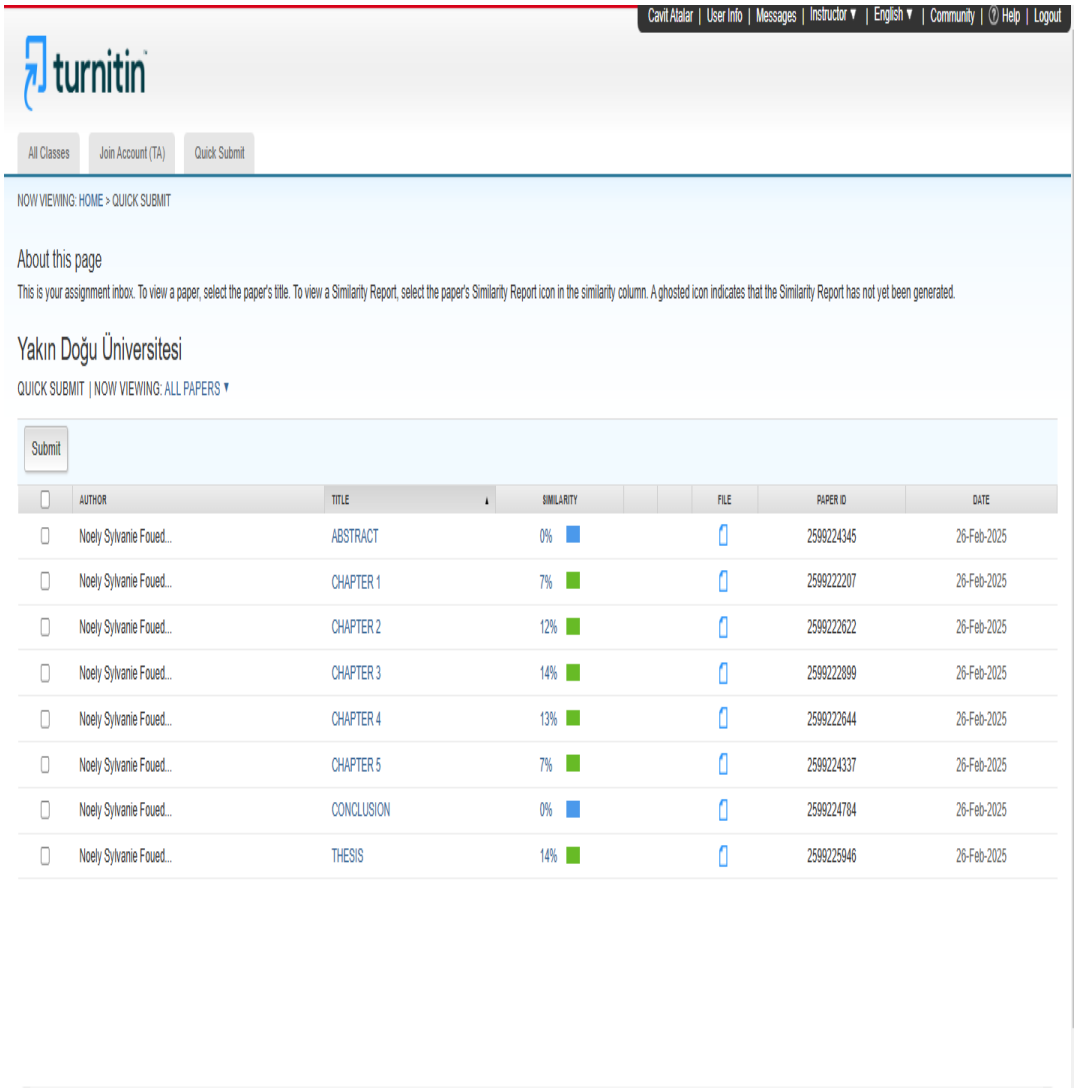

## APPENDIX C

## ETHICAL APPROVAL LETTER

# YAKIN DOĞU ÜNİVERSİTESİ

# ETHICAL APROVAL DOCUMENT

Date: 10/04/2025

To the **Institute of Graduate Studies**

The research project titled "**MODELING MISCIBLE $CO_2$ INJECTION FOR ENHANCED OIL RECOVERY: AIN DAR AREA**" has been evaluated. Since the researcher will not collect primary data from humans, animals, plants or earth, this project does not need through the ethics committee.

**Title**: Prof. Dr.

**Name Surname:** Cavit ATALAR

**Signature:**

**Role in the Research Project:** Supervisor